Resistivity and Surface Wave Seismic Surveys in Geotechnical Site Investigations

Wisén, Roger

2005

Citation for published version (APA):
Wisén, R. (2005). *Resistivity and Surface Wave Seismic Surveys in Geotechnical Site Investigations*. [Doctoral Thesis (compilation), Engineering Geology]. Engineering Geology, Lund University.

Total number of authors:
1

ISRN LUTVDG/TVTG-1016-SE
ISBN 91-973406-5-0

Resistivity and surface wave seismic surveys in geotechnical site investigations

Roger Wisén

Doctoral Thesis

Engineering Geology
Lund Institute of Technology
Lund University

2005

LUND INSTITUTE
OF TECHNOLOGY
Lund University

Printed by KFS AB, Lund 2005

Papers

Paper 1	Wisén, R., Auken, E. and Dahlin, T., 2005, Comparison of 1D laterally constrained inversion and 2D smooth inversion of resistivity data with a priori data from boreholes, *Near Surface Geophysics*, 3, 71-79.
Paper 2	Wisén, R., Christiansen, A.V., Dahlin, T. and Auken, E., 2005, Experience from two resistivity inversion techniques applied in three case studies of geotechnical site investigation, *Journal of geotechnical and geoenvironmental engineering*, ASCE, Submitted.
Paper 3	Wisén, R. and Christiansen, A.V., 2005, Laterally and Mutually Constrained Inversion of Surface Wave Seismic Data and Resistivity Data, *Journal of Environmental and Engineering Geophysics*, 10, 251-262.
Paper 4	Wisén, R., Zhang, D. and Dahlin, T., 2005, 3D effects on 2D resistivity imaging: modeling and field surveying results, *Geophysical Journal International*, manuscript.
Paper 5	Wisén, R. and Bjelm, L., 2005, Resistivity imaging as a site investigation method in urban environments, *Engineering Geology*, Submitted.

Related papers

Wisén, R., Dahlin, T. and Bernstone, C., 1999, Resistivity and inductive electromagnetics for delineation studies of leakage from a waste deposit in southern Sweden, *Proceedings of the EEGS-ES, Budapest, Hungary, 1999*.

Wisén, R., Bjelm, L. and Dahlin, T., 2000, Resistivity imaging as a preinvestigation method in urban environments, *Proceedings of the EEGS-ES, Bochum, Germany, 2000*.

Wisén, R. and Bjelm, L., 2001, Resistivity imaging as a complement to geotechnical investigations for delineation of inter-morainic sediments in a clay till, *Proceedings of the EEGS-ES, Birmingham, England, 2001*.

Wisén, R., Auken, E. and Dahlin, T., 2002, Comparison of 1D Laterally Constrained Inversion and 2.5D inversion of CVES resistivity data with drilling data as apriori information, *Proceedings of the EEGS-ES, Aveiro, Portugal, 2002*.

Wisén, R., Christiansen, A.V., Auken, E. and Dahlin, T., 2003, Application of 2D laterally constrained inversion and 2D smooth inversion of CVES resistivity data in a slope stability investigation, *Proceedings of the EEGS-ES, Prague, Check Republic, 2003*.

Wisén, R., Rydén, N., Bengtsson, D. and Henriksson, K., 2003, The application of MASW in a geotechnical site investigation, *Proceedings of the EEGS-ES, Prague, Check Republic, 2003*.

Wisén, R., Dahlin, T. and Auken, E., 2004, Resistivity imaging as a tool in shallow site investigation – a case study, *Proceedings of the ISC2-2004, Porto, Portugal*.

Socco, L.V., Boiero, D., Foti, S. and Wisén, R., 2005, Body and Surface Wave Analysis for Dynamic Characterisation from Seismic Reflection Data, *Proceeding of 24th GNGTS (Gruppo Nazionale Geofisica della Terra Solida – National Group of Solid Earth Geophysics) Congress, Rome, Italy, 2005*, In print.

Acknowledgements

First of all, I would like to thank my main supervisor at Engineering Geology in Lund, Torleif Dahlin. He has been a support during all the years of my PhD studies. In one way or another he has contributed to all the projects that I have been working with and the enthusiasm with which he performs his own work is encouraging.

Torleif was also the person that introduced me to Esben Auken at the Hydrogeophysics Group in Aarhus. Esben became one of my supervisors and together with Torleif, he has had an important role in shaping this project. I appreciate the time I have spent in Aarhus and I have learnt a lot. Working with Esben is fun, tough and productive; nothing is done without a purpose and nothing gets through unquestioned.

I want to thank Leif Bjelm for signing me up as a PhD student, being my main supervisor during the first years of my PhD studies. During this time I got a broad view of methods and methodology for site investigation and I did a lot of the field work that gave the data I have later used for evaluation of different processing methods.

I am grateful to Mats Svensson at Tyréns AB. When my funding at Lund University was coming to an end he came with the idea to apply for new funding from Sven Tyréns foundation, which is the owner of Tyréns AB. This worked out just fine and since June 2004 I have been an employee of Tyréns AB, at the department of geotechnics in the southern region, while still working full time on my PhD studies. Mats has also contributed as a supervisor and through his position outside the university he could see things in a slightly different way than I. He has also been very generous with his time, helping me out with just about everything I have asked for.

I do not know any superlatives that can describe how glad I am for having a colleague like Peter Jonsson at the department in Lund. Thanks for everything and especially for the review of my thesis.

I want to thank Claudio Strobbia, Sebastiano Foti and Valentina Socco for inviting me to Turin to work with them. I especially would like to thank Valentina for helping me to prepare the material for the last case study and allowing me to use the Surface Wave Analysis Toolbox (SWAT) that is developed at Politechnico.

I would like to acknowledge: Nils Rydén for all help and discussions regarding surface wave seismics; Anders Vest Christiansen, at the Hydrogeophysics group in Aarhus, for discussions on inverse modelling in general and excellent cooperation regarding the work with paper 2 and 3; Dahai Zhang, at that time a post-doc at the department in Lund, for the cooperation regarding paper 4; Henrik Möller, who is my boss at Tyréns AB; The rest of the people at the geotechnics department at Tyréns; Bo Holm Jacobsen, Head of department at the geophysics laboratory, Aarhus university, who taught me geophysical inverse modelling; All the PhD students active previously or at present in Lund; Master thesis workers that I have worked together with; The rest of the people at the department in Lund; Everyone that I have spent time with at the geophysics laboratory at Aarhus University and the rest of staff at the Hydrogeophysics group; Everyone that I have cooperated with and met at the geophysics laboratory in Turin; Everyone that have helped me in the field or in other ways; Richard Owen for proof reading the manuscript of my thesis.

I greatly acknowledge the Citytunnel Project, Malmö city, Tyréns AB, The Swedish Geotechnical Institute and Politechnico in Turin for allowing me to get access to field areas and data in their projects which I have been active in.

My funders: Sven Tyréns foundation for funding two years of my PhD studies; NORFA for scholarships to visit Aarhus University; The ROSE school for the Marie Curie fellowship to visit the University in Pavia and Politechnico in Turin.

My final and biggest “THANK YOU” goes to my family: My parents, Mats and Inger Wisén, that have brought me up and encouraged me to be the person I am; Sofia and Samuel who are the love of my life and two very patient persons.

Abbreviations

1D	One Dimensional
1D-LCI	One Dimensional Laterally Constrained Inversion
2D	Two Dimensional
2D-LCI	Two Dimensional Laterally Constrained Inversion
3D	Three Dimensional
CPT	Cone Penetration Test
CVES	Continuous Vertical Electrical Sounding
DC	Direct Current
GPS	Geodetic Positioning System
IP	Induced Polarisation
LCI	Laterally Constrained Inversion
MCI	Mutually Constrained Inversion
PACES	Pulled Array Continuous Electrical Sounding
SW	Surface Wave
SASW	Spectral Analysis of Surface Waves
SCPT	Seismic Cone Penetration Test
STDF	Standard Deviation Factor
VES	Vertical Electrical Sounding
VLF	Very Low Frequency

Abstract

The adaptation of geophysical methods for civil engineering purposes represents an important contribution to the development of geotechnical site investigation methodology. The term "geotechnical site investigation" here refers to all investigations performed prior to or during construction; i.e. investigations to support and refine a conceptual geological model as well as to provide a model of geotechnical design parameters. At any stage in the site investigation process, geophysical methods provide information to facilitate the interpolation of geological, geotechnical and hydro-geological structures between positions where detailed information, e.g. from drilling, are available. Geophysical methods have the potential to provide information that describes sections, areas or volumes; such information that would not be readily available from any other investigation method.

Common to almost all geophysical methods is the need for inverse modelling of the observed data. The modelling result can be interpreted directly in terms of the physical properties that it describes.

DC resistivity and surface wave seismics are two methods that perform well in geotechnical site investigations. This thesis focuses on the use of these two methods and different approaches for inverse modelling; the thesis illustrates and comments on the value of these approaches, e.g. through field studies.

- 2D smooth inversion, the commonly used technique for inversion of profiling resistivity data, is a robust technique also for data from complicated geological environments. However, this method is unable to produce sharp layer interfaces, which sometimes makes the resulting models difficult to interpret.
- 3D smooth inversion of resistivity data results in improved models in environments with prominent three-dimensional structures.
- The recently developed laterally constrained inversion of resistivity data provides a few-layer model together with estimates of the uncertainty of model parameters. When this technique is used together with 2D smooth inversion the interpretability of the results is improved.
- The laterally constrained inversion of dispersion curves from surface wave seismic data for a layered shear wave velocity model was developed within this thesis work. It provides a more stable inversion process compared to individual inversion of the dispersion curves.
- The new concept of mutually constrained inversion is implemented for the first time for combined inversion of resistivity and surface wave seismic data. It produces a better model estimate than separate inversion of the two data types and still allows for differences in geometry between the shear wave velocity and the resistivity models.
- By constraining the model geometry with a priori information, the effects from problems with hidden or suppressed layers, non-uniqueness and equivalence in the inversion can be reduced. The laterally constrained inversion allows the inclusion of a priori information on the model so that the uncertainties of the geophysical model parameters are reduced and the final geophysical model is improved.

These methods for measurement and inversion of geophysical data provide cost-effective, fast and robust tools for describing geological units. If they are used to complement the traditional geotechnical methods, an improved material model is achieved. This in turn leads to a safer design and at the end most probably a reduction of the construction costs.

Sammanfattning

Anpassningen av geofysiska metoder till infrastrukturtillämpningar är en viktig del i utvecklingen av geoteknisk förundersökningsmetodik. Det som här benämns geotekniska förundersökningar hänvisar till alla undersökningar som görs före eller under konstruktion, alltså sådana som syftar till att stödja och förbättra en konceptuell geologisk modell så väl som sådana som syftar till att ta fram en modell av geotekniska designparametrar. I varje steg i förundersökningsprocessen tillhandahåller geofysiska metoder information som underlättar vid interpolering av geologiska, geotekniska och hydrogeologiska strukturer mellan punkter där detaljerade sonderingsundersökningar har utförts. Geofysiska metoder har potential att beskriva sektioner, ytor eller volymer. Detta är information som inte är lätt tillgänglig från någon annan undersökningsmetod.

Gemensamt för nästan alla geofysiska metoder är behovet av inversmodellering av observerade data. Resultaten från inversmodellering kan tolkas direkt med avseende på de fysikaliska egenskaper de beskriver.

DC-resistivitet och ytvågsseismik är två metoder som fungerar väl i geotekniska förundersökningar. Denna avhandling fokuserar på användandet av dessa två metoder och olika tillvägagångssätt för geofysisk inversmodellering samt diskuterar och belyser värdet av att tillämpa dessa tekniker, bl.a. genom fältstudier.

- Den vanligast använda tekniken för inversion av profilerande resistivitetsdata, 2D-inversion med en cellindelad modell, är robust även för komplicerade geologiska miljöer. Denna teknik är dock oförmögen att skapa modeller med skarpa lagergränser vilket ibland gör resultaten svårtolkade.
- 3D-inversion med cellindelad modell ger bättre resultat i geologiska miljöer med framträdande 3D strukturer.
- En nyligen utvecklad metod för lateralt bunden inversion använder lagerindelade modeller. Utöver en slutlig modell över markens resistivitetsfördelning erhålls från inversionen också en uppskattning av modellparametrarnas osäkerheter. Detta förbättrar möjligheterna till tolkning av resultaten.
- Lateralt bunden inversion av dispersionskurvor från profilerande ytvågsseismiska data resulterar i en skjuvvågshastighetsmodell. Metoden utvecklades inom ramarna för detta avhandlingsarbete. Denna metod stabiliserar inversionen av yvågsseismiska data vilket ger upphov till en förbättring av inversionsresultatet jämfört med separat inversion av enskilda dispersionskurvor.
- Gemensamt kopplad inversion av olika datatyper är ett nytt koncept som här tillämpas för första gången för samtidig inversion av resistivitets- och ytvågsseismiska data. Metoden ger en förbättring av de resulterande modellerna jämfört med separat inversion av de två datatyperna och tillåter geometriska skillnader mellan resistivitets- och skjuvvågshastighetsmodellerna.

- Genom att styra modellgeometrin med a priori-information mildras effekterna av problem med dolda eller undertryckta lager, icke-unika lösningar eller ekvivalens vid inversion av geofysiska data. Lateralt bunden inversion tillåter denna typ av a priori information i inversionen vilket leder till en förbättring av den slutliga geofysiska modellen.

Dessa metoder är kostnadseffektiva, snabba och robusta verktyg för att beskriva geologiska enheter. Om de används som komplement till de traditionella geotekniska undersökningsmetoderna kan en förbättrad materialmodell erhållas vilket i sin tur leder till säkrare design och slutligen sannolikt till en reducerad konstruktionskostnad.

Table of contents

1. Introduction

During the last decades or even the last years several geophysical methods have experienced significant development. Much due to this, the adaptation of geophysical methods for civil engineering purposes represents an important contribution to the development of site investigation methodology. It is important to acknowledge that geophysical methods provide information that describes sections, areas or volumes; information that would not be readily available from any other investigation method. Therefore, geophysics provides information that facilitates the interpolation of geological, geotechnical and hydrogeological structures between discrete investigation points e.g. boreholes at any stage in the site investigation process.

Some seismic methods have been adopted more rapidly in geotechnical engineering than other geophysical methods, mainly because one of the results from certain seismic measurements is the stress-strain relationship at small strain (Stokoe et al., 2004). The stress-strain relationship is a mechanical property that is used directly in geotechnical design. However, also other geophysical methods measuring non-mechanical properties, e.g. electric or electro-magnetic methods, significantly contribute to geotechnical site investigation.

In Sweden the term “geotechnical site investigation” is often strongly connected to geotechnical design and soil mechanics. In this thesis the term refers to all investigations performed prior to or during construction. That means investigations to support and refine a conceptual geological model or a model of geotechnical design parameters.

Common to almost all geophysical methods is the need for inverse modelling of the measured data, hereafter referred to as inversion. Inversion is most often the last step in the construction of a geophysical model. The inverted model can be interpreted directly in terms of the physical properties that it describes; this is rarely the case on the measured data. However, the geophysical data and the inverted models have limitations that are critical to know.

This thesis presents some applications of surface wave seismic and resistivity methods and different inversion techniques to geotechnical site investigations. Evaluation of these methods is made and examples of commonly used algorithms for geophysical inverse modelling, as well as newly developed algorithms, are presented.

1.1. Aim and considerations

The main objective of the thesis work has been to evaluate and develop methods and methodologies for site investigations with geophysical methods. DC resistivity and SW (surface wave) seismic methods have been chosen as the core methods. This choice is based on the ability of the methods to perform well in different environments and to support each other. Results from other geophysical and geotechnical methods are used as reference data. The focus is on how the geophysical models, i.e. the resistivity model from electrical resistivity tomography and/or the shear wave velocity model from SW seismic measurements, are estimated through inverse modelling. This includes:

- An evaluation and comparison of existing algorithms for the inversion of CVES (Continuous Vertical Electrical Sounding) resistivity data. The evaluation regards well established as well as newly developed algorithms.
- An evaluation and comparison of existing algorithms for 2D and 3D inversion of CVES resistivity data.

- Development and evaluation of a new algorithm for the inversion of SW seismic data.
- Development and evaluation of a new concept for the combined inversion of SW seismic and resistivity data.
- Evaluation of resistivity measurements in an urban environment.

The main part of the thesis consists of five technical papers that have been accepted, are under revision, have been submitted or will be submitted for publication in peer-reviewed journals.

1.2. Limitations

Different approaches to geotechnical site investigation are presented but are not evaluated. There are many ways to treat geophysical data and the approach presented here is not complete, but a selection of methods that were found valuable in geotechnical site investigations. The methods discussed exclude for example the important borehole based measurements, e.g. logging.

The presented case studies are examples of how the methods can be applied. In some cases the results are as they were presented in the papers or reports from where they originate, and in other cases new results from processing techniques that were not available or not originally considered are presented.

The conditions for a site investigation approach including geophysical surveys as discussed here must be considered ideal. Such conditions are rare and most likely only possible in large projects. Therefore, since the majority of geotechnical projects are fairly small this approach can not be used uncritically but must be adjusted from case to case.

1.3. Outline

The thesis work is published as five papers in peer-reviewed journals covering subjects from near-surface geophysics to geotechnical engineering. This summary comprises:

- an introduction with objectives, limitations and outline of the thesis.
- a summary of the papers;
- a description of geotechnical site investigation;
- a description of the methods used;
- a presentation of a number of examples to support the aim of the thesis;
- conclusions of the material presented here and;
- a brief discussion on the future of engineering geophysics and the methods used.

Part of the thesis focuses on the use of inverse modelling as a tool in applied geophysics. To reduce the size of the summary the mathematical details of this topic are given in an appendix. The five technical papers, also found in appendices, are summarised below.

2. Summary of papers

2.1. Paper 1

The first paper “Comparison of 1D laterally constrained inversion and 2D smooth inversion of resistivity data with a priori data from boreholes” was published in Near Surface Geophysics, 2005. This paper shows how LCI (laterally constrained inversion) can provide significant additional information in the interpretation of CVES data. In this case a 1D formulation of the forward response was used for the LCI (1D-LCI) and it was used in combination with a 2D smooth inversion scheme. It is concluded that 2D smooth inversion resolves lateral changes well while 1D-LCI results in well-defined horizontal layer interfaces. In geological environments where the lateral variations are not too pronounced the 1D-LCI contributes to a geological interpretation of the resistivity measurements with better interpretation of depths to layer interfaces. The 1D-LCI offers an estimate of the uncertainty of the model parameters, which is helpful when evaluating the integrity of the model. Furthermore, with the 1D-LCI it is possible to constrain model parameters with a priori information e.g. for the depth to layer interfaces based on borehole information. The inclusion of a priori information in the inversion reduces the effects of non-uniqueness and 2D-effects in 1D-LCI; revealing further details and decreased uncertainty of the resistivity model.

2.2. Paper 2

The second paper “Experience from two resistivity inversion techniques applied in three case studies of geotechnical site investigation” is submitted to the Journal of Geotechnical and Geoenvironmental Engineering. This paper presents to the geotechnical community how the combination of in situ geotechnical testing and continuously measured geophysical data is a useful tool in geotechnical site investigation. An improved methodology combines 2D (two-dimensional) smooth inversion and 2D-LCI (2D laterally constrained inversion) to significantly increase interpretability. The 2D smooth inversion has high horizontal resolution while the 2D-LCI has a high vertical resolution. The possibility to add a priori information in the 2D-LCI increases the confidence in the inverted model and limits ambiguity.

The paper includes two case studies from Sweden and one from Denmark. In a site investigation for a railway trench a geotechnical data set is used as a priori information to increase the model resolution of the inversion of the resistivity data. A slope stability study employs resistivity data together with refraction seismic and geotechnical drill log data. Both of these case studies utilise a multi-electrode resistivity system. In the third case study the PACES (pulled array continuous electrical sounding) system is employed in the planned position of a freeway to map the uppermost 15-20 m. This is done in order to estimate the distribution of the geological formations which is important information for freeway construction.

2.3. Paper 3

The third paper “Laterally and mutually constrained inversion of surface wave seismic and resistivity data” was published in the Journal of Environmental and Engineering Geophysics in September 2005. It presents a development of LCI for SW seismic data. In combination with the 1D-LCI of resistivity data this algorithm makes it possible to perform mutually constrained inversion (MCI) of surface wave seismic data and resistivity data.

The advantages and limitations of LCI and MCI are evaluated on synthetic SW data and on data from a case study in southern Sweden. The main conclusions are that there is a significant increase in resolution of the seismic shear wave velocity model when LCI is used compared to that from individual inversion of synthetic seismic data alone. Adding mutual constraints to resistivity data further improves the model resolution of all parameters in the shear wave velocity model.

When applied to field data, model resolution improves significantly when LCI or MCI is used, and resistivity and velocity models correlate structurally with better correlation to lithological interfaces identified in drill logs.

2.4. Paper 4

The fourth paper “3D effects on 2D resistivity imaging: modelling and field surveying results” is a manuscript which will be submitted to the Geophysical Journal International. It presents a comparison of 2D and 3D smooth inversion of profiling resistivity data together with three examples. The existence of 2D effects on 1D resistivity modelling is a well known problem; however, former studies show that 3D effects in 2D surveying are less evident. The results presented here show that there is real advantage in performing 3D inversion in many environments. A comparison between 2D inversion and 3D inversion was made with analysis of data from two different synthetic models and three field datasets. From the synthetic study it is clear that 3D inversion gives higher contrast and fewer inversion artefacts than 2D inversion. From the field studies it is also evident that 3D inversion results in models with higher contrast. With only limited ground truth data it is not always possible to determine which model is closest to the true one; however, where ground truth data is available it is clear that the 3D inversion gives a better result. In addition it is shown that the choice of array configuration has a significant influence on the result, with multiple gradient array configuration generally giving better results than the other options.

2.5. Paper 5

The fifth paper “Resistivity imaging as a site investigation method in urban environments” is submitted to Engineering Geology. It presents a case study from southern Sweden where resistivity measurements are used in a geotechnical site investigation in the city centre of Malmö. An extensive resistivity campaign was performed in an area where an underground railway station will be built. Pipes, fences and underground constructions that can affect the resistivity survey negatively often prevent collection of useful resistivity data. The presented data are partially affected negatively by such structures. However, an effort is made to reduce these effects and their influence on the final result. The aim of the survey is the mapping of the limestone surface whereas more detailed interpretation is avoided. The combined interpretation of drilling data and the resistivity results gave a detailed model of the upper and lower boundaries in between which the surface of intact limestone is likely to be found, a result that can be very valuable at all stages in the site investigation process.

3. Site investigation

3.1. Introduction

The successful design of earth works and foundations requires a model of the material properties and their geometrical distribution. Unlike more homogeneous materials, the determination of a material model for geo-materials is relatively complex. This is due to the high degree of variation of material properties as well as to the extent and homogeneity of different geological formations. Moreover, in the case that the geo-materials have undesirable properties for a specific design, it is usually not possible to choose another material.

Both introductory and detailed, practical descriptions of site investigation procedures are available (e.g. Bell, 1993; Blyth and de Freitas, 1984; BSI, 1999 and; Clayton et al., 1995). The two latter are both very comprehensive and deal with the planning and procurement of a site investigation, the different stages in site investigation and individual methods. The main Swedish contributions are *Handboken Bygg: Geoteknik* (In Swedish, Liber förlag, 1984) that has a practical approach to site investigation and *Site investigations in rock: Investigations, prognoses, reports - recommendations* (Bergman and Carlsson, 1988) that summarises the knowledge and experience of that time and recommends a basic work procedure for site investigation. Two field manuals that contain general advice and method descriptions for geotechnical (SGF, 1996) and environmental (SGF, 2004) investigations are available in Swedish from the Swedish Geotechnical Society.

Even though the acceptance of geophysical methods and methodology has increased significantly over the last decades, geophysical methods are generally still not being used to their full potential in geotechnical site investigation. Many examples (e.g. Ward, 1989b; Dahlin et al., 1999; Foti, 2000; Dahlin et al., 2001; Stanfors et al., 2001; Rankka et al., 2004; Rydén, 2004; Stokoe et al., 2004; Turesson and Lind, 2005) show that geophysical methods can be as useful in geotechnical site investigation as it has proved to be in groundwater, environmental and geological investigations.

3.1.1. Geological information, uncertainties and hazards

The main risk in geotechnical engineering is the uncertainty of encountering an unexpected geological condition that implies a threat of possible damage. Therefore the formulation of a preliminary engineering geological model is an important step to provide an understanding of the expected site ground conditions, and thereby facilitate the planning and design of a project. Figure 1 describes how geological and geotechnical knowledge develop at different stages in a site investigation. Early in a project, after a desk study and field reconnaissance, the geological knowledge accumulates rapidly while there is almost no geotechnical knowledge. When geophysical investigations, geotechnical in-situ investigations and geotechnical laboratory tests are performed geotechnical knowledge is rapidly accumulated.

In site investigation it is necessary to assess the geological hazards and in order to do that, it is important to get the right geological information at the right time. The technical, geological, contractual, economic and political complexity of large underground construction projects makes it imperative to have clearly defined responsibilities, a structured flow of information, stringency in decision making and precision and accuracy in performing analyses of hazards and risks (Sturk, 1998). The use of geophysical information provides significant input in an early stage of site investigation. If geophysical data is collected late in the process much of the potential in applying geophysical methods is lost.

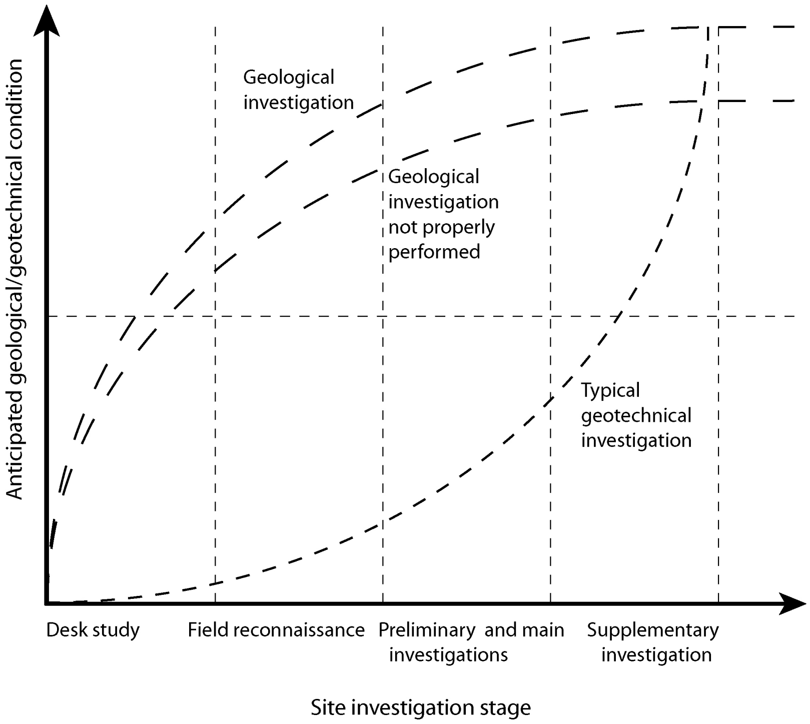

Figure 1 **The diagram describes how geological and geotechnical knowledge develops at different stages in a site investigation. Note that the anticipated ground conditions are relative to the separate investigations. During desk study and field reconnaissance geological knowledge accumulates rapidly while there is almost no geotechnical knowledge. However, during ground investigation geotechnical knowledge is rapidly accumulated (Modified from Fookes et al., 2000).**

3.1.2. Objectives of site investigation

Site investigation involves exploration of the ground conditions at and below the surface (Bell, 1993). The objectives for a site investigation (BSI, 1999 and Clayton et al., 1995) can be summarised as:

- Site selection: Where possible a choice of sites should be provided and the suitability of different sites for the planned works determined.
- Foundation and earth works design: Provide a suitable and economic design.
- Temporary works design: Often the temporary works impose greater stress on the ground than the final construction. The difficulties in construction due to temporary works must therefore be thoroughly investigated and the construction methods designed accordingly.

- Effect of changes: Determine the effect on the planned and adjacent constructions and the environment due to natural changes or changes imposed by the planned works.
- Investigation of defects or failure of existing works: This is important in the advancement of soil mechanics but also very valuable for obtaining data for future works in similar ground conditions
- Environmental investigations are today frequently performed. The main objectives of environmental effects are mapping of contaminated land, groundwater and the environmental and health effects from these contaminants.

Compared to the other objectives site selection is a process that requires information over relatively large areas. Since geophysical methods are cost-effective they provide a valuable contribution to fulfill this objective, especially fast methods, e.g. magnetometry and some electro magnetic methods are valuable. Geophysical investigations for delineation of contaminants that have increased ion content can include electrical and electro-magnetic methods that are sensitive to changes in resistivity.

3.1.3. Approaches to site investigation

A complete site investigation consists of a desk study, a field reconnaissance, a detailed investigation for design and a construction review. The desk study and field reconnaissance begin the site investigation and should be completed before the ground investigation (BSI, 1999). If contract conditions permit and the project is such that the design can be altered during its construction the site investigation should continue throughout the construction (Peck, 1969). The interaction between site investigation, design and construction is summarised in Figure 2. It must be specified from the beginning how data from the site investigation is used during and after the investigation. This is especially important when it comes to geophysical information since this type of data can be processed and interpreted in different ways at different stages in a project.

Depending on the project size a site investigation can include everything from a desk study and a geotechnical advice for small projects to a complete ground investigation consisting of all the parts mentioned in the beginning of this chapter. For projects where the design can be revised during construction the observational method (Terzaghi and Peck, 1967; Peck, 1969) is useful. This approach consists of an initial limited investigation with aim of establishing a general model of the ground conditions. From this model the most probable conditions together with the most unfavourable deviations should be established. During construction measurements of selected quantities are carried out and if necessary predefined actions and/or modifications are made.

In all these approaches geophysics can be applied to facilitate the creation of geological and mechanical material models as discussed in the previous chapter and in the introduction of this thesis.

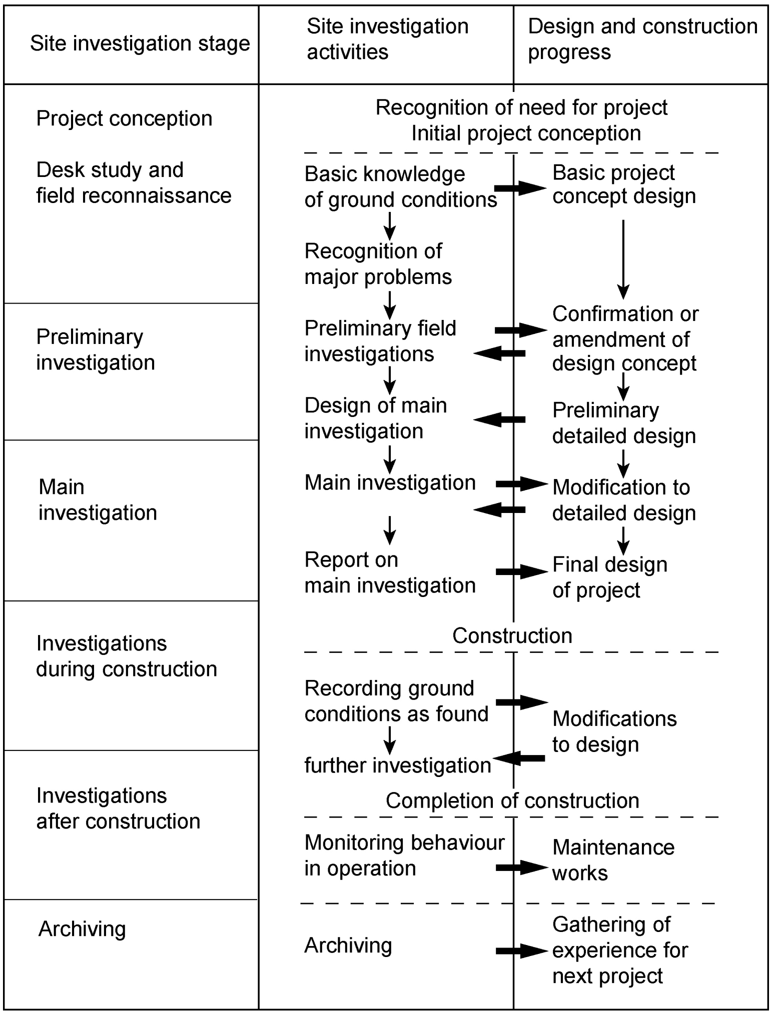

Figure 2 **Site investigation phases connected with design and construction stages of a project (modified from IAEG, 1981). As can be seen in the figure important decisions are made already early in the site investigation process which puts high demands on planning.**

3.2. The different stages of site investigation

3.2.1. Desk study and field reconnaissance

Site investigation is always initiated with a desk study that aims at evaluating the ground conditions based upon existing information and to outline a plan for the following stages of the site investigation. It is of utmost importance to have the most complete picture possible of the geology before new investigations are carried out. In large projects and for sites with a complex geology a desk study can save time and reduce the cost of the site exploration. In Sweden basic national information for the desk study is listed on one common web page (Kartplan, 2005). Information is available from Lantmäteriet (Swedish surveying office), SGU (Geological Survey of Sweden), Sjöfartsverket (Swedish Maritime Administration) and SMHI (Swedish Meterological and Hydrological Institute). SGU keeps a public database of all wells produced in Sweden. They also provide geological maps of soil, rock and hydrogeology as well as aerial photography and geophysical maps from investigations of magnetometry, gravimetry, VLF (very low frequency) and radiometry. Information of more local character is to be found at e.g. municipal offices or at consultant companies. However, no public geotechnical or geophysical archive with experience from projects exists in Sweden. As described in Figure 2 such a database could provide valuable background information from previous investigations in the geographical vicinity of new projects.

The desk study is followed by a field reconnaissance that consists of a visual examination of the site. After the desk study and field reconnaissance a first conceptual geological model should be produced giving a preliminary general description of the geometry, composition and condition of the geological units which are present.

3.2.2. Ground investigation

The ground investigation verifies or rejects and refines the geological models compiled in the desk study. The information from the investigation must be sufficient to produce an economic and safe design for new works, to assess any hazards associated with the ground and to meet tender and construction requirements (BSI, 1999). The primary objective is to establish a model of the geotechnical design parameters, describe the groundwater conditions and where appropriate the geometry and nature of discontinuities. The investigations should cover all ground in which temporary or permanent changes may occur as a result of the construction (BSI, 1999).

The methods used in ground investigation may include but are not limited to different types of drilling, probing, sampling, bearing capacity tests, laboratory tests and geophysical measurements. The extent of the ground investigation depends on the geological conditions, the type and size of the project and the information discovered during the desk study and during the investigation.

Interpretation as well as reporting from a site investigation should be performed as a continuous process. It is important that the geological and geophysical models are always updated so that the best methods can be implemented at the right time and place to provide optimal information. Reports should be separated in two parts: one descriptive part that covers work procedures and results; and one part that contains analysis, conclusions and recommendations. This should be the case regardless of the size of the investigation.

3.2.3. Geophysical surveying in ground investigation

In a geophysical survey different techniques can be used to measure a variety of physical properties, each of which is described by certain theoretical principles. Geophysical methods are cost efficient and provides often new information. However, the need for prior geological knowledge in order to make a correct interpretation of geophysical data and a proper choice of methods must be acknowledged. Early in the site investigation process geophysics can assist in refining a general geological model so that it contains local variations and major discontinuities; this model can then be used for optimal design of further investigations. During the detailed investigation (e.g. a drilling program) geophysics can be used to facilitate the interpolation of geological, geotechnical and hydrogeological properties between the discrete investigation points. Many geophysical methods have the potential of providing information that describes sections, areas or volumes; such information would not be readily available from any other investigation method. This information increases the resolution and decreases the uncertainty of the model developed during site investigation.

When selecting a geophysical method it is necessary to consider the resolution capability, the capacity to reveal certain conditions and the ability to assess specific physical properties. It happens that poorly chosen methods fail, leading to false or confusing interpretations. A procedure for choosing geophysical methods must consider the following issues (modified from Clayton et al., 1995):

- What is the objective of the survey? For example, to assess depth to bedrock, or to locate the position of old mine shafts or the determination of a certain physical property. Table 1 presents the connection between available geophysical methods, objectives and specific problems.
- What is the physical property to be measured? For some objectives this is obvious, i.e. small strain stiffness can only be determined if the shear wave velocity is measured, but otherwise the best method to use is one where the contrast in the physical property for the particular objective is highest.
- Which method is most suited for the geometry of the target? A geophysical target can vary from a horizontal boundary between bedrock and sediments, a vertical dyke or the determination of the geometry and size of a mechanically distinct zone.
- What is the required vertical and lateral resolution and depth penetration?
- Is there previous published experience on the use of method for the specific purpose? If available, this can save a lot of time and increase the efficiency of the survey.
- How much “noise” is there on the site? The signal to noise ratio has to be carefully considered when selecting method.
- Is the sub-soil geometry sufficiently simple to allow interpretation? Different geophysical data are processed in different ways resulting in models with different parameterisation.
- Is more than one geophysical method needed to meet the objectives? For example hidden layers in seismic interpretation might be found with resistivity measurements.

There are many available geophysical methods for engineering purposes, of which only a few will be discussed here. For detailed theoretical descriptions of available methods, literature on geophysics or applied geophysics should be consulted (e.g. Telford et al., 1990; Reynolds, 1997; Parasnis, 1997; Sharma, 1997).

Table 1 Objectives and specific problems in geophysical investigation for geotechnical applications (modified from BSI, 1999).

Objective	Problem	Example	Methods and remarks
Geological	Stratigraphical	Sands and gravel over bedrock with water table low in sands and gravel	Seismic refraction, radar
		Sands and gravel overlying clay with water table high in sands and gravel	Resistivity
		Clay over bedrock	Resistivity, seismic refraction
	Erosional	Buried channel	Seismic refraction, resistivity
		Buried karstic surface	Resistivity
	Structural	Buried faults, dykes	Resistivity, seismic refraction, seismic reflection, surface wave seismic, magnetic, gravimetric (large faults)
Resource assessment	Water	Location of aquifer	Resistivity, radar, seismic refraction
		Location of saline/potable interface	
	Sand and gravel	Sand, gravel over clay	Resistivity
	Rock	Intrusive in sedimentary rocks	Magnetic
	Clay	Clay pockets	Resistivity
	Archeological remains	Foundations, buried walls, crypts	Magnetic, electromagnetic, resistivity and radar
Hazard assessment	Cables and pipes	Trenches on land	Magnetic, electromagnetic field detectors, (radar)
	Shafts, audits and caverns	Shafts, sink holes and mine workings	Resistivity, magnetic, electromagnetic, radar, infra-red air photography (on clear areas), cross hole seismic, surface wave seismic, micro gravity
	Leakages in barriers	Leakages through earth dams	Resistivity, self potential (e.g. permanent installations)
	Pollution	Pollution plume from landfill	Resistivity, electromagnetic
	Landfills	Delineation of landfills	Resistivity, induced polarisation
Engineering properties	Young's Modulus, Shear modulus, density and porosity	Dynamic deformation modulus	Surface wave seismic, cross-hole seismic, down-hole seismic, borehole geophysics
	Effects of ground treatment	Effects of stabilisation of unconsolidated clay or organic soils with lime or cement	Resistivity
	Rock rippability	Choice of excavation method	Seismic

Some practical aspects for the planning of a geophysical investigation are:

- What is the extent of the investigation? For example, is one profile enough or are several parallel or crossing profiles required to meet the objective(s)?
- What other investigations are required to verify the interpretation? As mentioned earlier, no geophysical survey can be properly interpreted without reference data.
- Are there any records of the ground conditions available? These should then be used to refine the results from the geophysical survey.
- How shall the presentation of the results be organised and designed? How are the results communicated?
- How shall the investigation be planned in time? Has the best season of the year been chosen for the geophysical survey? Some surveys can be considerably harder or impossible to do when the weather is unsuitable. Are there other activities in the project that puts requirements on the choice of time?
- Accurate positioning and levelling surveys are very important. GPS (geodetic positioning system) increase the possibilities of accurate positioning of measurements. The choice of datum for positioning data must be consistent with the datum of other positioning surveys and maps that are used in the project.

3.3. Geophysical parameters and geotechnical design parameters

The use of geophysical methods for estimating geotechnical design parameters is not common. Mechanical properties estimated indirectly from geophysical measurements usually have a lower resolution than when estimated from invasive sounding methods. Measurements using traditional geotechnical methods (e.g. probing or laboratory methods) normally have a relatively small uncertainty at the measurement point. The uncertainty increases both with distance and with the degree of disturbance of the material. Sample volume also influences the uncertainty of the result.

In order to choose the appropriate geophysical method it is important to have an idea of the relationship between the physical properties and the desired geotechnical design parameters. Geometry and heterogeneity of geological units and aquifers are important parameters, and with a few exceptions these are the parameters that geotechnical literature claims as useful targets for geophysical surveys. Interesting examples where geophysical measurements are applied are common in the literature e.g. Dahlin et al. (2001) for slope stability investigations and Stanfors et al. (2001) for rock quality investigations prior to e.g. tunnel constructions.

The estimation of G_0 (shear modulus at small strain, see Figure 3) from shear wave velocity measurements is probably the only application where a surface based geophysical method has been generally accepted by the geotechnical community for determination of a geotechnical parameter. It has been shown that surface wave methods can be used for pavement system analysis (e.g. Nazarian, 1984; Rydén et al., 2004), and that seismic down-hole, cross-hole or surface wave methods can be used for the determination of G_0 in fine-grained soils (e.g. Massarsch, 2004). For the purpose of determining velocity in materials there are probing methods like the seismic cone (SCPT), a CPT equipment with down-hole receivers that can be used for shear wave velocity estimation (Butcher et al., 2005). Since G is different at different strain levels many methods, e.g. pressuremeter tests or triaxial tests, are required to get a well determined relationship (Figure 3).

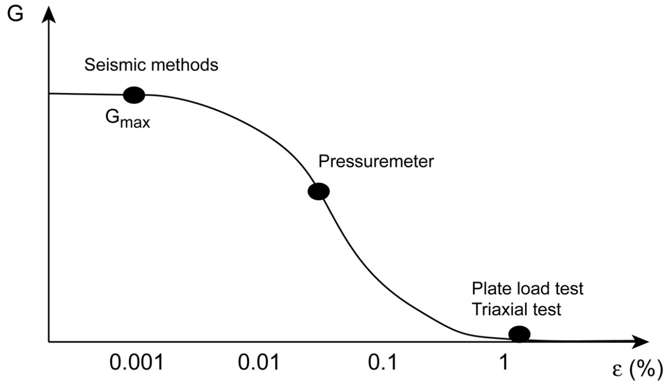

Figure 3 The relationship between G and strain together with the range of methods that can help to resolve this relationship. Seismic methods provide important information on the small strain G, called G_{max} or G_0 (after Jardine et al., 1986).

Quick clay formations can be investigated using laboratory tests, geotechnical soundings and resistivity measurements (Rankka et al., 2004). Quick clay is clay with high sensitivity and whose structure collapses completely when it is remoulded. The sensitivity is the relation between the undisturbed and the fully remoulded undrained shear strength. Most quick clays have been formed in marine sediments through a process of leaching which results in a decreased ion concentration in the pore water. In these formations low salt concentration is a prerequisite for the existence of quick clay. Since resistivity is strongly connected to the change in ion concentration resistivity measurements are useful for determining in which zones of an investigated area the salt concentration is high enough for quick clays not to occur. Since there are other factors that also influence the resistivity of the clay resistivity measurements must be used in combination with other geotechnical methods.

Grain size distribution is generally not used as a parameter in soil mechanical models but is very important for the understanding of soil behaviour. An actual attempt to estimate grain size distribution from geophysical measurements is presented by Rey et al. (2005) who apply resistivity measurements for estimation of rock mineral content in a conductive matrix through a relationship between bulk resistivity, resistivity of inclusions, resistivity of the matrix and content of inclusions.

Hydraulic parameters are also important. Theoretically a quantitative estimation of water content can be made using for example time domain reflectometry or logging with radioactive probes. Archie’s law (Archie, 1942) presents an empirical relationship between resistivity and porosity and water saturation.

3.4. Summary

It can be concluded that there are three points that must be considered when determining the necessary requirements on geological information:

- type of information - Choice of methods and to what extent the data should be processed and interpreted.

- timing in the project for data collection - The right information at the right time.
- amount and quality of the data - The amount and quality of data should neither be sub- nor super-optimised.

Up to here the geophysical methods have been seen from the perspective of planning a site investigation, and the role for geophysical methods in geotechnical site investigation has been discussed. In the following chapters resistivity measurements and surface wave seismic measurements will be presented and examples will be shown on how these methods can be applied in geotechnical site investigations.

4. Measurement methods

This chapter describes the DC resistivity and SW seismic methods since these two methods are central in this thesis. As mentioned in Section 1.1 these methods have the ability to perform well in many environments and to support each other. A short background and an introduction are given for both the methods. The measurement and data processing techniques are discussed and short descriptions of the forward modelling algorithms are given.

4.1. Resistivity method

Techniques for data acquisition and methods for interpretation of resistivity measurements have been continuously developed since 1912 when Conrad Schlumberger presented the idea of using electrical measurements to investigate subsurface conditions. The method has been used extensively (e.g. Ward, 1989a; Reynolds, 1997) and today there exist advanced techniques for measurement and processing of resistivity data.

From resistivity measurements an image of the subsurface resistivity variation is obtained. Different geological materials have different electrical resistivities (Figure 4). Some geological materials have overlapping resistivities; however, within a limited area and with geological knowledge, the resulting resistivity model can be interpreted for the distribution of geological units.

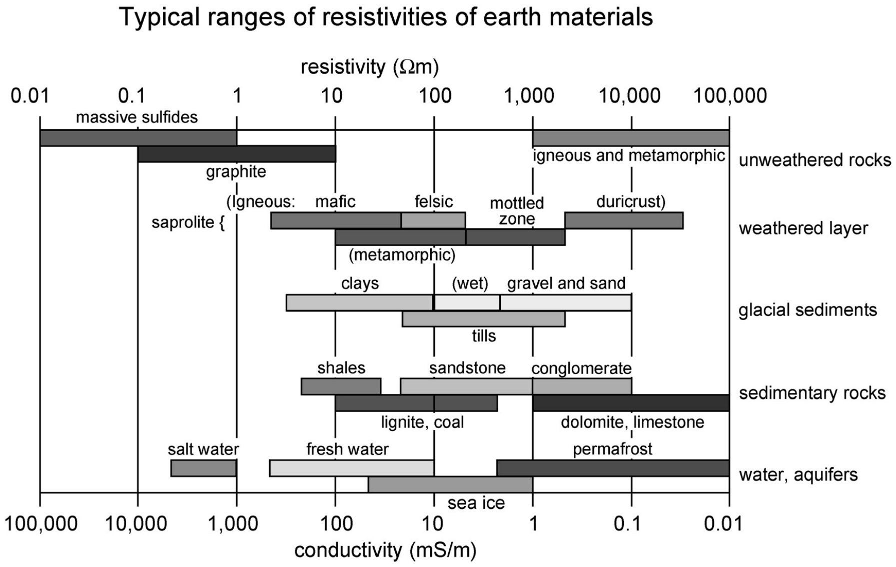

Figure 4 **Typical resistivities of natural soil and rock materials (modified from Palacky 1987). Many materials have large resistivity ranges and different materials can have overlapping resistivities. However, within a limited area of investigation the resistivity range for a material is usually limited. With knowledge on the expected geology from ground truth, resistivity measurements can provide very valuable information.**

Resistivity measurements have many different applications, both environmental and engineering (e.g. Dahlin, 1996; Pellerin, 2002). Resistivity mapping is a common method for the mapping of groundwater aquifers, their recharge areas and vulnerability (Larsen et al 2002; McGrath et al., 2002; Sørensen et al., 2005), delineation of landfill structures and leakage (Bernstone et al., 2000; Leroux and Dahlin, 2005), site investigation for construction (Dahlin et al., 1999) and geological hazard assessment (Hack, 2000; Suzuki et al., 2000; Rankka et al., 2004).

When electrical resistivity measurements are made a direct current is transmitted between two electrodes, and the potential difference between two other electrodes is measured. The apparent resistivity can then be calculated as:

$$\rho_a = K \times \frac{U}{I} \ (\Omega m) \qquad \textit{Equation 1}$$

where U is the measured potential, I is the current and

$$K = 2\pi \left[\left(\frac{1}{r_1} - \frac{1}{r_2} \right) - \left(\frac{1}{r_3} - \frac{1}{r_4} \right) \right]^{-1} \qquad \textit{Equation 2}$$

is the geometrical factor depending on r1, r2, r3 and r4 that are electrode distances as shown in Figure 5a. If the resistivity distribution in the ground is homogeneous, the apparent resistivity is equal to the true resistivity. However, this is never the case in reality and therefore a number of apparent resistivity data covering different investigation volumes (a sounding or a CVES profile) are measured to assess the resistivity distribution. The performance, in depth penetration and ability to assess certain structures, depends on the maximum separation, the internal positioning of the electrodes and the number of measurements.

The Wenner, Schlumberger and dipole-dipole array configurations shown in Figure 5b, c and d are all well known collinear arrays as are their pros and cons. Wenner is less sensitive to noise and is favourable to use for mapping of horizontally layered structures. The depth penetration of the Wenner array configuration is smaller than for the others. The dipole-dipole array configuration is much more sensitive to noise but has a greater depth penetration and is favourable for mapping vertical structures. Compared to these arrays the Schlumberger array configuration has intermediate quality both for noise sensitivity and for the type of structures that is mapped. Multiple gradient array configuration (Dahlin and Zhou, 2004) (Figure 5e) is slightly more sensitive to noise than the Wenner array configuration but has otherwise good capabilities. The gradient and dipole-dipole array configurations are well suited for multi-channel systems that are available today (Dahlin and Zhou, 2005).

4.1.1. Data collection

The CVES method has been used for many years and is well documented (e.g. Griffiths and Turnbull, 1985; Overmeeren and Ritsema, 1988). CVES measurements are often performed with a multi-electrode roll-along measurement system (Figure 6). Throughout this work the ABEM Lund Imaging System (Dahlin, 1996) (Figure 7) was used. For roll-along measurements four cables are connected to 81 electrodes that are placed along a line; after recording, one cable is moved from the beginning of the line to the end thus providing 20 new electrode locations. This CVES system allows for very flexible data collection. Based on the target and the actual geophysical problem, any configuration and data density that is allowed by the 81 electrodes can be programmed and, if desirable, altered during the measurement sequence.

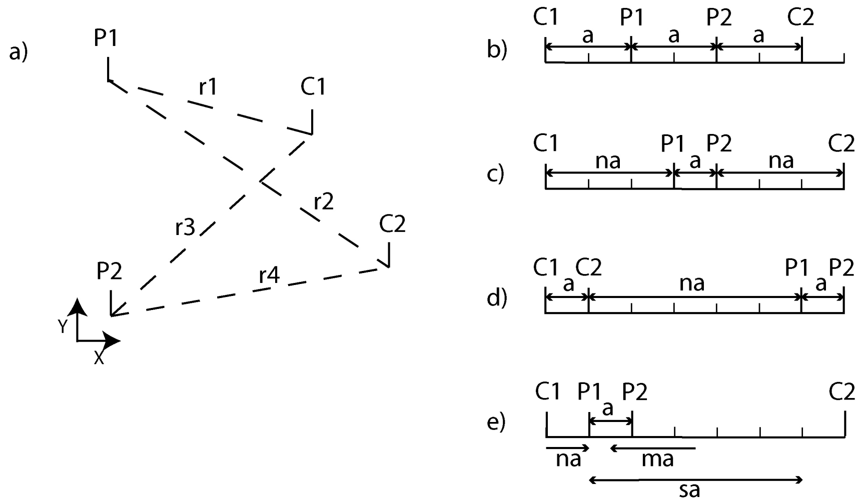

Figure 5 a) Principal of a four electrode measurement setup with two potential electrodes and two current electrodes on the ground. b) The Wenner array. a is the internal electrode distance. c) The Schlumberger array. a is the distance between potential electrodes and na is the distance between the current and potential electrodes. d) The dipole-dipole array. a is the distance between the electrodes in the current and potential dipoles and na is the distance between the current and potential dipoles. e) The multiple gradient array. a is the distance between the potential electrodes, na is the distance between the first current electrode and the first potential electrode, ma is the distance between the midpoint of the potential dipole and the midpoint of the current dipole and s is the number of potential dipoles with internal distance a that can be distributed in the array.

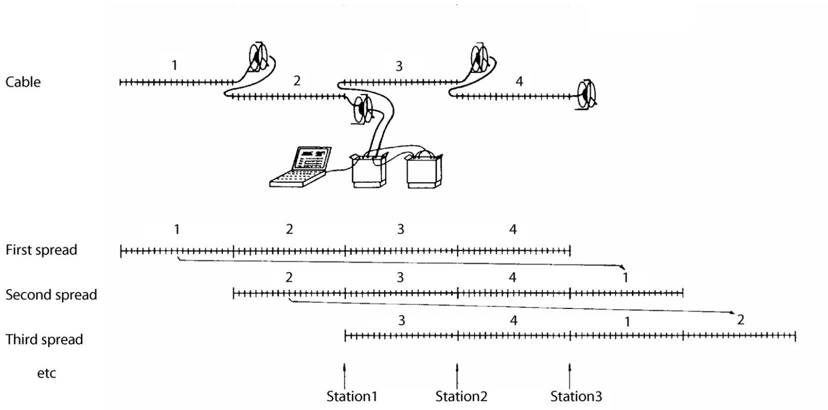

Figure 6 For roll-along measurements four cables are connected to 81 electrodes that are placed along a line; after recording, one cable is moved from the beginning of the line to the end thus providing 20 new electrodes locations (modified from Overmeeren and Ritsema, 1988).

Figure 7 Photograph of one version of the ABEM Lund Imaging System including the instrument SAS4000, an electrode selector ES-1064, multi-conductor cables, electrodes, a battery and various connectors.

In Denmark the PACES system is often used in large scale for groundwater investigations. This system consists of a small tractor which pulls the electrodes mounted on a towed electrode streamer (Sørensen, 1996; Sørensen et al., 2005) (Figure 8). The tractor is equipped with processing electronics and the electrodes are cylindrical steel tubes with a weight of about 15 kg each. Two electrodes are maintained as current electrodes, the remaining electrodes serve as potential electrodes in 8 different configurations (Figure 9b). A sketch of the system is shown in Figure 9a. Data collection is continuous at a speed of approximately 1.5 m/s with one full sounding saved each second. The maximum penetration depth of the system is 20 to 25 m depending on soil conditions and the production rate is 10 to 15 line-km per day. Data from this system is presented in Paper 2.

Figure 8 Photograph of the PACES system. (left) The small caterpillar seen from the side. A portable bridge is mounted on one side and the electrode streamer is visible behind the caterpillar. Note the wheel that measures travelled distance. (right) The operator standing on a small plough mounted just behind the caterpillar for improvement of the electrodes contact with the ground. The cylinder mounted on the cable just behind the plough is the first electrode.

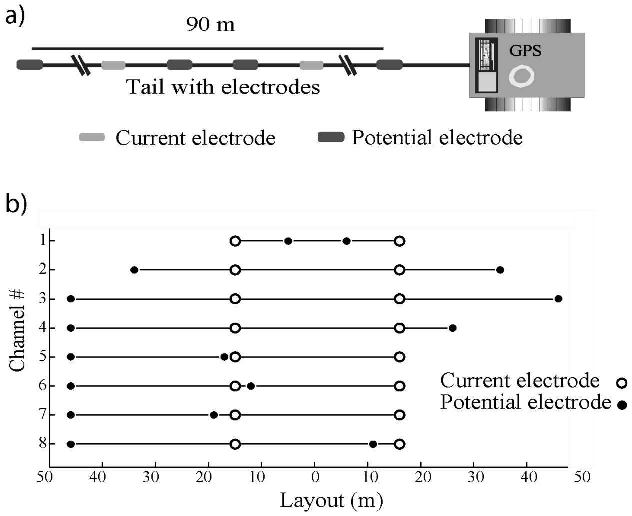

Figure 9 a) A sketch of the PACES system with b) an eight electrode configuration. The total length of the electrode array is approx. 90 m.

The 3D resistivity surveying presented in this thesis is performed as a set of parallel 2D surveys, i.e. measurements are only made in one direction over the target area. The distance between the lines is twice that of the in-line electrode distance. Compared with 3D surveys where measurements are made in more than one direction (e.g. Dahlin et al., 2002) this approach is fast and logistically simple and has at least in some cases similar resolution capability (Papadopoulos et al., 2005). While it is necessary to plan a 2D survey with respect to the strike of the geological structures, a 3D survey and inversion will be much less sensitive to the angle at which the measurement profiles cross structures.

4.1.2. Processing of apparent resistivity data

Basic processing of resistivity data includes plotting of pseudo-sections and/or sounding curves with subsequent removal or weighting of bad data.

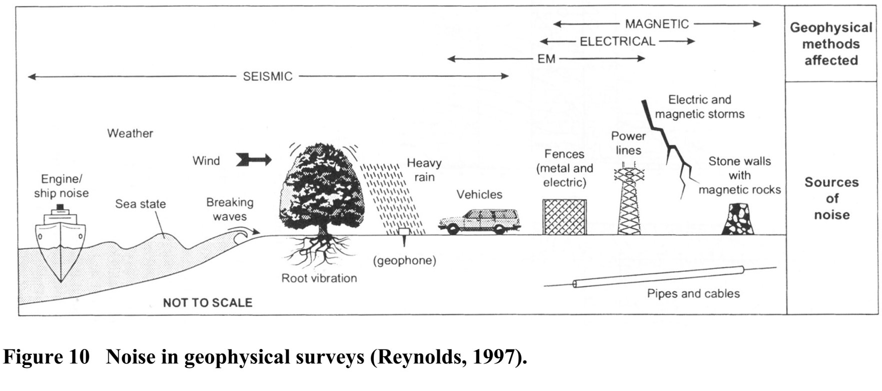

Figure 10 Noise in geophysical surveys (Reynolds, 1997).

The pseudo-section or sounding curve gives an initial idea of the resistivity distribution in the ground, but inverse modelling of the data is generally needed for further interpretation. Geophysical methods are sensitive to different varieties of noise. A large part of the noise sources are related to human activity, as illustrated in Figure 10. Before inverse modelling is performed bad data need to be manually culled as they often influence the inversion process negatively. The signal to noise ratio must be sufficiently high. If this ratio is too low the data will be noisy, however, it can still be useful. Outliers consist of erroneous data points, e.g. affected by temporary problems with instruments or large electrode grounding resistance. These data are usually easily detected and removed. Bad data affected by manmade conductive objects, e.g. fences or cast iron pipes, in galvanic contact with the ground can be a much larger problem. This data can be harder to recognise and they usually constitute a large quantity of the data resulting in a significant decrease of the model resolution. If it is possible to locate the sources in advance the best way to minimise the effect is simply by planning the survey to avoid the noise sources. If it is necessary to measure in an area e.g. with a metal pipe, the problems will be minimised if the measurement profile is placed perpendicular to the pipe. If the conductive objects are perpendicular to the measurement it has been shown that pre-processing of the data can remove these effects (Vickery and Hobbs, 2002).

Figure 11 Example of resistivity profiling close to an iron fence. a) This fence is placed 1 m outside the fence in b) and consists of a small iron rail that is in very good galvanic contact with the ground. b) A fence isolated from the ground by concrete foundations and the position of two resistivity sections.

Figure 11 present pictures with two different types of fences. In many cases fences have concrete foundations that isolate them sufficiently from the ground to allow more or less undisturbed measurements. This is the case in Figure 11b. However, if the fence is in galvanic contact with the ground, as the one in Figure 11a it will significantly influence the measurements because of current channeling.

In Figure 12 the resistivity model after inversion of data from measurements with 3 m electrode separation and approximately 40 m depth penetration at a distance of about 2 m from the fence in Figure 11a is presented. It is, as seen, not possible to make a geological interpretation due to the current channeling. The resistivity model shows a very low resistivity and the data misfit is very large which indicates that the data is bad. Figure 13 presents results from a measurement with 1.5 m electrode separation and about 20 m depth penetration at a distance of about 10 m from the fence in Figure 11a. Also these results show unnaturally low resistivity at depth, which is an effect from current channeling, but the data misfit is small and hence it is likely that a reasonable interpretation of the upper part of the model can be made.

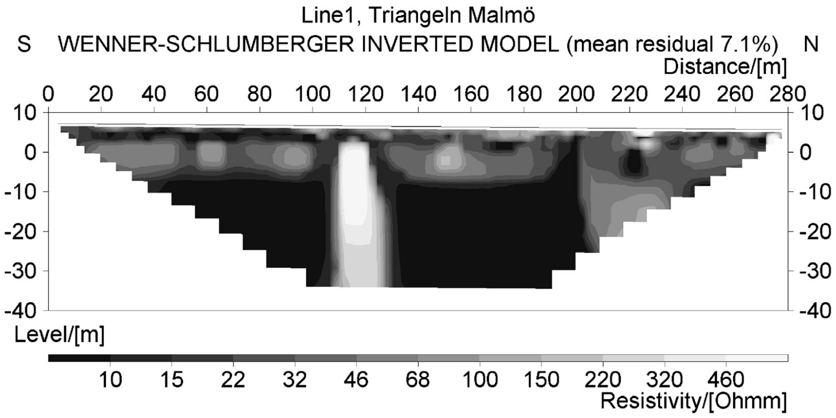

Figure 12 **Results from measurement in the position of the white line in Figure 11b. The electrode distance used was 3 m giving an approximate depth penetration of about 40 m. The resistivity of almost the entire section is lower than 10 Ωm and the mean residual error is high. This indicates that it is strongly affected by the conductive iron fence.**

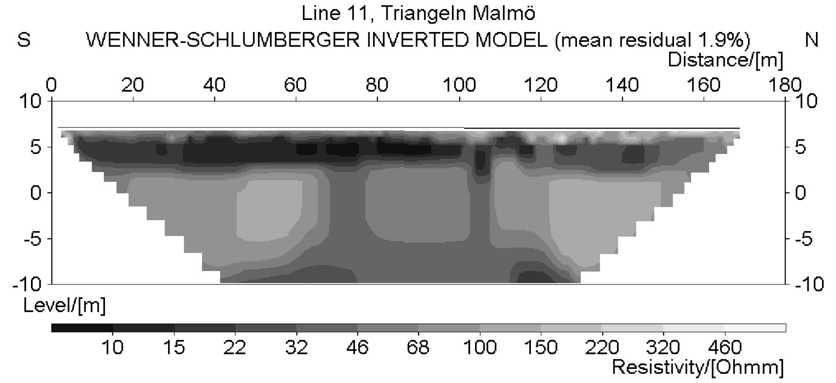

Figure 13 **Results from measurement in the position of the black line in Figure 11b. The electrode distance used was 1.5 m giving a depth penetration of about 20 m. The resistivities in this section are decreasing with depth, which might be an effect from disturbances at distance. However the mean residual error is low, indicating that the section is not as affected by the iron fence as the section in Figure 12.**

4.1.3. Forward models for apparent resistivity calculations

In this Section the forward responses for resistivity modelling are mentioned together with references to publications that provide information for a deeper understanding. In this work these algorithms have been used as they appear in the evaluated codes.

Forward responses for a 1D layered model can be calculated as a summation of pole-pole responses over a layered earth as described by Telford et al. (1990). This is the formulation used in the 1D-LCI algorithm (Auken et al., 2004).

Forward responses for a 2D model are calculated with a 2D finite difference method. The resistivity of the model cells can vary arbitrarily in x-z plane (described by the direction along the measurement line and depth) but no variation is allowed perpendicular to this plane (Figure 14b).

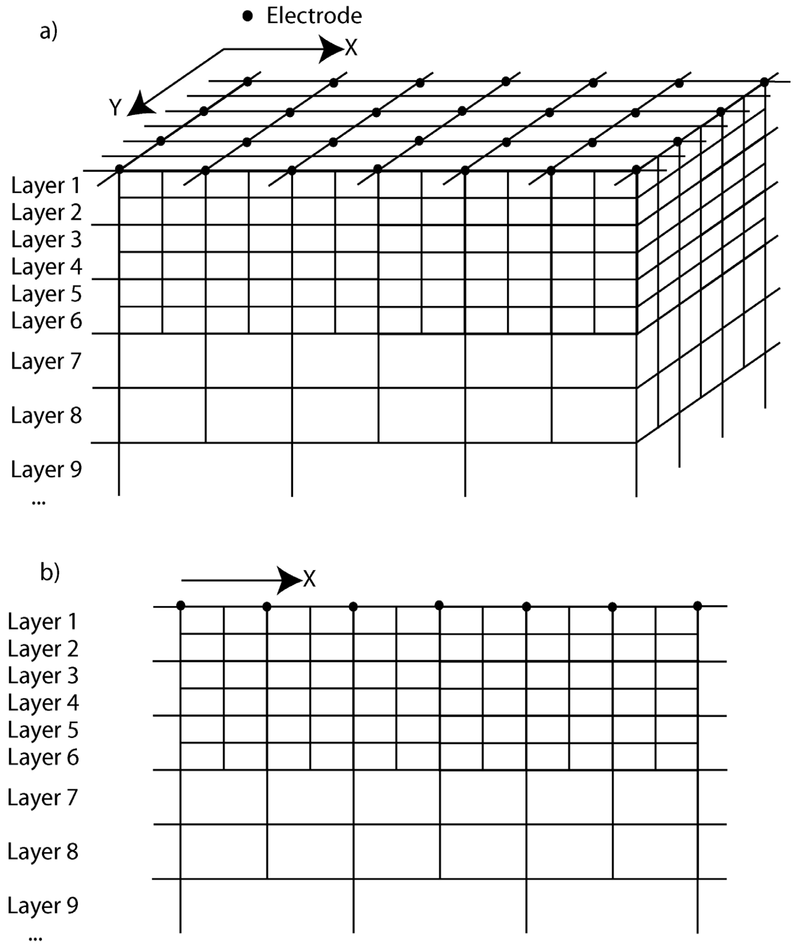

Figure 14 a) Principal sketch of a grid for 3D modelling. b) Principal sketch of a grid for 2D modelling.

For the 2D smooth inversion and the 2D-LCI (Auken and Christiansen, 2004) the 2D forward responses are calculated by finite difference methods as described by Loke and Barker (1996) and McGillivray (1992). For 2D-LCI the finite difference grid is superimposed on the layered model (Figure 15) as described by Auken and Christiansen (2004).

As for the 2D case the 3D forward response is calculated by a finite difference method utilising a 3D grid instead (Figure 14a).

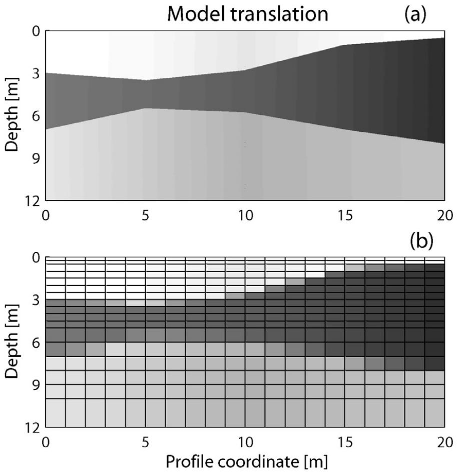

Figure 15 **a) The parameterised layered model used for inversion. b) The layered model superimposed on the finite-difference grid (from Auken and Christiansen, 2004).**

4.2. Surface wave seismic method

In seismic methods the propagation of a wave is observed in order to characterise mechanical properties of the ground and possible discontinuities. Surface wave methods utilise the dispersive nature of e.g. Rayleigh waves in a layered medium to obtain a shear wave velocity (V_s) profile with depth. Surface wave methods have been used in different fields of science since the middle of the 20th century and for geotechnical applications for a few decades. A thorough and up to date description of the available techniques is found in Socco and Strobbia (2004).

The use of the method in engineering applications accelerated in the 80's when the spectral analysis of surface waves (SASW) (e.g. Nazarian, 1984; Svensson, 2001) was introduced, since then multi-station techniques (e.g. Park et al., 1999; Foti, 2000) that convey a stable analysis have been increasingly used.

4.2.1. Data collection

Collection of seismic data is preferably performed with a multi-channel system. The systems available for refraction seismic or reflection seismic data collection are also well suited for collection of SW data but some considerations are necessary: because of the need for low frequency data (in order to increase the investigation depth) geophones for SW data collection typically need to be sensitive at lower frequencies than geophones for refraction or reflection surveys (geophones with a sensitivity peak at 4.5 Hz have proved to be very useful but 10 Hz geophones are often sufficient); the techniques used in reflection seismic surveys to reduce the amount of ground-roll have to be restrained, e.g. geophone groups or high pass filters should not be used in acquisition. For most of the data presented in Section 6.2.4 a 24-channel seismograph and 4.5 Hz geophones were used. The data collection was performed with the geophones coupled to the ground by spikes or using a land-streamer where the geophones are mounted on heavy steel plates connected by a cable and pulled after a vehicle (Svensson, 2004) (Figure 16).

Figure 16 Photographs of the land-streamer and 4WD. Note the Geometrics Geode mounted on the rear of the 4WD.

For some datasets 48-96 channels have been acquired with a multi-shot approach. In practice the source is moved an array length away from the geophones instead of moving the geophones. A number of common practice shot gathers are then concatenated to give larger dataset.

In the case study presented in Section 6.2.4 the source consisted of a sledgehammer dropped on a plate for better coupling. A more powerful impact source was used in the case study presented in Section 6.6 where the data originally was collected in a reflection seismic survey. In all case studies presented here the aim has been to collect data in a profiling manner, i.e. a number of seismic datasets are collected along a profile.

4.2.2. Data processing

The wave field measured in time and space (t-x) domain using a multi-station technique consists of a set of traces, a seismogram. In this the surface waves may be possible to identify but it is not possible to estimate their properties, e.g. velocity at different frequencies. To achieve this, the data is transformed into the frequency-wavenumber (f-k) domain (or sometimes into frequency-phase velocity (f-V_{Ph}) domain) where the properties can be more readily evaluated. This is done through one of many available approaches (see e.g. Socco and Strobbia, 2004). In the f-V_{Ph} or f-k domain the energy distribution of the different body and surface wave events can be studied and the fundamental mode dispersion curve extracted. Since the processing results in one fundamental mode phase velocity, V_{Ph}, dispersion curve for each dataset and this dispersion curve is assumed to be dependent on a 1D V_S model of the site this data can be considered a SW seismic sounding. Figure 17 shows an example of a shot gather in both t-x domain and f-V_{Ph} domain. The wave field transformation and dispersion curve extraction outline the basic processing for analysis of fundamental mode surface wave data.

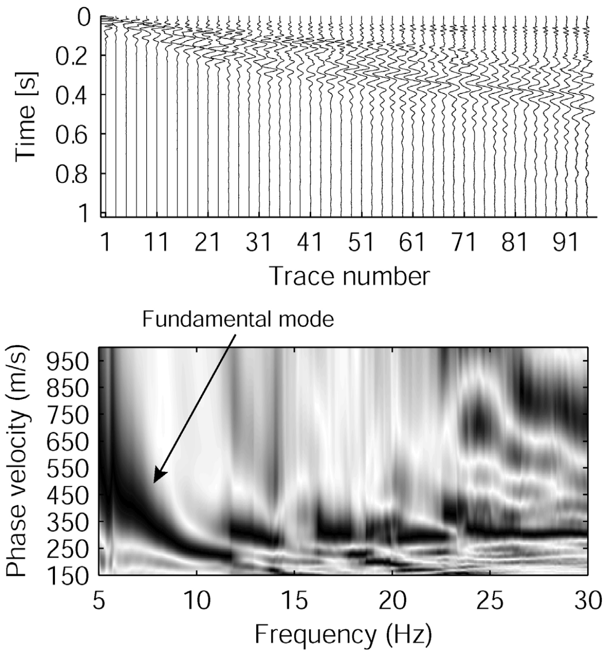

Figure 17 **A 96 channel shot gather from a seismic survey. a) t-x domain. The distance between traces is 1 m. Only traces with odd number position are plotted. b) f-V_{Ph} domain. The fundamental mode is identified at 10-19.5 Hz. Higher modes are also present at higher frequencies.**

Even if measurements are made with great care, there are still some things that can prevent the estimation of a correct dispersion curve. The distribution of energy between different modes is one such problem. There is always a large portion of energy travelling in higher modes and in some situations this might prevail over the occurrence of energy in the fundamental mode. This problem is difficult to handle, but approaches that include the analysis of higher modes exist. These are e.g. multimodal approaches (e.g. Beaty and Schmitt, 2003; O'Neill, 2003), full wave field (Forbriger, 2003a and b) or f-V_{Ph} analysis (Rydén, 2004). In this study only fundamental mode dispersion curve analysis is considered.

4.2.3. Forward model for dispersion curve calculation

For the development of the LCI for SW data the stiffness matrix method (Kausel and Roesset, 1981) was chosen for calculation of the theoretical dispersion curves for a 1D V_S model. In Appendix 1 the algorithm is described in detail.

Inputs to the model are Poisson's ratio, V_S, thickness and density of each layer. For each frequency (*f*) a number of wave-numbers (k) are calculated, one for each mode of propagation. In this work only the fundamental mode is used in the inversion.

5. Geophysical inverse modelling

5.1. Introduction

This chapter contains a general discussion on the application of geophysical inverse modelling with special focus on the application presented in the thesis. For details on the algorithms references are made to Appendix 1. The appendix contains basic theory for inverse modelling and a detailed description of the application of inverse modelling for laterally constrained inversion of SW data.

Inversion of geophysical data is most often the last step in the construction of a geophysical model. The inverted model can be interpreted directly for the physical features that it describes, which is often not the case for the measured data. However, the inverted model has limitations that must be known. Data collection is time consuming and it is often not possible to obtain the data quantity and quality that is needed to resolve a given geological model. Jackson (1972) states that geophysical data by nature is insufficient, inconsistent and inaccurate; therefore the geophysical model is a simplification of the true underlying model. The geophysical model will have problems with hidden or suppressed layers, non-uniqueness, equivalence and lack of resolution in parts of the model. A sensitivity analysis can be performed for any model that comes from inversion of geophysical data. Such an analysis can be made quite easily for the few-layered parameterised models used in LCI, as described in Section 5.4 and Appendix 1.

There are ways to get an improved estimate of the inverted model. One is the use of a priori information in the inversion and another is combined inversion of different datasets. This will be discussed later in this Chapter.

The inversion algorithms described here optimise a model result through an iterative scheme. An initial model is updated based on how the model response compares to the observed data. When a stop criteria is reached the iterative process stops and the final model is the result from the inversion. The stop criteria can for example consist of a minimum improvement of the residual between two consecutive iterations or an absolute value of the residual. The residual is a measure of the difference between the observed and modelled data.

5.2. 2D and 3D smooth inversion of CVES data

Continuous vertical electrical sounding data is traditionally processed using a 2D smooth inversion (Oldenburg and Li, 1994; Loke and Barker, 1996). It has been common to use the smoothness-constrained inversion, using L^2-norm* solution that works well for models with smooth changes. However, a limitation of 2D smooth inversion is that it is unable to produce sharp layer interfaces. This has been improved to some extent with the robust, or L^1-norm (Claerbout and Muir, 1973) solution can be used for the 2D smooth inversion (Loke et al., 2003). In all case studies presented here the 2D smooth inversion of Loke and Barker (1996) with L^1 or L^2-norm solution was used for inversion of the resistivity data.

---

* Norm is a term used to describe a measure of size. Here this measure is included in the objective function that is to be minimised in the iterative inverse modelling. The norm indicates the power of the elements that are measured i.e. L^1, L^2 or L^{inf}. Higher norm gives higher power to larger elements. If data is expected to scatter widely, which is the case for apparent resistivity data, a low order norm (L1 or L2) is used since it gives more equal weight to all sizes of errors. (After Menke, 1989)

The inversion can be constrained e.g. by changing the overall smoothing or choosing different smoothness-constraint in different directions to enhance certain structures. The latter is used for example in the case study from Lockarp, presented in Section 6.2.2, where the horizontal smoothness-constraint is four times the vertical.

For 3D smooth inversion the same approach is used as for 2D smooth inversion, with the difference that the model in this case consists of a 3D grid. It should also be mentioned that 3D inversion is considerably more time-consuming than 2D inversion, even though the development of faster computers have made it feasible. Another aspect of 3D inversion is that it requires a dense data coverage in order to be meaningful, which again falls back on the data collection with increased investigation time and cost as an effect. Where a 3D environment is prominent, the 3D resistivity survey with subsequent 3D inversion can give increased detail and accuracy of the resulting resistivity model compared to that given by 2D inversion. In certain cases, however, the 2D survey and 2D inversion is sufficient.

5.3. Laterally and mutually constrained inversion

The LCI and MCI perform a parameterised, layered inversion of many datasets by tying neighbouring models together with lateral constraints on the model parameters (Auken and Christiansen, 2004; Auken et al., 2004) as illustrated in Figure 18b. The models are few-layered 1D-models that should reflect the geology locally and the lateral constraints can be seen as a priori information on the lateral geological variation of the different model parameters in the field area. Applying lateral constraints result in a layered and laterally smooth pseudo 2D model.

a)

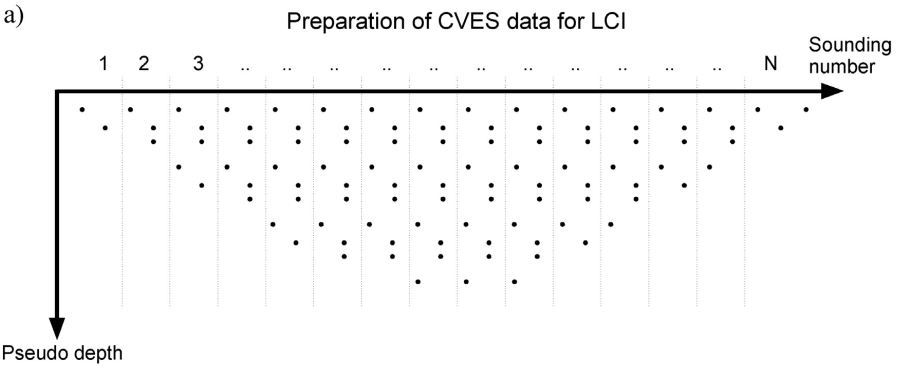

b)

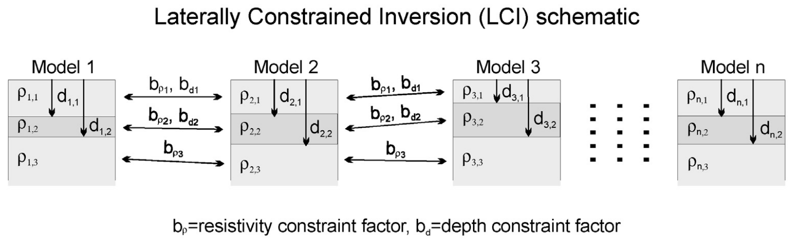

Figure 18 a) The CVES data set and the way it is divided into separate soundings for LCI. b) A schematic of the LCI model setup. The model is created from a number of 1D models with layer resistivities, ρ, and depths to layer boundaries, d. Each model is connected with its neighbours by constraints on the resistivities, b_ρ, and depths, b_d.

5.3.1. 1D and 2D LCI of CVES data

Laterally constrained inversion of resistivity data with a 1D formulation for the forward responses is referred to as 1D-LCI. For this approach this work shows that boundaries between the geological units are easier to localise in the LCI model compared to models from 2D smooth inversion (Paper 1). The layered pseudo 2D-model (consisting of a series of 1D-models) and corresponding data are inverted simultaneously with applied constraints. Before 1D-LCI is performed a CVES data set needs to be divided into separate soundings, this is done by dividing it into sections that each comes to contain the data for one sounding as is shown in Figure 18a.

Laterally constrained inversion that utilises a 2D forward response is referred to as 2D-LCI. The forward response is calculated like in 2D smooth inversion. Before the forward response is calculated in the 2D-LCI the set of neighbouring 1D-models are translated to a finite difference grid as described in Section 4.1.3 and Figure 15. The model in the 2D-LCI is described at nodes with layer resistivity and layer thickness, interpolated to build a full 2D-model.

5.3.2. LCI of SW data

Similar to the 1D-LCI for resistivity data, the LCI of SW data utilises a 1D forward response for the calculation of fundamental mode dispersion curves. A set of neighbouring 1D V_S models build up a pseudo 2D model, where each 1D V_S model corresponds to a dispersion curve. V_S, thickness and depth are the primary model parameters while Poisson's ratio and density are treated as fixed model parameters in the inversion (even though the possibility exists to let also these model parameters be optimised in the inversion process) since it has been shown that the impact on the final result from changes in Poisson's ratio and density are very small (Nazarian, 1984) compared to the impact from changes in V_s.

In Section 6.2.4, Section 6.6 and in Paper 3 it is shown that performing LCI instead of independent inversion of SW data significantly improves the final result.

5.3.3. Combined inversion

There is a difference between joint inversion and combined inversion that should be noted. As an example consider two datasets of different types collected at one site. Independent inversion of these datasets produces two results correlated only by their common origin, the ground conditions. The mutually constrained inversion, MCI, produces two dependent model results. In the inversion one or several corresponding model parameters, e.g. geometry, are coupled (but not fixed) to each other. The degree of coupling is determined by constants, the *mutual constraints*. Joint inversion implies that certain model parameters are shared so that only one model result is produced through the inversion. This is equivalent to the special case of combined inversion where the coupled model parameters are fixed to each other.

Examples of joint or combined inversion of different geophysical data are presented by e.g. Vozoff and Jupp (1975), Schmutz et al. (2000) and Hertrich and Yaramanci (2002). Mutually constrained inversion of transient electro magnetic data and DC resistivity data is presented by Christiansen et al. (2004). Examples of inversion combining seismic and DC resistivity methods include: underground vertical seismic profiling (VSP) and DC resistivity (Dobroka et al., 1991); CVES and seismic travel times (Gallardo and Meju, 2004) and refraction seismic and VES (Kis, 2002). In Hering et al. (1995) basic ideas for a joint inversion algorithm for VES and SW seismic data are presented, and in Misiek et al. (1997) two applications of this inversion algorithm are presented. Comina et al. (2002) also presents joint inversion of VES and SW data based on the work of Hering et al. (1995) and Misiek et al. (1997).

5.3.4. MCI of SW and CVES data

A fundamental assumption for combined inversion of VES and SW data is that the electrical and elastic interfaces are correlated, that is, the layer parameters have some kind of relationship.

The term mutually constrained inversion, MCI, is used to describe the process in which two or more datasets with different geophysical properties and/or sensitivities are inverted, such as SW data and CVES data. The MCI produces the same number of models as the number of individual soundings (VES or SW dispersion curves), with a correlation between the models established through equality constraints between corresponding parameters as outlined in Figure 19.

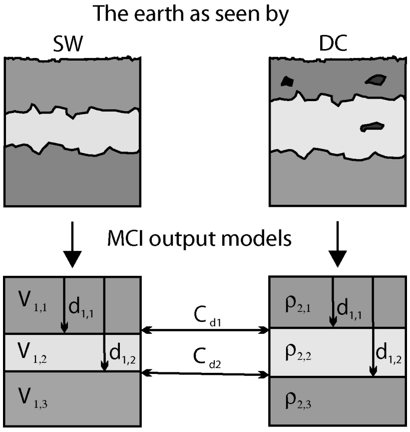

Figure 19 Schematic illustration of the MCI model concept, where different data types are connected via constraints on the model parameters. The resistivity model is described with layer resistivities, ρ, and depths to layer boundaries, d. The shear wave velocity model is described by layer velocities, V, and depths to layer boundaries, d. The models are connected to each other by constraints on depths to layer boundaries, Cd.

The MCI was originally developed to combine electromagnetic and DC resistivity data (Christiansen et al., 2004), but because of the soft bounds between the two models, the approach is quite robust and can be used in a general approach.

5.3.5. A priori data in inverse modelling

A priori information can be added to the dataset e.g. as depth to layers to constrain geometry. The use of lithological data from drillings as a priori information has been shown to be a successful approach (e.g. Jackson, 1979; Paper 1) and the use of a refraction seismic model is discussed in Paper 2 and in Section 6.3.2.

In the LCI each model parameter can be constrained. The strength of an a priori constraint should be based on the uncertainty of the a priori information. If a priori data agree with the geophysical data, the depth to layer interfaces in the geophysical model result will coincide with the a priori data. If, on the other hand, the a priori data and the geophysical data disagree this will be evident as a deviation of the model parameter from its given a priori value and/or as a high data misfit corresponding to that model.

The 2D smooth inversion algorithm allows for the inclusion of a priori information by constraining the resistivity in fixed regions or by loosening the smoothness constraints along layer boundaries. Information about depth to a layer boundary in one single position cannot be used for these constraints. If a number of data points describing a layer boundary are available, these could be used, but interpolation is then required.

5.4. Analysis of model resolution

For a parameterised inversion as in the LCI and MCI it is possible to perform a sensitivity analysis of the model parameters, which is helpful for evaluating the integrity of the model. This analysis is influenced by the sensitivity of the forward response, the amount and uncertainty of the geophysical data, the amount and uncertainty of the a priori information and the lateral and mutual constraints. The result is the a posterior covariance of the model parameters and from this the standard deviation of each model parameter is calculated. A more thorough description of the model parameter analysis is given in Appendix 1.

When the model parameters are represented as logarithms in the inversion (which is the case here), the analysis is presented as a standard deviation factor (STDF) on the parameters. The theoretical case of perfect resolution has a STDF=1. Well-resolved parameters are defined to have a STDF<1.2, which is approximately equivalent to an error of 20%. Moderately resolved parameters fall within 1.2<STDF<1.5, poorly resolved parameters 1.5<STDF<2, and unresolved parameters have a STDF>2. The analysis requires that the inverse problem is locally linear and that the inversion has converged, i.e. the data misfit is at least smaller than the expected observational error of the data.

For smooth inversion it is not possible to achieve an analysis of the model parameters uncertainties as described above. Other methods, that have not been used here, are available such as the area of investigation analysis presented by Oldenburg and Li (1999).

6. Examples from field investigations

6.1. Introduction

In this chapter a number of case studies are presented in order to show some examples of what can be achieved with the methods presented in this thesis. The common denominator for these projects is that they are all performed within, or parallel to, geotechnical site investigations. However, the target for the surveys, e.g. positioning of the bedrock level or an aquifer, can be common for almost any application.

6.2. Case study 1 – Resistivity and SW seismic surveys prior to railway trench construction

6.2.1. Introduction

In 1997 a government decision was made to build a tunnel under Malmö city to improve connections between the main Swedish railway system and an existing bridge and tunnel connecting Sweden with Denmark. This project, named the Citytunnel Project, consist of 17 kilometres of railway, of which 6 kilometres run in parallel tunnels under the city, two new stations one of them subterranean and an extension of the central station. Works began in 2004 and is expected to be completed in 2011 at a cost of about one billion Euros. Since 1995 major ground investigations have been performed. Resistivity measurements were made for the connection outside Malmö through the municipality of Lockarp where a railway trench of about 2 km length and 10 m depth will be excavated. The reference data from almost 50 auger drillings and a few cores were made for material classifications. From these, information about the lithology was extracted. The positions of these drillings are shown in Figure 20. Most of the auger and all the core and hammer drilling were performed before acquisition of the resistivity data.

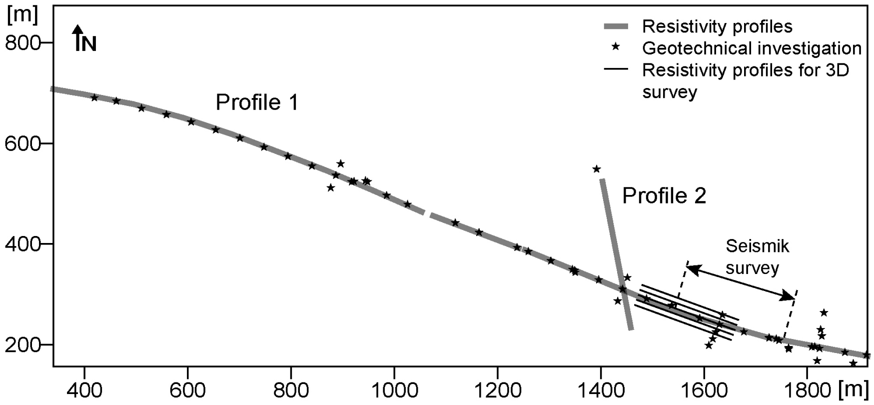

Figure 20 Map over the positions of the geophysical investigations and reference data in Lockarp.

Geology

The sedimentary geological environment consists of Quaternary deposits underlain by the Danian limestone. Based on geological background information and geotechnical investigations the geological and hydrogeological conceptual model for the Malmö area in Figure 21 was selected from Håkansson (1999). Based on experience from resistivity tomography and borehole logging in the surrounding area, the different geological units were assigned resistivity values. Five units as described in Table 2 and Figure 21 were identified.

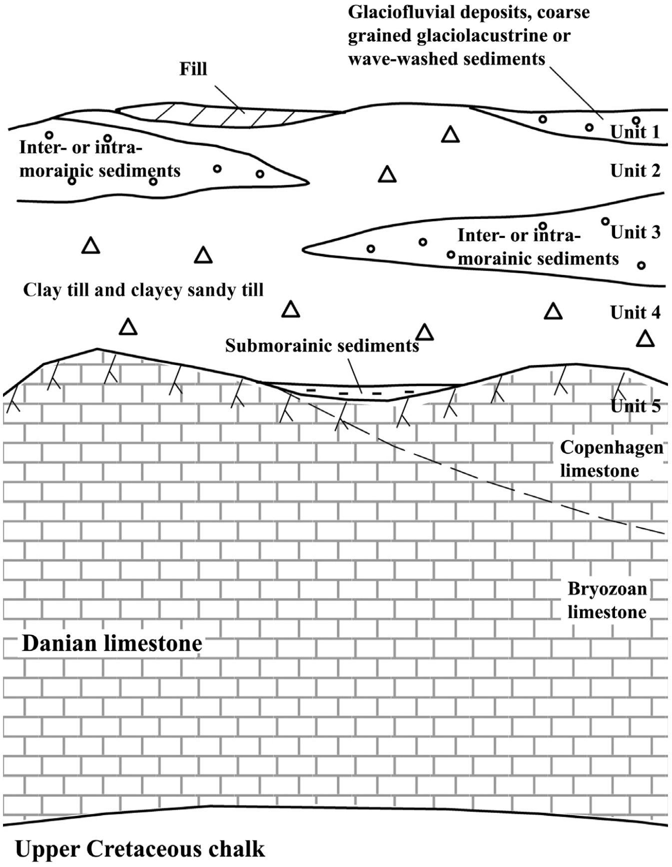

Figure 21 Generalised geological model. Five units are used to describe the geology and hydrogeology: Units 1 to 4 consist of Quaternary deposits and unit 5 of limestone (modified from Håkansson, 1999).

The possibility of a large hydraulic conductivity in the limestone, Unit 5, and the inter-morainic sediments, Unit 3, makes the groundwater situation an important issue for environmental review, design and construction. To understand the groundwater situation it is necessary to know how the main aquifers are distributed. Therefore, the main aim of this investigation was to determine the depth to limestone, soil composition, and soil layering. Resistivity imaging was a natural choice because the resistivity contrast between the different geological units is high.

Table 2 A summary of the geological units, their properties and possible resistivity intervals.

Unit	Material	Comment	Expected thickness [m]	Expected resistivity [Ωm]
1	Post- or late glacial sediments, mainly sand and silt.	Situated above the groundwater surface.	0.5 - 2	100 - 1000
2	Clay till, alternating with sand and silt layers.		2 - 5	20 – 100
3	Inter-morainic sediments, mainly sand and silt.	The unit is found only in parts of the area. It was deposited on the lower clay till, Unit 4.	0 – 3	50 – 400
4	Clay till, silty and often containing sand.		2 – 10	20 – 75
5	Danian limestone. Top meters often crushed and mixed with the lower clay till, Unit 4.	Undulates slightly and rises about 10 m from east to west in the field area. The groundwater pressure level in the limestone can be found at a few meters belowe the ground level.		100 - 600

Geophysical data collection

During the year 2000 approximately three kilometres of CVES resistivity measurements were collected (Figure 20). More resistivity data was collected in 2004 for an evaluation of the 3D smooth inversion (Figure 20). The seismic data was collected on two occasions (2001 and 2004) in order to evaluate the SW method.

The resistivity survey was performed with a multi-electrode ‘roll-along’ system with a minimum electrode distance of 2 m, a maximum electrode distance of 148 m and a combination of the Wenner and Schlumberger electrode configurations.

The seismic survey was performed with a 24-channel seismograph and 4.5 Hz geophones spaced 1 m apart with the geophones coupled to the ground by spikes or using a land-streamer as described in Section 4.2.1. The source was a sledgehammer impacting on a steel plate for better coupling. The aim was to collect a dataset that consists of a number of seismic soundings along a measuring line. The spacing of the soundings differs along the line but is in general 10 m. For most datasets 48 channels were used for analysis.

6.2.2. 2D smooth inversion and LCI of CVES data

In the 2D smooth inversion of the resistivity data the horizontal smoothness constraints were set four times stronger than the vertical, promoting horizontally elongated features. For the 2D-LCI a five-layer model was used.

Results and interpretation

Apparent resistivity data and inverted models from profiles 1 and 2 are shown in Figure 22 and Figure 23, respectively. Profile 1 follows the planned position of the railway trench and profile 2 is roughly perpendicular crossing at coordinate 1178 m. Profile 1 contains about 11 000 apparent resistivity data points and profile 2 contains about 3500 apparent resistivity data points.

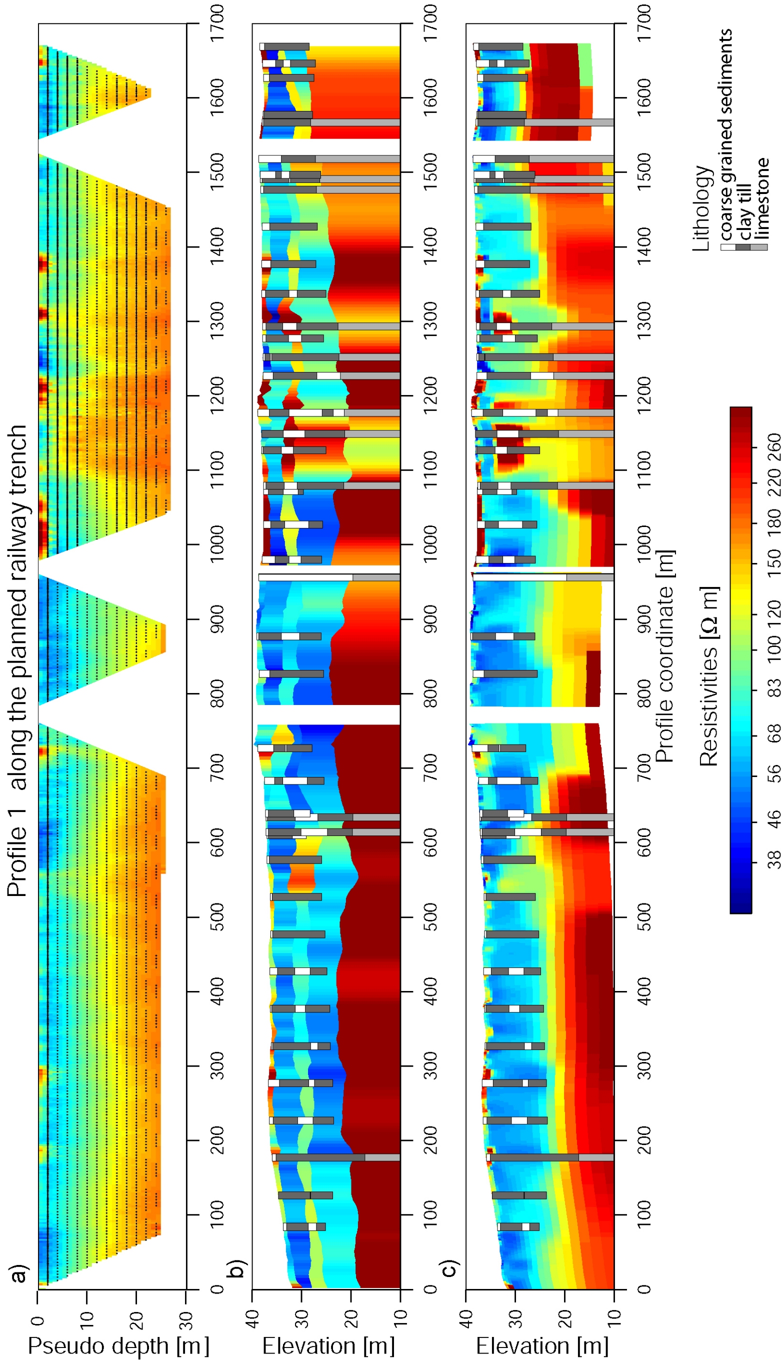

Figure 22 a) Pseudo section of apparent resistivity for profile 1, which follows the planned position of the railway trench. Resistivity model from: b) the 2D-LCI using lithological information from drill log data as a priori information in the inversion; c) the 2D smooth inversion.

A resistivity model with five layers agrees with the expected geological and geophysical model. The high-resistivity, bottom layer is interpreted as limestone (unit 5 in Figure 21). The thick, low-resistivity layer is interpreted as the two clay-tills (unit 2 and 4). The high-resistivity layer, sometimes present within the low-resistivity layer, is interpreted as inter-morainic sediments dividing the two clay-tills (unit 3). The high-resistivity features in the top of the profile are interpreted as post- or late-glacial sediments (unit 1).

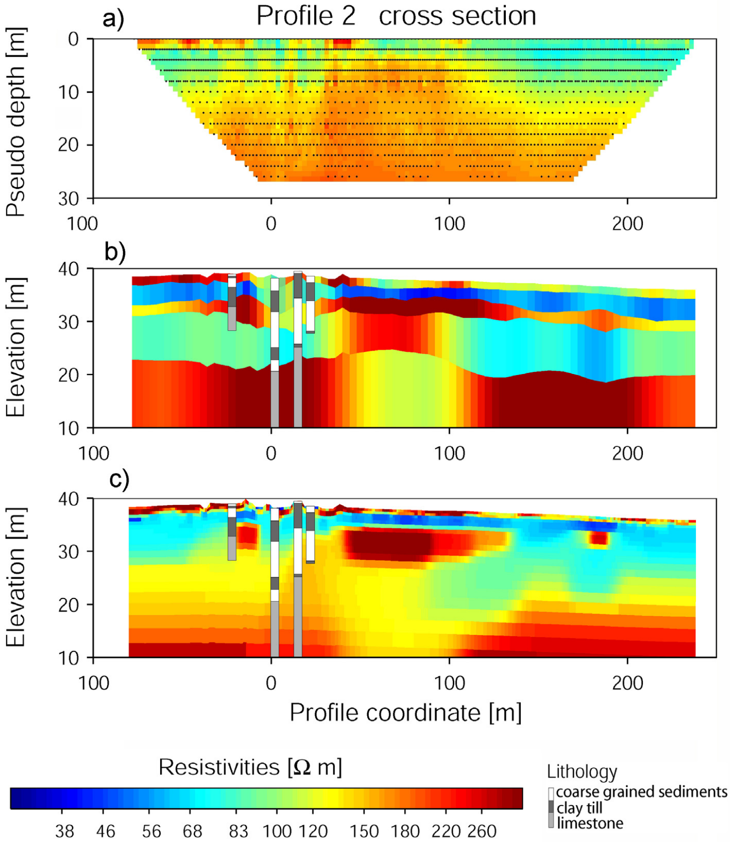

Figure 23 **a) Pseudo section of apparent resistivity for profile 2, which crosses profile 1 at coordinate 1178 m. Resistivity model from: b) the 2D-LCI using lithological information from drill log data as a priori information in the inversion; c) the 2D smooth inversion.**

The overall standard deviation of the residual error between measured data and model response is less than 2% for inversion results from the 2D smooth inversion and between 2% and 4% for the 2D-LCI. For individual data sets it can be as low as 0.3% indicating high quality data and a satisfying model fit.

Discussion

The 2D smooth resistivity models in Figure 22c and Figure 23c clearly show the presence of high-resistive inter-morainic sediments. Because of the smoothness constraint, it is difficult to detect sharp boundary interfaces and determine the depth to layer interfaces. The presence of Unit 3, inter-morainic sediments, seems to cause depressions in the depth to and resistivity of Unit 5, originating from high-resistive equivalence in Unit 3. This is a probable explanation to why the depth to Unit 5 does not always agree with depth to the limestone as found in the drill logs. From the 2D smooth resistivity models it is possible to determine the horizontal extent and depth to Unit 3, the inter-morainic sediments; however, it is difficult to determine a boundary for the bottom of the inter-morainic sediments and the top of the limestone.

The 2D-LCI models in Figure 22b and Figure 23b clearly describe the horizontal layer interfaces of the different geological units. The inter-morainic sediments (Unit 3) can be identified and their thickness properly assessed, much due to the presence of a priori information that solves equivalence problems. The a priori information added consists of layer boundaries as defined by drill log data with an assumed standard deviation of 12%. One example of where equivalence problems are reduced can be found in profile coordinate 1000-1360 m in profile 1 where there is a significant difference in the thickness and resistivity of layer 3 compared to the model from 2D smooth inversion.

Layer three throughout most of both profile 1 and 2 have significantly higher resistivity than what is the case for the corresponding areas of the 2D smooth inversion result. The result from 2D smooth inversion shows no evidence of high-resistive inter-morainic sediments (Unit 3) between the positions where it is most evident; however, in the result from 2D-LCI the resistivity of this layer is clearly higher than the resistivity of the clay tills.

From the interpretation of the geophysical investigations it is concluded that there exists one large structure of inter-morainic sediments between coordinates 1100 m and 1200 m on profile 1, which can also be seen around coordinate 0 m on profile 2. A few smaller units of inter-morainic sediments are also present. The limestone appears to rise about 10 m from east to west in profile 1. While the 2D-LCI models show good correlation to lithological interfaces, the 2D smooth inversion models show high horizontal resolution. The combined interpretation of these two models makes a good basis for detailed geological interpretation.

6.2.3. 3D smooth inversion of CVES data

The dataset consist of 5 parallel profiles of 200 m length with 10 m distance and 5 m in-line electrode separation. For the data presented in this Section the multiple gradient array configuration was used data collection. Figure 24 show the 2D and 3D inversion result for the this data. The residual average error from the separate 2D inversions is 0.9% and the error for the 3D inversion is 1.3%.

All models can be divided into a low-resistive upper part (<80 Ωm) and a high-resistive lower part (>100 Ωm) with the border just below 15 m depth. Through the low-resistive part of the model runs a 15-20 m wide high-resistive belt (>100 Ωm). This belt starts at about 3 m depth and continues down to about 6 m depth.

The geological interpretation of these models matches the geological expectations. The low-resistive upper part of the model is interpreted as the two clay tills, the high-resistive lower part of the model is interpreted as the limestone and the high-resistive belt is interpreted as the inter-morainic sediments.

The 3D inversion results show a slightly larger contrast between the low-resistive part and the high-resistive belt. The 2D inversion results show a decrease in resistivity in the part of the model below the high-resistive belt. In previous studies of this area (see Section 6.2.2) it has been shown that this is caused by high-resistive equivalence and that there is no correlation with the undulation of the limestone level. The effect on 2D inversion results is quite strong and it is reduced significantly by the 3D inversion.

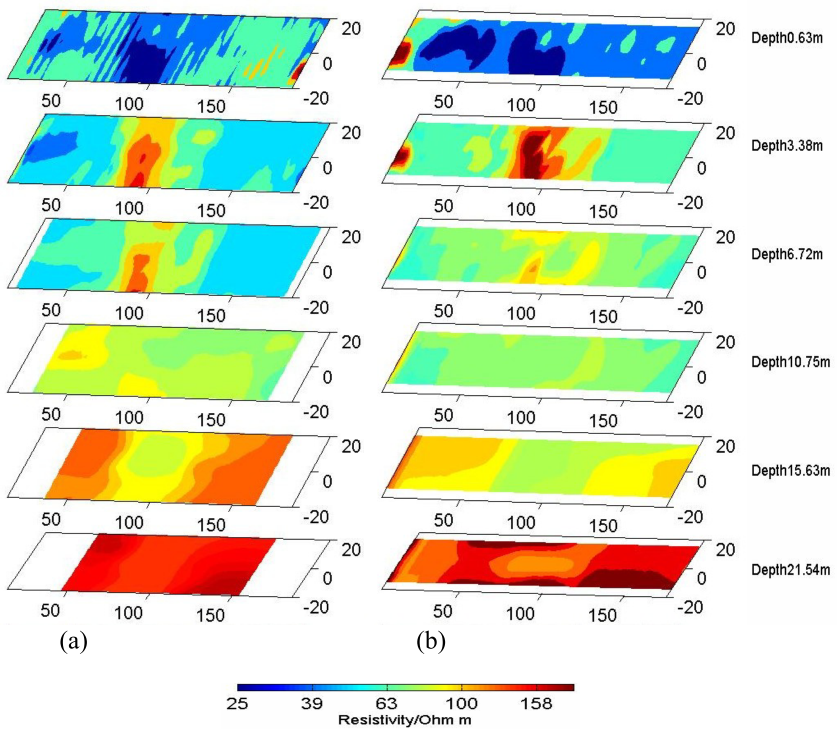

(a) (b)

Figure 24 Inversion results from gradient array dataset collected in Lockarp, Sweden: (a) 2D L_1 norm; (b) 3D L_1 norm.

6.2.4. LCI and MCI of SW and CVES data

The processed SW seismic dataset contains 21 separate dispersion curves with different profile coordinates. The lowest frequency of the fundamental mode varies from 9-22 Hz with an average of 11.5 Hz and the upper limit of the frequency varies from 13-55 Hz with an average of 25 Hz. A standard deviation of 5% was assumed for all dispersion data. This figure is a rough estimate of the uncertainty of the experimental data; the same standard deviation that is used for resistivity data. O'Neill (2003) shows that the standard deviation of SW data is frequency dependent with smaller errors at high frequencies and larger errors at low frequencies, compared to what is assumed here. To estimate the standard deviation of SW data it is necessary to collect more than one dataset, which was not done for any of the data presented here.

In this case study, the two different data sets have very different sampling density. They are combined as shown schematically in Figure 25a. Every 1D sounding has a corresponding 1D model. The constraints between the models are based on the following:

Every DC model is constrained to its nearest neighbouring DC models in both directions (Figure 25b). Similarly, every SW model is constrained to its neighbouring models on each side (Figure 25c). The neighbouring SW and the DC models are then constrained to each other, as illustrated in Figure 25d.

All lateral constraints, C_l, are scaled according to the model separation, d, using

$$C_l = C_r \sqrt{\frac{d}{d_r}}$$

where C_r is a reference constraint for a reference distance, d_r. Therefore if the distance between two constrained models is twice that of the reference distance, the constraint values between the two models are multiplied by a factor of $\sqrt{2}$, which gives a less tight constraint. If the distance is smaller than d_r the reference distance, C_l, is set to C_r. The reference distance is in this case twice the minimum electrode distance i.e. $C_r = 4$ m. The mutual constraints are scaled in the same way.

Combining the constraints described above yields the full set of constraints as sketched in Figure 25.

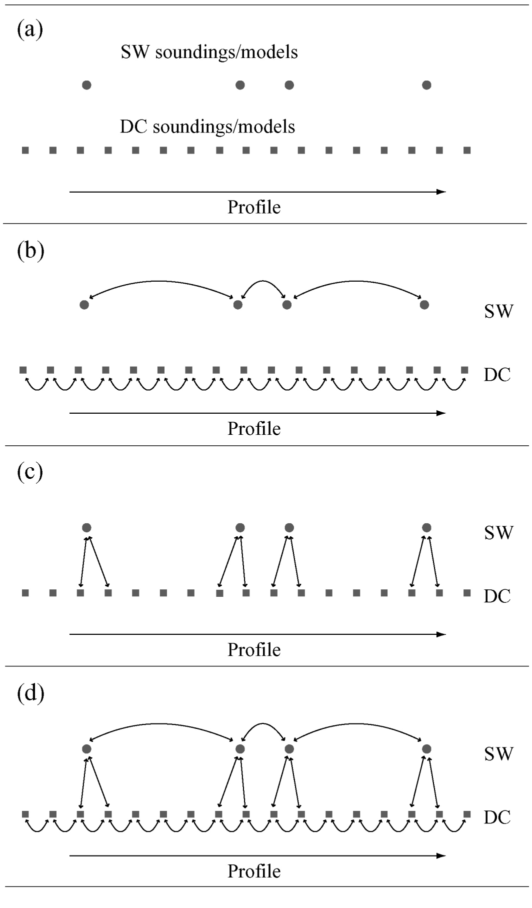

Figure 25 Schematic illustration of lateral and mutual model constraints indicated by arrows. a) A simplified sketch of the distribution of SW and DC soundings and their corresponding models. b) Lateral constraints internally between the DC and internally between the SW are applied. c) Mutual constraints between the DC and SW are applied. d) A summary of the total set of constraints.

For the seismic LCI model four layers are used. With a three-layer model it was not possible to achieve a satisfyingly low data misfit and a five-layer model was found to be poorly resolved. For the resistivity model five layers are used. For the MCI it is necessary to have an equal number of model parameters for each 1D-model to constrain between the resistivity and velocity models respectively. Thus, an equal number of layers in the resistivity and velocity models are required. Here, both the resistivity and velocity models have five layers. However, the seismic model is effectively re-parameterised to four layers (which is the number of layers used for the independent inversion and LCI) by very tightly constraining the velocities between layers three and four. In practice, this regularisation is achieved with a vertical constraint, as described in Appendix 1. Layer resistivity and velocity is allowed to vary approximately 10% between neighbouring models and interface depths by at least +/- 1 m over a distance of 4 m.

In all modelling performed in this study Poisson's ratio equals 0.4 and the density equals 2 g/cm^3. These figures are based on results from geotechnical investigations performed in the area around Malmö.

Results and interpretation from independent inversion and LCI

Figure 26(a) presents the resulting V_s models after independent inversion on all SW data with the analysis of the model parameters STDF in Figure 26b and the normalised data misfits in Figure 26c. The normalised data misfit is 1 if the data is fit at the assumed observational error of 5%. The model in Figure 26a shows V_s of the bottom layer ranging from 800-1800 m/s and depths to this layer ranging from 8-21 m. Figure 26b shows that very few model parameters are resolved. The normalised data misfit in Figure 26c is around 0.5 for all soundings, which is well below the assumed observational error.

Figure 26d presents the resulting V_s model after LCI on all SW data, Figure 26e presents the accompanying analysis of model parameters STDF and Figure 26f presents the normalised data misfit for each dataset. In Figure 26d lithology from drill logs has been added for comparison. In the drill logs, white represents sorted sediments, dark grey represents clay till and light grey represents limestone. The model in Figure 26d shows V_s of the bottom layer ranging from 850-1650 m/s and depths to this layer ranging from 10-17 m. Most model parameters, including all velocities and depths, are well-resolved or resolved. Only thicknesses are generally poorly resolved or unresolved. The normalised data misfit is only slightly higher than for the independent inversion and still well below the observational error.

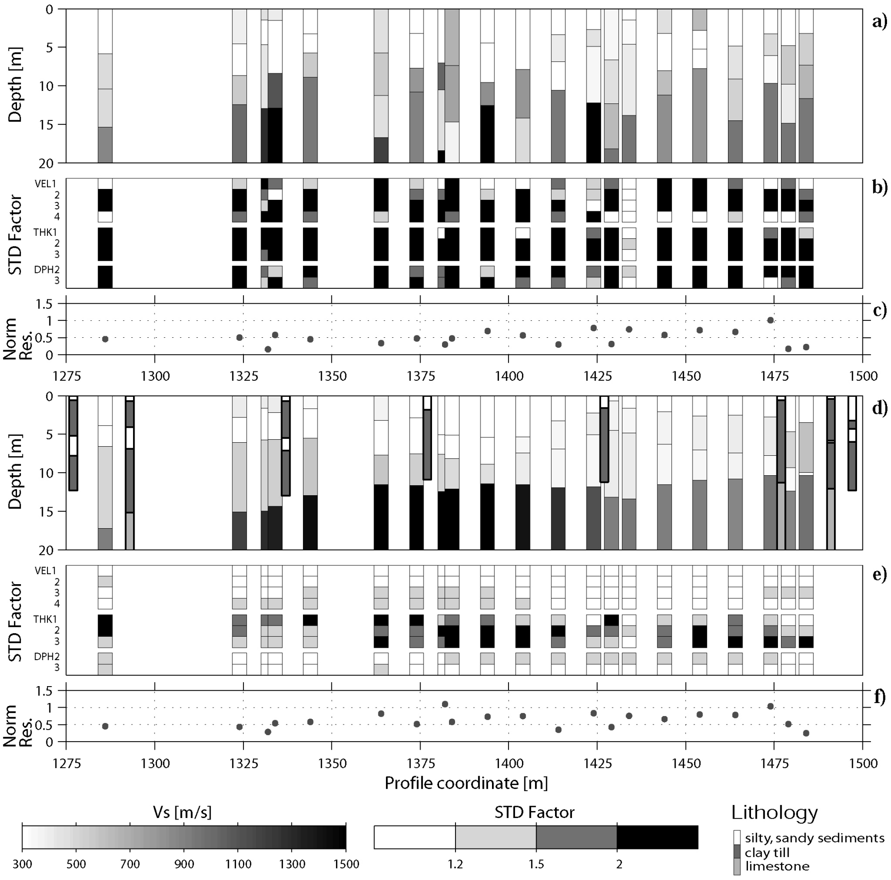

Figure 26 **Result from inversion of SW data. a) Vs model from independent inversion on all SW data. b) Model resolution analysis of the model in (a). c) Normalised data misfit presented for each dataset. d) LCI on all SW data. e) model resolution analysis of the model in (d). f) Normalised data misfit presented for each dataset. In the LCI model lithology from drill logs is present. In the drill logs, white represents sorted sediments, dark grey represents clay till and light grey represents limestone.**

The effect from performing LCI instead of independent inversion can be seen in the model in Figure 26d. The model parameters are now much more consistent along the measuring profile. Figure 26e shows the STDF factors of the model in Figure 26d. When comparing with the result for independent inversion in Figure 26b it can be seen that in particular velocities and depths are improved.

The alternative ways to improve model resolution while employing a single surface wave mode would be to use a model with fewer layers or to use many more layers with fixed thickness and soft vertical constraints between layer velocities. The first alternative would not fit the data for most dispersion curves and hence only be useful for a very small part of the data. The second alternative would result in a smooth model without physical resemblance to the sedimentary layered geology that is present. Of course, incorporating higher modes and/or broader frequency ranges would also assist, but this study is restricted to the fundamental mode only.

Results and interpretation from MCI

The information from the CVES data is combined with the SW data to investigate the possibility to improve the V_S-models by adding more information about the thickness of layers and depths to interfaces. Figure 27a presents the resulting V_S and resistivity model after MCI on all SW and CVES data. Figure 27b presents the resolution analysis of the seismic model parameters and Figure 27c presents the normalised data misfit for each SW dataset. Since there is about 5-10 times more CVES resistivity data than SW data, the impact of the seismic data on the resistivity model is very small. The resistivity model presented here has been verified earlier (Paper 1) and will not be analysed. The V_s model in Figure 27a shows V_s ranging from 800-1450 m/s and depths to this layer ranging from 9.5-13.5 m. Most model parameters, including all velocities, depths and most thicknesses are well-resolved or resolved. The normalised data misfit corresponding to the SW data is only slightly higher than that for the independent inversion and actually lower than that for the LCI on SW data alone. It is also well below the observational error.

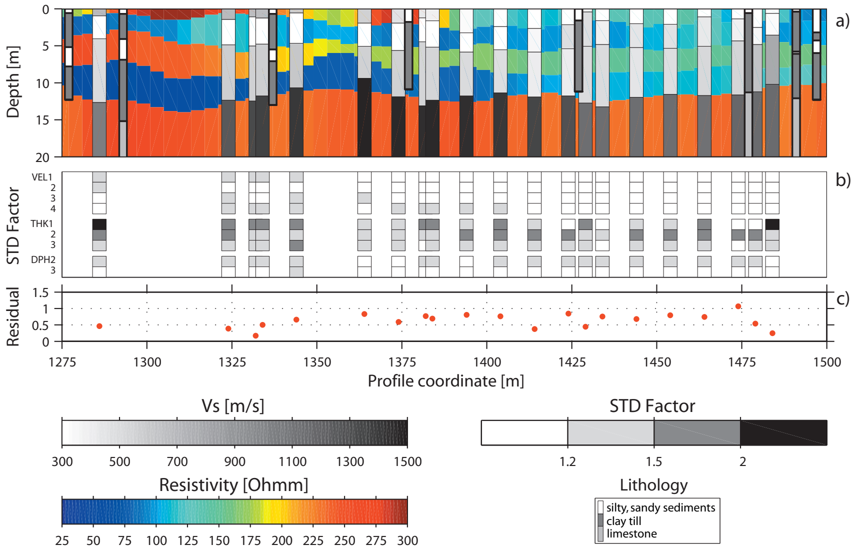

Figure 27 Results from combined inversion of SW and CVES data. a) Resistivity (color) and Vs (grayscale) model after MCI. b) Model resolution analysis of the Vs model in (a). c) Normalised data misfit presented for each dataset. In the LCI model lithology from drill logs is present. In the drill logs, white represents sorted sediments, dark grey represents clay till and light grey represents limestone.

The main difference between the V_s model in Figure 27a and the model in Figure 26d is the improvement of the STDF of the thickness and the variation of model parameters. Information on thickness of the high-resistivity top layer found in the CVES profile helps constrain the shear wave velocity of that layer. Due to the additional information on depths to layer interfaces the velocity of the bottom layer improves. Moreover, the geophysically interpreted interfaces in Figure 27a correlate better with lithological interfaces identified in drill logs than the one in Figure 26d.

Figure 28 presents the measured data and model response for the model at profile coordinate 1429 m. For this dataset the root mean square error is 1.6% for independent inversion, 2.1% for LCI and 2.2 % for MCI. Combined, these model responses fit well within the expected observational error of 5%. The largest misfit occurs at the lowest frequency. At frequencies above 15 Hz the misfit seems to decrease with frequency. The model response from LCI and MCI agrees well and both differ from the model response from independent inversion. This is due to influence from neighbouring models through the lateral and mutual constraints. Even though the model resolution is improved in this case, it is not the new improved model that is the main benefit from performing MCI, but rather the knowledge that the resistivity model and the seismic model actually correspond geometrically. This information is important and can be used in the geological and geotechnical interpretation of other resistivity data in this area.

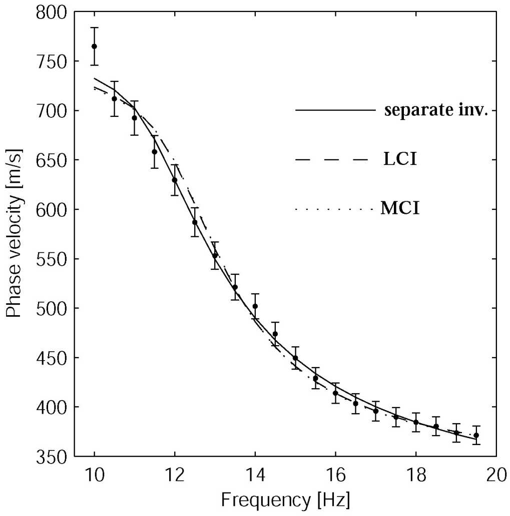

Figure 28 **Observed data and model responses from the seismic model at profile coordinate 1429 m.**

6.3. Case study 2 – Resistivity and refraction seismic survey in slope stability investigation

6.3.1. Introduction

In May 1997 a slope failure caused a 200 m by 60 m area of clay deposits to slide into the Trosa River valley, in Vagnhärad south of Stockholm, Sweden, causing severe damage to residential houses and infrastructure, as shown in Figure 29. The slope failure was caused by an increase of the pore-water pressure in the clay, due to increased water pressure in the sandy and silty till below the clay. Many geotechnical tests and soundings were performed in the area in order to investigate properties of the clay, but no reliable information about the surface level of the bedrock was obtained since this was not the scope of those investigations.

Figure 29 A photograph of a residential area in Vagnhärad after the slope failure within the Trosa River valley in 1997 (Andersson et al., 1998).

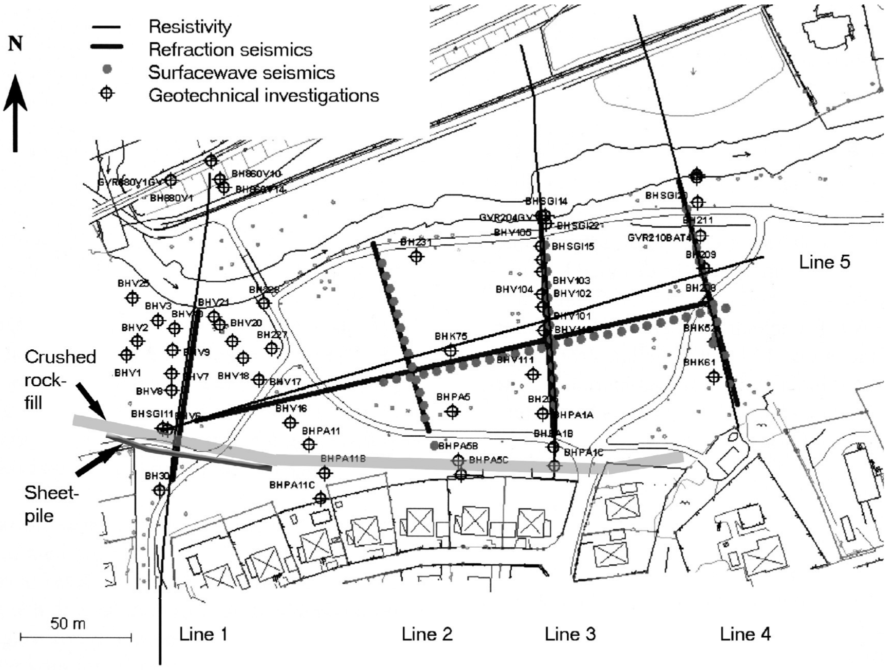

Figure 30 Detailed map of the investigated area showing location of the geophysical survey profile lines.

In a project funded by the Swedish Rescue Agency, Engineering Geology at Lund University and the Swedish Geotechnical Institute the applicability of geophysical methods for slope stability investigations was evaluated. The main goal of the geophysical surveys was to determine the geometry of the bedrock and sediments along the valley slopes, since geometry is an important property in stability calculations. The report from this project (Dahlin et al., 2001) shows that a combination of CVES resistivity imaging and refraction seismic surveying is a successful approach. Figure 30 shows the position of the river, roads, remaining houses and geophysical survey profile lines.

Geology

The geological setting is a depression in the crystalline bedrock filled with mainly varved glacial clay. Gradual erosion in and around the Trosa River, which runs through the valley, and small landslides in the river have reduced the thickness of the clay deposits and increased the steepness of the valley slopes. The geological model consists of four units:

1. A surface layer of fill material from human activities. This layer is generally above the groundwater level.
2. Several meters of unconsolidated clay. Geotechnical investigations found layer thicknesses of up to 14 m. The sediments are thin at the top of the valley walls and increase in thickness towards the bottom of the valley.
3. Sandy and silty till with a thickness up to a few meters. This unit is only sometimes found under the clay; when present this layer acts as a confined aquifer.
4. Crystalline bedrock.

Figure 31 shows a principal sketch of the geological setting in the valley.

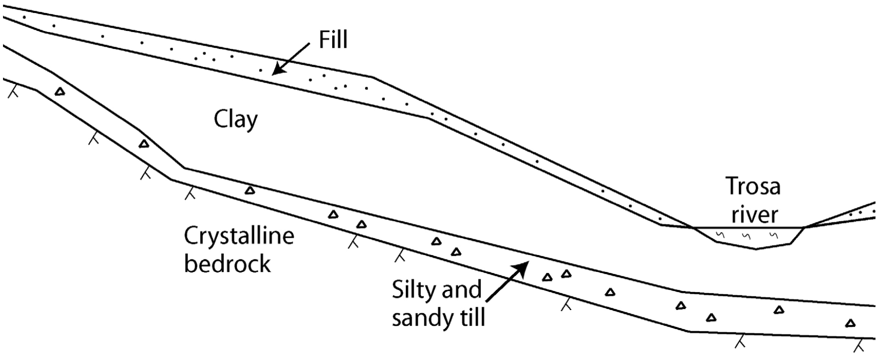

Figure 31 Principal sketch of the geological setting in the investigated area. The section is perpendicular to the valley. A thick clay layer is partially covered by fill material from human activities and underlain by silty, sandy till and crystalline bedrock.

Geophysical data collection

The resistivity survey was performed as CVES measurements with a multi-electrode ‘roll-along’ system. Minimum electrode distance was 2 m, maximum electrode distance 148 m and the electrode configuration was a combination of Wenner and Schlumberger. About 550 m of seismic refraction profiling was performed with a 24-channel seismograph, employing 10 Hz vertical geophones at a station distance of 2 m, and an explosive source.

6.3.2. 2D smooth inversion and 2D-LCI of CVES data

Results and interpretation from seismic refraction surveys

Traditionally refraction seismic data, in the form of first arrivals, are used to analytically calculate a model of V_P. The velocity at which these waves travel depends on different material parameters such as density, porosity, water content, type of rock material and degree of weathering. Typical velocities for compressional, P-waves in different geological materials are presented in Figure 32.

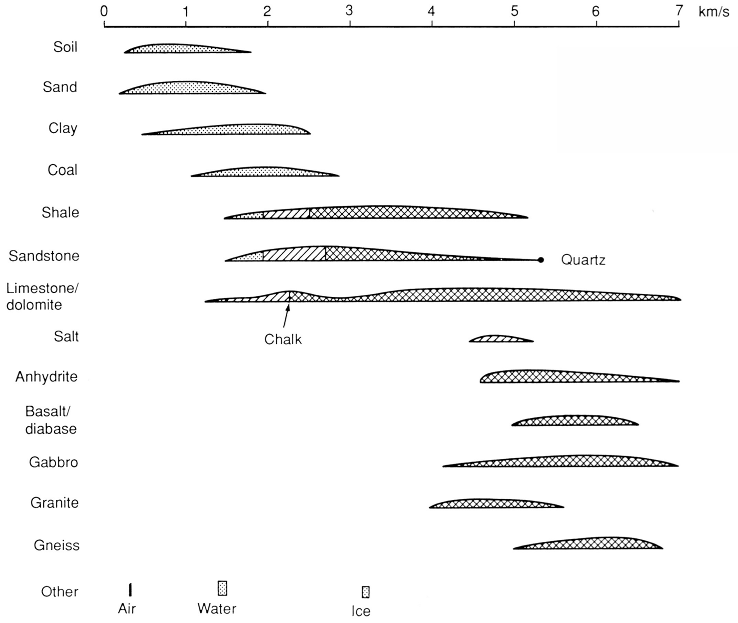

Figure 32 Typical velocities for P waves in geological materials (Milsom, 1996).

Three layers are identified in the compressional wave velocity model (Figure 33): the first layer is less than 3 m thick with velocities varying between 330 m/s and 950 m/s; the second layer has a thickness between 5 m and 17 m and velocities varying between 1040 m/s and 1700 m/s; and the third layer has velocities varying between 3900 m/s and 5100 m/s.

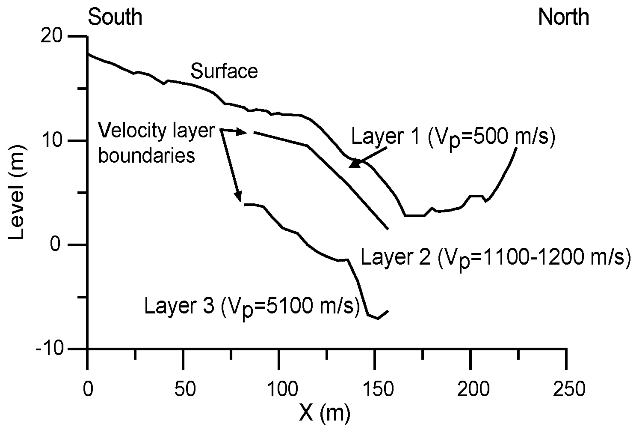

Figure 33 A three-layer velocity model interpreted from the seismic refraction data along profile 1.

The top layer has velocities consistent with dry soil material, which is most likely the fill material, Unit 1. The velocities of the second layer are interpreted as saturated clay and/or sandy and silty till, Unit 2 and 3. These units are not possible to differentiate in the refraction seismic velocity model. The third layer has velocities that are interpreted as the bedrock, Unit 4.

Results and interpretation from CVES data

Apparent resistivity data and the resulting 2D-LCI, with and without a priori information, and 2D smooth inversion models for profiles 1, 3 and 5 are shown in Figure 34, Figure 35 and Figure 36, respectively. The residual errors after inversion are quite low, between 1% and 3%. Four layers were used for the 2D-LCI. In all profiles three resistivity units are clearly defined in the models resulting from the 2D-LCI without a priori information (b) and the 2D smooth inversion (d): a thin, high-resistivity layer in the top of the section; a low-resistivity layer with a thickness between 0 to 10 m; and a high-resistivity layer in the bottom. The high-resistivity layer in the top is interpreted as the dry fill material, Unit 1; the low-resistivity layer is interpreted as clay, Unit 2; and the high-resistivities in the bottom of the sections is interpreted as the sandy and silty till, Unit 3, or the bedrock, Unit 4. In these resistivity models it is not possible to clearly separate the sandy and silty till (Unit 3) and the bedrock (Unit 4).

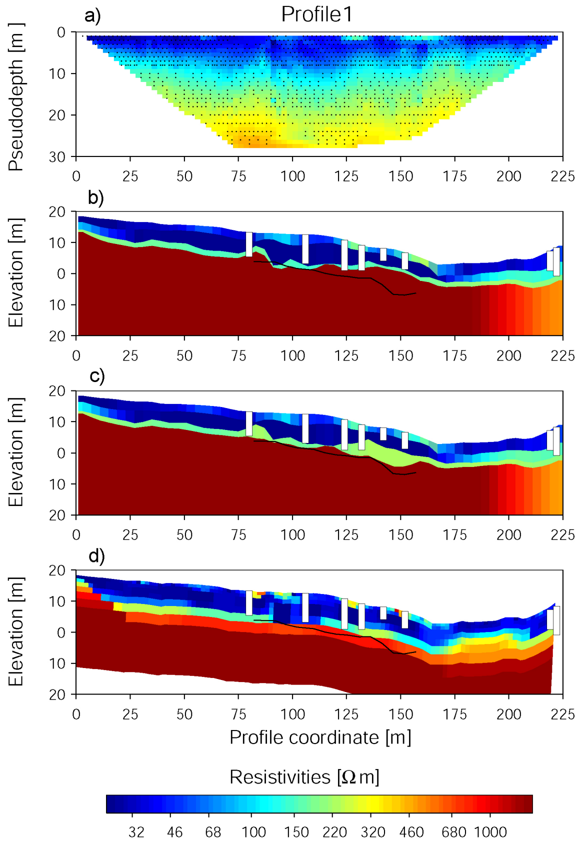

Figure 34 a) Apparent resistivity pseudo sections for profile 1. Resistivity models from: b) 2D-LCI; c) 2D-LCI with layer interfaces from the refraction seismic model as a priori information; d) 2D smooth inversion.

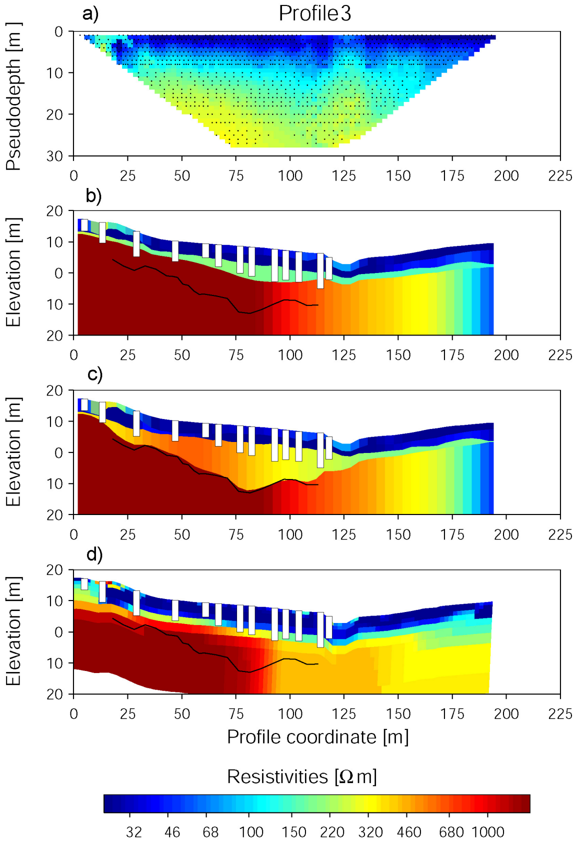

Figure 35 **a) Apparent resistivity pseudo sections for profile 3. Resistivity models from: b) 2D-LCI; c) 2D-LCI with layer interfaces from the refraction seismic model as a priori information; d) 2D smooth inversion.**

A priori information consisting of the depth to the seismic bedrock refractors was added with a 10% standard deviation. When the seismic bedrock refractors are used as a priori information, four resistivity units are defined in the 2D-LCI models. In some positions, e.g. along profile coordinates 125 to 150 m in Figure 34a, a fourth layer appears that has intermediate resistivities between the low-resistivity layer and the high-resistivity bottom layer, and it is interpreted as sandy and silty till, Unit 3.

As part of the geotechnical investigation, data was acquired to define the properties of the clay. The depth to bedrock was not determined at all or not determined with sufficient accuracy; therefore, this information is only used when interpreting the resistivity models, as an indication of the minimum depth to bedrock.

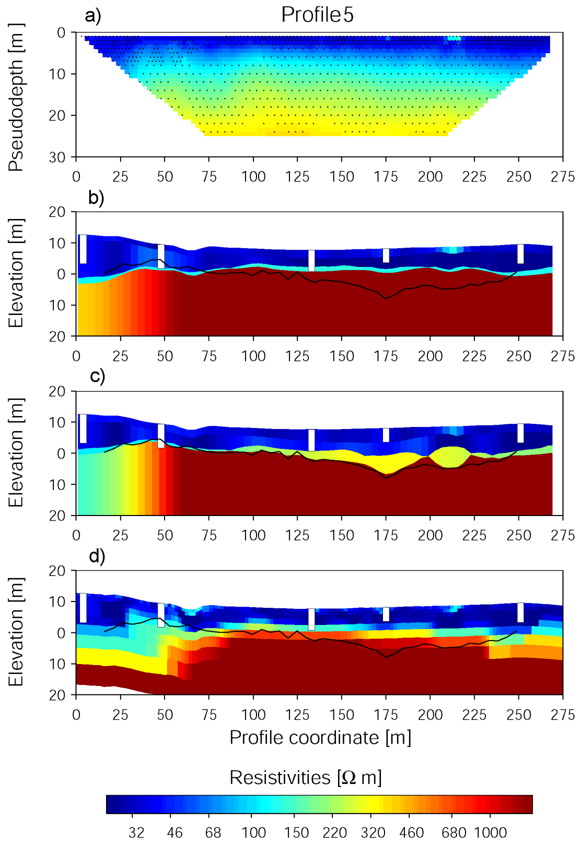

Figure 36 **a) Apparent resistivity pseudo sections for profile 5. Resistivity models from: b) 2D-LCI; c) 2D-LCI with layer interfaces from the refraction seismic model as a priori information; d) 2D smooth inversion.**

Discussion

The thickness and resistivity of layer 3 are poorly resolved. In the 2D-LCI without a priori data (Figure 34b, Figure 35b and Figure 36b) this layer is generally thin and has a resistivity that is similar to the low-resistivity second layer. When the seismic refraction model is used as a priori information the thickness of layer 3 changes completely and follows that of the seismic model. With a change in thickness, the resistivities of layers 3 and 4 also change. There are clearly equivalence problems in the third layer; the data misfit does not increase when a priori data is used.

The geometry of the clay, the sandy and silty till and the bedrock surface units can be derived from these geophysical models. From the 2D-LCI models with a priori information, the thickness of the third layer can be quantified which was one of the aims of the investigation. It is important to recognise that the depth to the bottom of this layer is resolved with the seismic data; hence, the certainty of the resistivity model is dependent on the certainty of the seismic model. Using the seismic model as a priori data for the resistivity imaging, it is possible to delineate the sand and silt till, Unit 3, and to estimate its resistivity.

6.4. Case study 3 – 3D resistivity survey for bedrock mapping

6.4.1. Introduction

The data in this case study was collected for a bedrock depth investigation prior to the design of a sludge deposit dam for a paper pulp industry in southern Sweden. The geological setting is described by a crystalline gneissic bedrock overlain by Quaternary deposits. The Quaternary deposits consist of till overlain by silt and clay. Figure 37 shows a map of the area with the position of the resistivity profiles and topography.

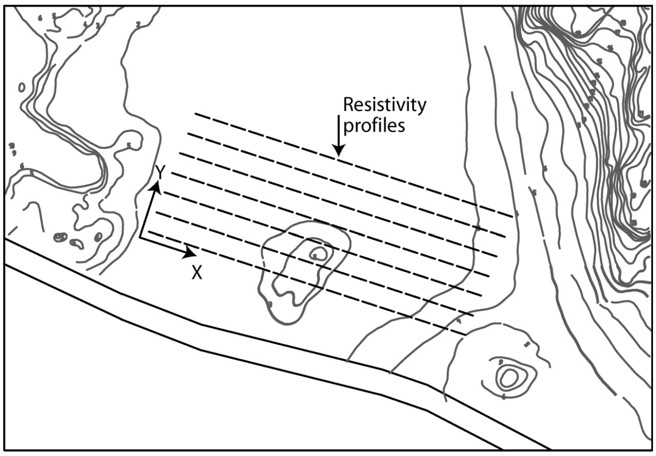

Figure 37 Map of the investigated area showing resistivity profiles and topography.

At one side of the area (between x=60 to 100 m and y=0 to 30 m, see Figure 38 for coordinates) an outcrop of bedrock is present on the surface. The height of the outcrop is maximum 2 m in an otherwise fairly flat area. On both sides, in the x-direction, the valley sides are present in the topography and bedrock is cropping out, the soil thickness is therefore expected to decrease in these directions. The valley continues towards increasing y-coordinate.

6.4.2. 3D smooth inversion of CVES data

The dataset consist of 7 parallel profiles of 160 m length with 10 m separation and 5 m in-line electrode separation. The multiple gradient array configuration was used and Figure 38 show the 2D and 3D inversion results.

The residual average error from the separate 2D inversions is 7.4% and the error for the 3D inversion is 7.7%. One feature with very high resistivity (>10000 Ωm) is evident in the upper and middle part of both the 2D and 3D inversion result. Except for this feature the resistivity down to about 13 m is low (<100 Ωm). Below this the resistivities are still quite low (from less then 100 to about 2000 Ωm). There is a significant difference between the result from 2D inversion and 3D inversion. The 3D inversion result show only high resistivities below a depth of about 15 m while The 2D inversion result show some very low resistive features at great depths. These features are artifacts from 3D effects in the 2D inversion. It is clear that in this case

3D measurements and a 3D inversion is necessary in order to get an accurate estimate of the resistivity distribution.

The high-resistivities in the deeper parts of the models are interpreted as crystalline rock. The comparatively high resistivities in the upper part of the models (corresponding to the position of the outcrop) are interpreted as crystalline rock that is less saturated. The low resistive features are interpreted as clay or silt.

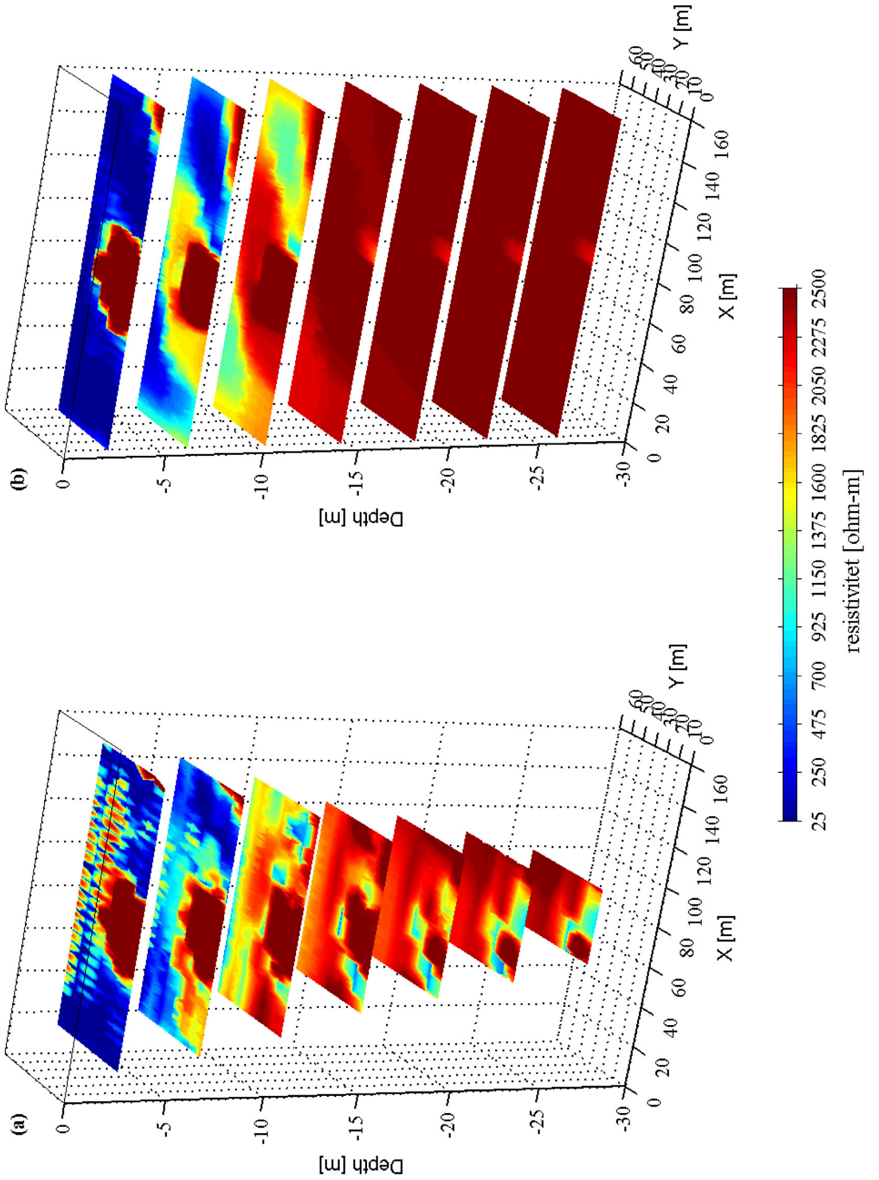

Figure 38 Inversion results from a gradient array dataset collected in Mörrum, Sweden. a) 2D L_1 norm. b) 3D L_1 norm.

6.5. Case study 4 – Urban resistivity measurements

6.5.1. Introduction

This case study was performed parallel to the site investigations included in the Citytunnel Project (see Section 6.2). A general geological description for central Malmö is similar to that for Lockarp that was given in Section 6.2.1 and Figure 21, with Quaternary glacial deposits underlain by limestone of Tertiary age dominating the geology. The maximum depth of the Quaternary deposits in the test area is about 5 m. The investigations include a large number of core drillings, geophysical borehole logging, reflection seismics and groundwater investigations. With the drilling and logging data as reference, an attempt was made to evaluate profiling resistivity measurements as a site investigation method in an urban environment. The test area is about 300×300 square meters (see Figure 39). During June 1999 to February 2000 a pilot study was performed with 15 resistivity profiles of between 100 and 300 meters length. The resistivity campaign was divided into two parts as shown in Figure 39. The first part aimed to cover as much of the area as possible. The quality of that resistivity data was evaluated, mainly with regard to problems originating from conductive manmade objects in galvanic contact with the ground. The second part aimed to map areas where no, or little, effects from these problems could be expected. Resistivity results with no or only few signs of negative effects from disturbances have then been used to map the surface of the limestone.

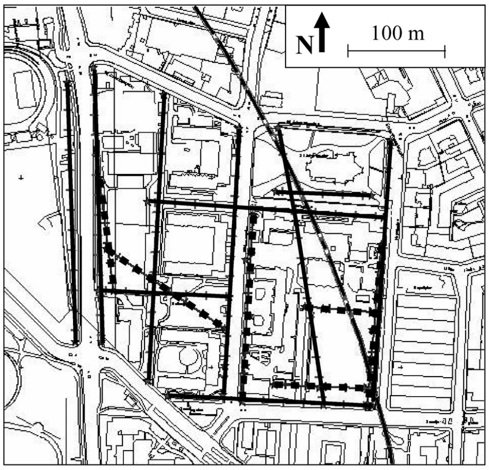

Figure 39 **Map of the study area showing position of resistivity investigations (Solid lines: campaign one; dashed lines: campaign two) and the planned position of the tunnel.**

The electrode configurations used were Wenner-Schlumberger and dipole-dipole. The maximum depth penetration was about 45 m but many profiles were made with smaller depth penetration to avoid coupling to man-made conductive objects.

6.5.2. 2D smooth inversion of CVES data

The discussion in Section 4.1.2 on how to deal with noise in apparent resistivity data springs from this case study. The inverted resistivity sections presented in Figure 12 and Figure 13 are two of the profiles measured in this area.

Quality control

In order to assess the quality of the inverted datasets the resistivity results were first compared with the depth to bedrock as interpreted from drilling data. An interpolated surface of the 70 Ωm boundary (see Figure 40) in all profiles was compared to an interpolated surface of depth to bedrock. The amount of resistivity data was set to the same as for the drilling dataset by extracting resistivity data in positions where drilling data exist.

The comparison is shown as interpolated surfaces for drilling data and resistivity data (Figure 41). When comparing these models some of the main topographic structures can be recognised. The absolute values do however differ because no calibration of the resistivity model was performed. The difference between the limestone surface level observed in the reference model and in the initial resistivity model is between 0 m and 3 m with an average of 1.5 m and a standard deviation of 0.95 m. This deviation is quite large but the resistivity level observed here does not only depend on the true level of the limestone surface but also on local variations in the resistivity of the materials. These variations are related to the properties of the limestone and the overlying glacial deposits.

It can be concluded that, despite some negative effects in the resistivity data from manmade conductive objects, it is possible to produce a model describing the relative variations in level of limestone surface. This model compares well with the drilling data.

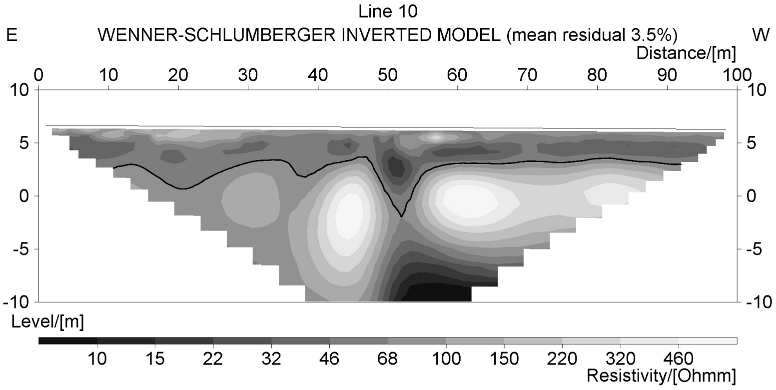

Figure 40 Example on inverted resistivity profile and how the border between the upper low resistive and the underlying high resistive layer has been interpreted.

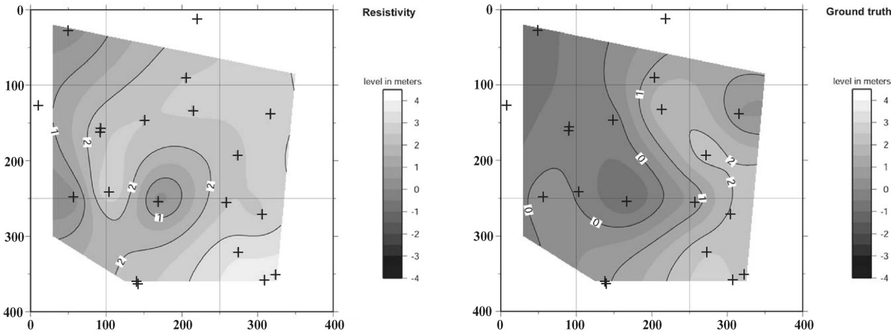

Figure 41 Comparison between interpolated surface from resistivity data, left, and drilling data, right. The density of the resistivity data is the same as that of the drilling data.

6.5.3. Rock-surface models

After verifying the quality of the resistivity data the information from the drilling and logging data was again interpreted with the resistivity results. This suggested a detailed model of the limestone surface. For the calibration, the lithological information from the drilling data was divided into three groups, Quaternary glacial deposits (clay till), crushed limestone mixed with clay till and intact limestone. The results from the new interpretation are two models of the limestone surface describing an upper and a lower boundary between which the surface of intact limestone is likely to be found (Figure 42).

When comparing the limestone surface model in Figure 42a with the reference model in Figure 41b a better description of the depth to the limestone, as shown in Figure 41a becomes evident. This is due to the depth calibration of the resistivity results that comes out of the combined interpretation. The model in Figure 42a is also more detailed than the models in Figure 41. The interpretation reveals that the level of the limestone surface in parts of the area seems to go deeper than what is evident from the models in Figure 41. This is partially due to the fact that the model from drilling data in Figure 41 is an interpretation of the material boundary between glacial deposits and limestone, and not between crushed and intact limestone. However, it also implies that local troughs in the limestone might have been overseen in the drilling campaign.

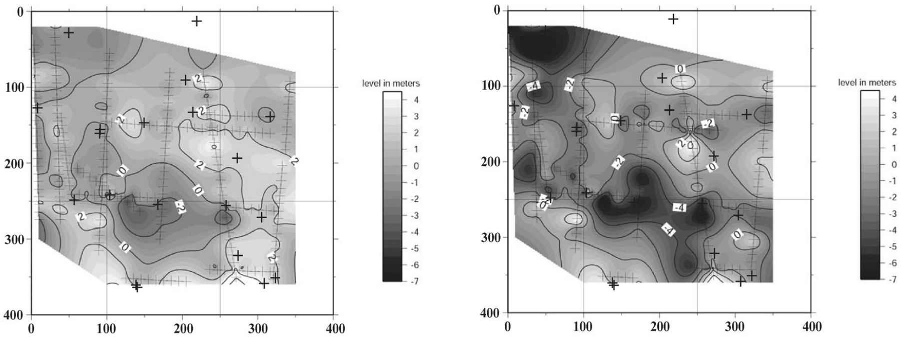

Figure 42 a (left) Model of boundary between clay till and limestone. b (right) Model of border between high quality and low quality limestone.

The main aim of the presented resistivity surveys was to describe the topography of the limestone. The combined interpretation of drilling data and resistivity results gave a more detailed model of the upper and lower boundaries in between which the surface of intact limestone is likely to be found, a result that can be very valuable at all stages in the site investigation process.

6.6. Case study 5 – Surface wave analysis and LCI of reflection seismic data

6.6.1. Introduction

The inter-regional EU project Sismovalp (Seismic hazard and alpine valley response analysis) aims to improve the knowledge of seismic characterisation of alpine areas. One of the chosen test sites is the urban area of Torre Pellice in the Pellice valley, Italy.

The data for this case study was collected as reflection seismic data perpendicular to the valley. An example of an seismogram is presented in Figure 43. Data collection was made with 10 Hz geophones, 2 m geophone distance, 240 active channels and without any attempt to reduce ground-roll in the acquisition. Data was collected for shots positioned at a 6 m distance through the array. An accelerated impact source of 250 Kg was used to generate seismic waves. The acceleration is achieved with vacuum that builds up when the weight is lifted in an airtight cylinder in which it is mounted. Only a part of the complete dataset is presented here. Analysis was made on parts of the complete seismograms that have high quality and consistent SW events (De Riccardis, 2005).

From previous work in the area it is known that the site has prominent 2D structures and the presence of velocity inversions. Because of difficult geological conditions and a noisy environment the data quality is varying. The remaining data with a sufficient quality gives dispersion curves with different frequency range and area coverage.

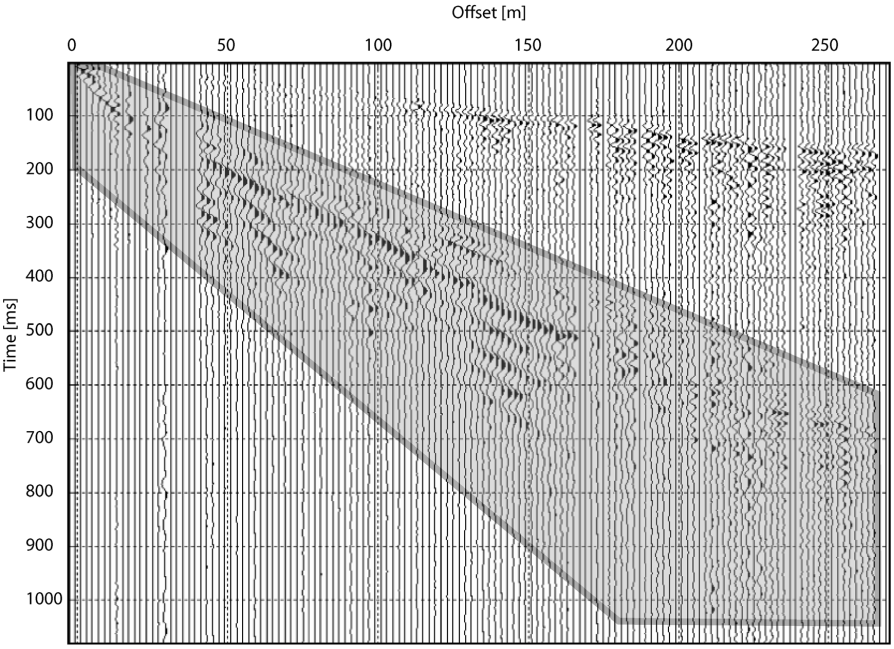

Figure 43 A seismogram showing the reflection seismic data from measurements in Torre Pellice. The part of the seismogram containing the Rayleigh wave events, or ground-roll, is marked with grey.

Geology

The site presents an overburden mainly composed by a layer of fluvial sediments with an expected thickness of 10 – 50 m over a layer of lacustrine sediments. The bedrock is crystalline and the depth is expected to be more than 100 m in the central part of the valley. The depth to the bedrock can be expected to be smaller in the upper part of the valley and at the same time the slope is expected to be steeper.

A seismic down-hole test in the vicinity shows velocities of about 150 m/s in the upper 5 m and then 300 – 400 m/s down to about 30 m, no information on the velocity of the bedrock is available from that test.

6.6.2. LCI of SW data

The starting model for all the 1D models in the inversion is based on an initial inversion of one of the dispersion curves from the center of the profile (at 88 m in e.g. Figure 44). The starting model has velocities of 150 m/s for layer 1 to 500 m/s for layer 5, and a velocity inversion for layer 4. The depth to layer 5 is 32 m.

Figure 44a presents the resulting Vs models from independent inversion of all SW data. It shows a bottom layer of V_s around 500 m/s and the depth to this layer is 30 – 35 m in the entire section. For a handful of the models the velocity of layer 5 is 600 m/s or more. The overlying layer has lower velocities and show tendencies of a velocity inversion. The uncertainties of the model parameters (Figure 44b) are generally high. The normalised residual is low as shown in Figure 44c. Only a few models between 88 and 95 m and one at 122 m have any resolution of the bottom layer parameters.

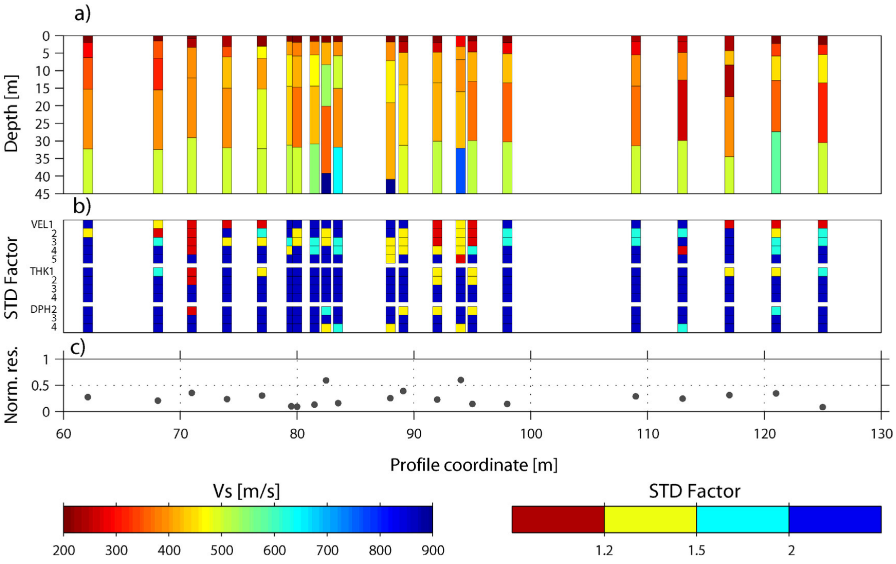

Figure 44 **Result from independent inversion on all SW data. The Profile coordinates increase towards the side of the valley. a) V_s model. b) Model resolution analysis of the model in (a). c) Normalised data misfit for each dataset.**

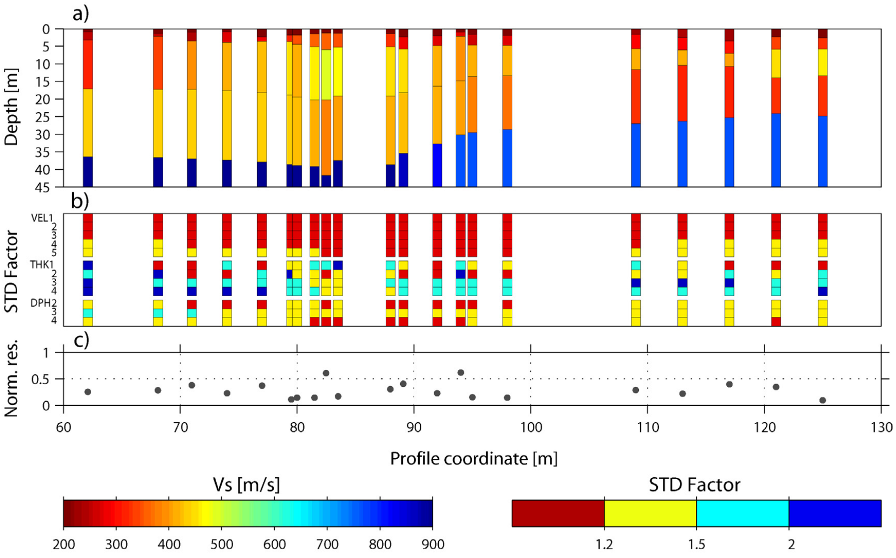

Figure 45 **Result from LCI on all SW data. a) V_s model. b) Model resolution analysis of the model in (a). c) Normalised data misfit for each dataset.**

For the LCI, the lateral constraints are scaled as described in Section 6.2.4; the reference constraint is 0.1 and the reference distance is 4 m. For a model separation of 4 m or less this implies that a difference of about 10% is allowed between corresponding model parameters of neighbouring models. The standard deviation of each data point is assumed to be 5%.

The effect of performing LCI instead of independent inversion can be clearly seen in the section in Figure 45. Almost all parameters (velocities and depth) are consistent along the profile and their uncertainty (Figure 45b) is significantly decreased. Only thickness values are generally poorly resolved or unresolved, which is of minor importance since the inversion is optimising the depths and not thicknesses. The normalised data misfit (Figure 45c) is well below the observational error. The depths to the bottom layer are between 30 and 40 m and changes smoothly throughout the profile. The velocities are 700 m/s or more.

The fact that the depths to and velocities of the bottom layer are only resolved in a handful of the models in the separate inversions (Figure 44a and b) indicate that there is very little information in the observed data about these parameters. It can also be noted in Figure 44 that where the uncertainties of these parameters are high, they have kept the values given to the starting model. The consistent bottom layer of relatively high velocities in the section in Figure 45a might therefore be an effect of the high velocities at depth estimated in a few of the 1D models spreading to all other models through the lateral constraints.

Since lateral variations are expected in the area an inversion was made using multilayer models with fixed geometry and lateral constraints only on velocity between the models. Vertical constraints where also used to get vertically smooth velocity changes and to allow information on velocities in the upper parts of the models to influence the deeper parts.

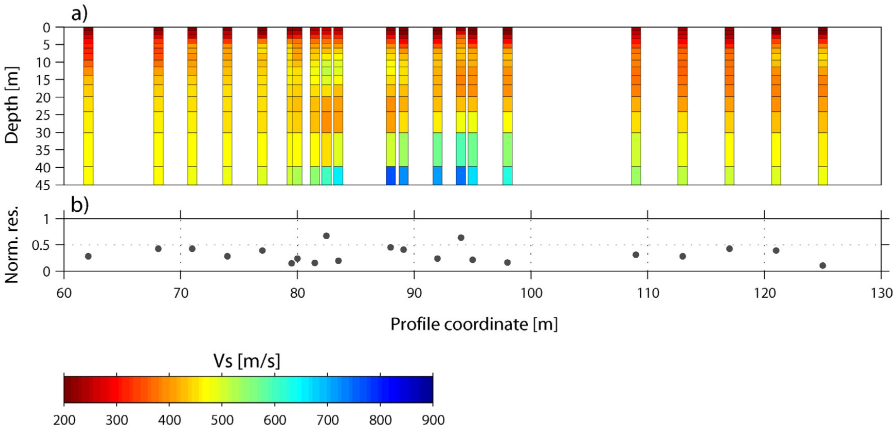

Figure 46 Result from LCI on all SW data with a multilayer model with soft vertical constraints on velocities. Layer thicknesses are fixed. a) V_s model. b) Normalised data misfit for each dataset.

The result from this inversion is shown in Figure 46. Due to the changed parameterisation of the models it is not useful to analyse the uncertainties of the model parameters. The normalised data misfit (Figure 46b) is well below the observational error. The V_s model in Figure 46a has many similarities to that in Figure 45a but shows a significant difference in the velocities in the lower parts of the model. From the model in Figure 46a it is clear that the high velocities in layer 5 only occur between 80 and 100 m. The vertical constraints work against the lateral constraints.

Where there is no information in the observed data of high velocities in the lower parts of the models, the low velocities in the upper part of the model spread downwards due to the vertical constraints.

The higher velocities below 30 m and between profile coordinates 80 and 100 m in the V_s model in Figure 46a are interpreted as bedrock.

7. Conclusions

The successful design and construction of earth works and foundations requires a model of the geological materials properties and their geometrical distribution. However, it is a fact that the establishment of material models for geo-materials is relatively complex. This is due to the high degree of variation of material properties as well as to the extent and in-homogeneity of different geological formations. Largely because of this, the adaptation of geophysical methods for engineering purposes represents an important contribution to the development of site investigation methodology. Geophysical methods can provide significant information early in the site investigation process, thus refining the geological model. Thereby the understanding of local variation and major discontinuities is enhanced. At any stage in the site investigation geophysics can be used to facilitate the interpolation of geological, geotechnical, hydrogeological and/or geophysical structures between discrete investigation positions. Continuous geophysical models also provide a decision support for where to conduct additional probing or drilling for an enhanced geological/geotechnical model.

It is important to acknowledge that many geophysical methods provide continuous information that would not be available from any other investigation method. The use of geophysics in geotechnical site investigation is however a field that is far from explored and only a few methods are so far accepted, e.g. seismic methods, for determination of small strain level stiffness, and borehole geophysics.

The geophysical information should not be used instead of other site investigation methods but rather as a complement to increase the resolution and decrease the uncertainty of the material models developed from site investigation. If geophysical methods are used as a complement to the traditional geotechnical methods an improvement of the quality of the material models is achieved and thereby risk of inferior design leading to increased construction costs or failure of structures is reduced.

This thesis discusses how geophysical methods can be used in practice in geotechnical site investigation. The term “geotechnical site investigation” in this case includes both early investigations for a conceptual geological model as well as detailed investigations for a model of geotechnical design parameters. The application of different geophysical models resulting from DC resistivity and surface wave seismic measurements through different approaches of modelling (established as well as new methods) is presented.

- In several examples it is shown how the different models from 2D smooth inversion and LCI describe a geological environment and how the information in the LCI models and the models from 2D smooth inversion in combination increase the reliability of the final geological interpretation. It is shown how a model from 2D smooth inversion reveals the lateral variation while a model from layered and laterally constrained inversion gives more accurate layer boundary estimates and a possibility to assess model parameter uncertainty. Two commercial software packages were used in this study. The software for 2D smooth inversion can be considered as the most widely used for 2D resistivity inversion while the software for LCI is considerably newer and not used to the same extent.

- A priori information that is used to constrain the inversion reduces negative effects from hidden or suppressed layers, non-uniqueness, equivalence and lack of resolution. This results in a geophysical model that better resembles the actual geological setting. This approach is exemplified both with drilling data and refraction seismic data as a priori information for model geometry. After the a priori information is added to the dataset for inversion the models are biased and the final result can not be compared with ground truth in an objective way. Therefore, in Paper 1 a case of inversion with a priori information is presented where only half of the potential a priori dataset is used. In that case it is shown how a small amount of a priori information can stabilise the inversion just as well as a larger amount and how unbiased geological information fits well with the geophysical model from inversion with a priori information.

- The use of LCI for profile oriented SW dispersion curves proves to be a useful way of stabilising the inversion of fundamental mode dispersion curves for a shear wave velocity model. Compared to individual inversion of each dispersion curve it is shown both for synthetic data and field data how LCI produces a much improved model estimate. The LCI of SW data was developed by incorporating the stiffness matrix method for calculation of SW dispersion curves (in this case only for the fundamental mode) in the LCI algorithm.
- The approach of combined inversion that uses two separate mutually constrained geometrical models differs significantly from the joint inversion where one geometrical model is used for both geophysical parameters. It is shown both for synthetic data and field data how the soft constraints on geometry between the two different models perform very well and produce a better model estimate while still allowing for differences in geometry. It is specifically shown how the higher data density in CVES datasets helps to constrain model geometry in a velocity model and thereby produces better estimate of the velocities.
- It is shown for both synthetic data and field data that a 3D resistivity dataset, consisting of a number of parallel CVES profiles, in some cases can give significantly improved resistivity models. Even though the 3D calculations are more time-consuming it can be justified for environments with prominent 3D structures that prevent good results with 2D techniques. It should, however, also be noted that in many geological environments the 2D inversion is sufficient providing that the surveys are designed properly with respect to the strike of the geological structures, as is shown by the case study in Section 6.2.3.
- With a careful assessment of the data quality it is possible to get good results from resistivity surveys also in urban environments. Pipes, fences and underground constructions can affect a resistivity survey negatively and often prevent the collection of useful resistivity data. In the case study presented here the data from resistivity surveying are partially affected by such structures. An effort is made to reduce these effects and their influence on the final result. The aim for the survey is mapping of the limestone surface whereas more detailed interpretation is avoided. The assessment of resistivity data quality supports the idea that it is possible to determine the main structures in the area, like the dip and local extremes of the limestone surface. The combined interpretation of drilling data and resistivity results

give a detailed model of the upper and lower boundary between which the surface of intact limestone is likely to be found, a result that can be very valuable at all stages in the site investigation process.

This collection of methods for measurement and inversion together provide a cost-effective, fast and robust tool for determining the main geological and geo-mechanical units also in urban areas. The possibility of estimating uncertainties of the geophysical model parameters makes it possible to critically analyse the results.

In short the conclusions from this work are that:

- The LCI used parallel to 2D smooth inversion of resistivity data makes it possible to significantly improve the interpretability of the results compared to using only 2D smooth inversion.
- With 3D smooth inversion of resistivity data good results are achieved in environments with prominent 3D structures.
- Combining these methods for resistivity measurements and inversion makes it possible to describe complicated geological environments.
- Moreover, through the use of a priori information in the inversion, optimum use is made of all data and uncertainty in the final geophysical model is minimised.
- The use of LCI for profile oriented SW data proves to be a useful way of stabilising the inversion of fundamental mode dispersion curves for a shear wave velocity model.
- The MCI of resistivity and SW data performs very well and produces a better model estimate while still allowing for differences in geometry between the two models.

8. Future development

8.1. Site investigation methodology

The development of individual methods and applications is important but, in the author's opinion, the most important developments in the future will be seen in integration of different methods; not only integration of different geophysical, hydrogeological or geotechnical methods for the interpretation or processing, but also in integration of concepts to get a more complete view of a problem. If information on a certain property is needed it is often not enough to measure at a few discrete points. Geological understanding and geophysics helps in the interpolation but huge differences in volume coverage, resolution and uncertainty between the different data types are challenges which must be dealt with. For example core drilling is a very precise sampling technique for point determination of lithology and rock quality while a resistivity model averages a much larger volume.

If a geophysical image is in conflict with information derived from geotechnical data it is likely that the results from surface based geophysical methods are not considered as reliable as those from geotechnical in situ methods. But geophysical methods are in fact true in situ measurements of undisturbed material, which is rarely the case for invasive geotechnical methods that alter the material before or while measurements are made. To solve this conflict a technique that recognises the different resolutions and uncertainties of all available data should be used. At the end this technique must present an objective estimate of the properties, their uncertainties and their spatial variation. Such a technique would make it possible to trace inconsistencies back to their source, e.g. the measurements or the processing, and hence provide a much more refined analysis than what is possible from a visual comparison. The LCI and MCI is one step towards such a technique. It allows different kinds of data, including geotechnical, to be inverted simultaneously for one final model (or two in the case of MCI) and quantifies the uncertainties of each data set.

8.2. The resistivity and surface wave methods

The methods described in this thesis are under constant development but are at different development stages.

For resistivity measurements there are a number of commercial solutions available for engineering applications, both when it comes to field equipment as well as processing software. As described in the thesis the approach to perform CVES measurements is established and well documented. However there are available techniques, such as the PACES system from Denmark (see Section 4.1.1), that are not used much elsewhere and which may be very useful for example in an investigation like that described in Section 6.2.

The possibility to perform induced polarisation (IP) measurements in combination with resistivity measurements should also be noted. This is a technique that has proved to be useful for distinguishing between natural soils and landfill-material that are both low resistive but that have different chargeability. The IP technique is not as developed as resistivity imaging (CVES), and it is often difficult to combine high data quality with high field productivity, but it has potential to be an important technique in environmental investigations.

The development of the surface wave methods can be compared with that for the resistivity methods. At present the surface wave methods are at a similar development stage as the resistivity methods where one or two decades ago. Surveys are generally performed as soundings with the aim of estimating a shear wave velocity profile with depth. In this case effects from 2D and 3D environments are normally ignored. Obviously this affects the results negatively and limits the applicability of the methods. A lot of research is focusing on this matter and in a decade surface wave seismic methods will probably be at a completely different stage of development and hopefully there will be methods and methodology available that can handle both 2D and 3D environments. As for the resistivity case this is strongly connected to the development of faster computers and the optimisation of algorithms.

References

Andersson, H., Bengtsson, P.E., Berglund, C., Larsson, R., Sällfors, G. and Öberg-Högsta, A.L, 1998, Skredet i Vagnhärad Teknisk/vetenskaplig utredning om skredets orsaker (The landslide in Vagnhärad technical/scientific investigation about the cause of the landslide), Swedish Geotechnical Institute, Rapport No 56, Linköping.

Archie, G.E., 1942, The electrical resistivity log as an aid in determining some reservoir characteristics, *Transactions of the Society of Petroleum Engineers of the American Institute of Mining*, Metallurgical and Petroleum Engineers, 146, 54-62.

Auken, E. and Christiansen A.V., 2004, Layered and laterally constrained 2D inversion of resistivity data, *Geophysics*, 69, 752-761.

Auken, E., Christiansen, A.V., Jacobsen, B.H., Foged, N. and Sørensen, K.I., 2004, Piecewise 1D Laterally Constrained Inversion of resistivity data, *Geophysical Prospecting*, in press.

Beaty, K.S. and Schmitt, D.R., 2003, Repeatability of multimode Rayleigh-wave dispersion studies, *Geophysics*, 68, 782-790.

Bell, F.G., 1993, *Engineering geology*, Blackwell Scientific Publications, ISBN: 0-632-03223-5.

Bergman, S.G.A. and Carlsson, A., 1988, *Site investigations in rock: Investigations, prognoses reports - recommendations*, Stiftelsen bergteknisk forskning - BeFo, Stockholm, BeFo 86:2/88.

Bernstone, C., Dahlin T., Ohlsson T. and Hogland W., 2000, DC-resistivity mapping of internal landfill structures: two pre-excavation surveys, *Environmental Geology*, 39, 360-371.

Blyth, F.G.H. and de Freitas M.H., 1984, *A geology for engineers*, seventh ed., Edward Arnold Ltd, ISBN: 0-7131-2882-8.

BSI, British Standards Institution, 1999, *Code of Practice for Site Investigations – BS 5930:1999*, British Standards Institution, London, ISBN: 0-5803-3059-1.

Butcher, A.P., Campanella, R.G., Kaynia, A.M. and Massarsch, K.R., 2005, *Seismic downhole procedure to measure shear wave velocity – a guideline prepared by ISSMGE TC10: Geophysical Testing in Geotechnical Engineering*, http://www.geoforum.com/tc10, 2005-10-11.

Christiansen, A.V., Auken, E., Foged, N. and Sørensen, K.I., 2004, Mutually and laterally constrained inversion of CVES and TEM data - A case study, *Near Surface Geophysics*, Submitted.

Claerbout, J.F. and Muir, F., 1973, Robust modelling with erratic data, *Geophysics*, 38, 826-844.

Clayton, C.R.I., Matthews, M.C. and Simons, N.E., 1995, *Site investigation*, Blackwell science Ltd, ISBN: 0-632-02908-0.

Comina, C., Foti, S., Sambuelli, L., Socco, L.V. and Strobbia, C., 2002, Joint inversion of VES and surface wave data, *proceedings of SAGEEP 2002*, Las Vegas.

Dahlin, T., 1996, 2D resistivity surveying for environmental and engineering applications, *First Break*, 14(7), 275-283.

Dahlin, T. Bernstone, C. and Loke, M.H., 2002, A 3-D resistivity investigation of a contaminated site at Lernacken, Sweden, *Geophysics*, 67, 1692-1700.

Dahlin, T., Bjelm, L., and Svensson, C., 1999, Use of electrical imaging in site investigations for a railway tunnel through the Hallandsås Horst, Sweden, *Quarterly Journal of Engineering Geology*, 32, 163-172.

Dahlin, T., Larsson, R., Leroux, V., Svensson, M. and Wisén, R., 2001, *Geofysik i släntstabilitetsutredningar* (Geophysics for slope stability investigations), Swedish Geotechnical Institute, Rapport No 62, Linköping.

Dahlin, T. and Zhou, B., 2004, A numerical comparison of 2D resistivity imaging with 10 electrode arrays, *Geophysical Prospecting*, 52, 379-398.

Dahlin, T. and Zhou, B., 2005, Multiple gradient array measurements for multi-channel 2D resistivity imaging, *Near Surface Geophysics*, accepted for publication 2005-09-21.

Dobroka, M., Gyulai, A., Ormos, T., Csokas, J. and Dresen, L., 1991, Joint inversion algorithm of seismic and geoelectric data recorded in an underground coal mine, *Geophysical Prospecting*, 39, 643-666.

Fookes, P.G., Baynes, F.J. and Hutchinson, J.N., 2000, Total geological history: A model approach to the anticipation, observation and understanding of site conditions, *Proceedings from GEOENG2000,* Volume 1, Melbourne, Australia, 370-460, ISBN: 1-58716-067-6.

Forbriger, T., 2003a, Inversion of shallow-seismic wavefields: I. Wavefield transformation, *Geophysical Journal International*, 153, 719-734.

Forbriger, T., 2003b, Inversion of shallow-seismic wavefields: II. Inferring subsurface properties from wavefield transforms, *Geophysical Journal International*, 153, 735-752.

Foti, S., 2000, *Multistation methods for geotechnical characterization using surface waves*, Doctoral thesis, Politecnico di Torino.

Gallardo, L.A. and Meju, M.A., 2004, Joint two-dimensional dc resistivity and seismic traveltime inversion with cross-gradients constraints, *Journal of Geophysical Research*, 109, B03311.

Griffiths, D.H. and Turnbull, J., 1985, A multi-electrode array for resistivity surveying, *First Break*, 3(7), 16-20.

Hack, R., 2000, Geophysics for slope stability, *Surveys in Geophysics*, 21, 423-448.

Hering, A., Misiek, R., Gyulai, A., Ormos, T., Dobroka, M. and Dresen, L., 1995, A joint inversion algorithm to process geoelectric and surface wave seismic data. Part I: basic ideas, *Geophysical Prospecting*, 43, 135-156.

Hertrich, M. and Yaramanci, U., 2002, Joint inversion of surface nuclear magnetic resonance and vertical electrical sounding, *Journal of applied geophysics*, 50, 179-191.

Håkansson, Å., 1999, *Inverse groundwater modelling – a tool for hydrogeological investigations: An example from the Malmö area*, Licentiate thesis, Lund University, Lund, Sweden.

IAEG, 1981, Engineering geological mapping, International Association of Engineering Geology – Commission on Site Investigation, *Bulletin of IAEG*, Nr 24.

Jackson, D.D., 1972, Interpretation of Inaccurate, Insufficient and Inconsistent Data, *Geophysical Journal Of The Royal Astronomical Society*, 28, 97-109.

Jackson, D.D., 1979, The use of a priori data to resolve non-uniqueness in linear inversion, *Geophysical Journal Of The Royal Astronomical Society*, 57, 137-157.

Jardine, R.J., Fourie A.B. and Burland, J.B., 1986, Studies of the influence of non-linear stress-strain characteristics in soil-structure interaction, *Géotechnique*, 36, 377-396.

Kartplan, 2002, http://www.lm.se/kartplan, 2005-07-28

Kausel, E. and Roesset, J.M., 1981, Stiffness matrices for layered soils, *Bulletin of the seismological journal of America*, 71, 1743-1761.

Kis, M., 2002, Generalised series expansion (GSE) used in DC geoelectric-seismic joint inversion, *Journal of applied geophysics*, 50, 401-416.

Larsen, F., Owen, R., Dahlin, T., Mangeya, P. and Barmen, G., 2002, A preliminary analysis of the groundwater recharge to the Karoo formations, mid-Zambezi basin, Zimbabwe, *Physics and Chemistry of the Earth*, 27, 765-772.

Liber förlag, 1984, *Handboken bygg: Geoteknik* (in Swedish), ISBN: 91-38-06077-9.

Leroux, V. and Dahlin, T., 2005, Time-lapse resistivity investigations for imaging saltwater infiltration in glaciofluvial deposits, *Environmental Geology*, Manuscript Number: HJ-2004-0111, (accepted).

Loke, M.H. and Barker R.D., 1996, Rapid least-squares inversion of apparent resistivity pseudosections by quasi-Newton method: *Geophysical Prospecting*, 44, 131-152.

Loke, M.H., Dahlin, T. and Acworth, I., 2003, A comparison of smooth and blocky inversion methods in 2-D electrical imaging surveys, *exploration geophysics*, 34(3), 182-187.

Massarsch, K.R., 2004, Deformation properties of fine-grained soils from seismic tests, in Viana da Fonseca, A. and Mayne P.W. eds. *Geotechnical and Geophysical site characterization*, 133-146.

McGillivray, P., 1992, *Forward modeling and inversion of dc resistivity and mmr data*, Doctoral thesis, University of British Columbia.

McGrath, R.J., Styles P., Thomas E. and Neale S., 2002, Integrated high-resolution geophysical investigations as potential tools for water resource investigations in karst terrain, *Environmental Geology*, 42, 552-557.

Menke, W., 1989, *Geophysical data analysis: discrete inverse theory* – Revised ed., San Diego Academic Press, International Geophysics Series.

Milsom, J., 1996, *Field geophysics*, John Wiley & Sons Ltd, England.

Misiek, R., Liebig, A., Gyulai, A., Ormos, T., Dobroka, M. and Dresen, L., 1997, A joint inversion algorithm to process geoelectric and surface wave seismic data. Part II: applications, *Geophysical Prospecting*, 45, 65-85.

Nazarian, S., 1984, *In situ determination of soil deposits and pavement systems by spectral analysis of surface waves method*, Doctoral thesis, University of Texas at Austin, Texas.

Oldenburg, D.W. and Li Y., 1994, Inversion of induced polarization data: *Geophysics*, 59, 1327–1341.

Oldenburg, D.W., and Li Y., 1999, Estimating depth of investigation in dc resistivity and IP surveys, *Geophysics*, 64, 403-416.

O'Neill, A., 2003, *Full-waveform reflectivity for modelling, inversion and appraisal of seismic surface wave dispersion in shallow site investigation,* Doctoral thesis, The University of Western Australia.

Overmeeren, R.A. van and Ritsema, I.L., 1988, Continuous vertical electrical sounding, *First Break*, 6(10), 313-324.

Palacky, G.J., 1987, Resistivity characteristics of geological targets, M.N. Nabighian ed. *Electromagnetic methods in Applied Geophysics,* Society of Exploration Geophysics, Tulsa, 53-130.

Papadopoulus, N.G., Tsokas, G.N., Tsourlos, P. and Sarris, A., 2005, Archeological investigations by means of resistivity inversion, *Proceedings of the 11th European Meeting of Environmental and Engineering Geophysics*, 4-7 September 2005, Palermo, Italy, Extended abstract: B023.

Parasnis, D.S., 1997, *Principles of applied geophysics*, 5th ed., Chapman & Hall, London, ISBN: 0-412-64080-5.

Park, C.B., Miller, D.R. and Xia, J., 1999, Multichannel analysis of surface waves, *Geophysics*, 64, 800-808.

Peck, R.B., 1969, Ninth Rankine Lecture: 'Advantages and limitations of the observational method in applied soil mechanics', *Géotechnique*, 19 (2).

Pellerin, L., 2002, Applications of electrical and electromagnetic methods for environmental and geotechnical investigations, *Surveys in Geophysics*, 23, 101-132.

Rankka, K., Andersson-Sköld, Y., Hultén, C., Larsson, R., Leroux, V. and Dahlin, T., 2004, *Quick clay in Sweden*, Swedish Geotechnical Institute, Rapport No 65, Linköping.

Rey, E., Jongmans, D., Gotteland P. and Garambois, S., 2005, Characterisation of soils with stony inclusions using geoelectrical measurements, *Journal of applied geophysics*, 57, In press, available online 9 august 2005.

Reynolds, J.M., 1997, *An Introduction to Applied and Environmental Geophysics*, John Wiley & Sons Ltd, Chichester, ISBN: 0-471-95555-8.

De Riccardis, A., 2005, Caratterizzazione sismica di una valle alpina (Val Pellice) (Seismic Characterisation of an Alpine Valley (Val Pellice - Italy)), Master Thesis, Politecnico in Turin, Turin, Italy.

Rydén, N., 2004, *Surface wave testing of pavements*, Doctoral thesis, Lund university, Lund, Sweden.

Rydén, N., Park, C.B., Ulriksen, P. and Miller, R.D., 2004, Multimodal approach to seismic pavement testing, *Journal of Geotechnical and Geoenvironmental Engineering*, ASCE, 130, 636-645.

Schmutz, M., Albouy, Y., Guérin, R., Maquaire, O., Vassal, J., Schott, J.J. and Descloitres, M., 2000, Joint electrical and time domain electromagnetism (TDEM) data inversion applied to the super sauze earthflow (France), *Surveys in geophysics*, 21, 371-390.

SGF, 1996, *Geoteknisk fälthandbok. Allmänna råd och metodbeskrivningar* (in swedish), Svenska Geotekniska Föreningen, Rapport 1:96.

SGF, 2004, *Fälthandbok, miljötekniska markundersökningar* (in swedish), Svenska Geotekniska Föreningen, Rapport 1:2004.

Sharma, P.V., 1997, *Environmental and engineering geophysics*, Cambridge University Press, Cambridge, UK, ISBN: 0-521-57632-6.

Socco, L.V. and Strobbia, C., 2004, Surface-wave method for near-surface characterization: a tutorial, *Near Surface geophysics*, 2, 165-185.

Stanfors, R., Triumf, C.A. and Emmelin, A., 2001, *Geofysik för bergbyggare* (Geophysics for rock engineers, in Swedish), Stiftelsen Svensk bergteknisk forskning, Stockholm, ISBN: 91-631-0633-7.

Stokoe, K.H., Joh, S.H. and Woods, R.D., 2004, The contribution of in situ geophysical measurements to solving geotechnical engineering problems, in Viana da Fonseca, A. and Mayne P.W. eds. *Geotechnical and Geophysical site characterization*, 97-132.

Sturk, R., 1998, *Engineering geological information: its value and impact on tunnelling*, Doctoral thesis, The Royal Institute of Technology, Stockholm, Sweden.

Suzuki, K., Toda, S., Kusunoki, K., Fujimitsu, Y., Mogi, T. and Jomori, A., 2000, Case studies of electrical and electromagnetic methods applied to mapping active faults beneath the thick quaternary, *Engineering Geology*, 56, 29-45.

Svensson, M., 2001, *Application of the SASW-technique in geotechnical in-situ testing*, Doctoral thesis, Lund University, Lund, Sweden.

Svensson, M., Möller, B. and Gunnarsson, A., 2004, Ytvågsseismisk undersökning av väg på masstabiliserad torvmosse (Surface wave seismic survey of road on mass stabilised peat, in Swedish), *Proceedings of XIV Nordic Geotchnical Meeting, May 19th-21th 2004*, H-153.

Sørensen, K.I., 1996, Pulled Array Continuous Electrical Profiling, *First break*, 14, 85-90.

Sørensen, K.I., Auken, E., Christensen, N.B. and Pellerin, L., 2005, An Integrated Approach for Hydrogeophysical Investigations: New Technologies and a Case History, *Near-surface Geophysics Volume II: Application and case histories*, Society of Exploration Geophysics, in press.

Telford, W.M., Geldart, L.P. and Sheriff, R.E., 1990, *Applied geophysics*, second edition, Cambridge university press, Cambridge, UK, ISBN: 0-521-33938-3.

Terzaghi, K. and Peck, R.B., 1967, *Soil mechanics in engineering practice*, second edition, John Wiley & Sons.

Turesson, A. and Lind, G., 2005, Evaluation of electrical methods, seismic refraction and ground-penetrating radar to identify clays below sands – Two case studies in SW sweden, *Near Surface Geophysics*, 3, 59-70.

Vickery, A.C. and Hobbs, B.A., 2002, The effect of subsurface pipes on apparent-resistivity measurements, *Geophysical Prospecting*, 50, 1-13.

Vozoff, K. and Jupp, D.L.B., 1975, Joint inversion of geophysical data, *Geophysical Journal of the Royal Astronomical Society*, 42, 977-991.

Ward, S.H., 1989a, Resistivity and Induced Polarization Methods, in *Investigations in Geophysics no. 5: Geotechnical and Environmental Geophysics, vol I*, ed. S. Ward, Society of Exploration Geophysicists, Tulsa, p 147-189.

Ward, S.H., 1989b, *Geophysics no. 5: Geotechnical and Environmental Geophysics, vol III: Geotechnical*, ed. S. Ward, Society of Exploration Geophysicists, Tulsa.

Appendix 1 – Geophysical inverse modelling and its application to laterally constrained inversion of surface wave seismic data

Table of contents

Appendix 1 – Geophysical inverse modelling and its application to laterally constrained inversion of surface wave seismic data

Appendix 1 – Geophysical inverse modelling and its application to laterally constrained inversion of surface wave seismic data

1 Introduction

Even though the techniques used in geophysical inverse modelling constitute a significant part of this thesis, the subject is too vast to be described in detail inside the thesis. Since the reader might not be familiar with discrete inverse theory, an introduction to the subject is given in this appendix. In addition an application of discrete inverse modelling to surface wave seismic data is presented (Wisén and Christiansen, 2005) (paper 3 in appendix 4). The inversion algorithm is described in more detail than in the paper, and also the forward model is presented here.

Basic literature on geophysical inverse modelling is for example William Menkes (1989) "Geophysical data analysis: Discrete inverse theory – Revised edition", where a detailed description of the subject is found.

2 Short introduction to inverse theory

This introduction deals with the linear inverse problem and discrete inverse theory. In reality inverse problems are often non-linear but for the sake of simplicity Chapter 2 describes only the linear case. However, in the application of inverse modelling to surface wave seismic data the non-linearity is evident and therefore, in Section 3.3 the non-linear inverse modelling is discussed.

Initially, a distinction should be made between forward modelling and inverse modelling. From a known set of model parameters here represented as a vector

$$\mathbf{m} = \left[m_1, m_2, ..., m_j, ..., m_M\right]^{\mathrm{T}} \qquad \textbf{Equation 1}$$

with M model parameters, a set of data

$$\mathbf{d} = \left[d_1, d_2, ..., d_i, ..., d_N\right]^{\mathrm{T}} . \qquad \textbf{Equation 2}$$

can be calculated by a model, **g**. The model is a function that describes the mapping from model space to data space, also known as the forward model:

$$\mathbf{d} = \mathbf{g(m)} \qquad \textbf{Equation 3}$$

With inverse modelling an attempt is made to estimate the model parameters to a known set of data. The most obvious part of the solution to the inverse problem is the estimate of the model parameters, but other aspects like standard deviation and probability distribution of the parameters can also be part of the solution. Formulation of the inverse problem is the first step. This includes dealing with the data, data uncertainty and model parameterisation. In geophysical inverse modelling data consist of discrete observations and for N observations the elements in a vector

$$\mathbf{d^{obs}} = \left[d_1^{obs}, d_2^{obs}, ..., d_i^{obs}, ..., d_N^{obs}\right]^{\mathrm{T}} \qquad \textbf{Equation 4}$$

will contain the measured values. Now consider

$$\mathbf{d} = \mathbf{Gm} \qquad \textbf{Equation 5}$$

where **G** is the mapping of the model parameters into the data space, also called the data kernel. The calculations are done as

$$d_i = \sum_{j=1}^{M} G_{ij} m_j \qquad i = 1...N, j = 1...M . \qquad \textbf{Equation 6}$$

An observed data, d_i^{obs}, is always connected to an observational error, e_i^{obs}, so that

$$\mathbf{Gm^{true}} = \mathbf{d^{obs}} + \mathbf{e^{obs}}. \qquad \textbf{Equation 7}$$

These errors are assumed to be uncorrelated and independent of time; checking these prerequisites is part of setting up the inverse problem.

Parameterisation is another important part of the problem. Which are actually the unknowns that are to be found behind the observed data? The model parameters can initially be divided into fixed and variable model parameters. The fixed model parameters are not estimated with the observed data but treated as constants. The variable model parameters, **m**, are the unknowns that the observed data can be used to estimate.

Now, the linear inverse problem can be formulated as

$$\mathbf{d^{obs}} = \mathbf{Gm^{true}} + \mathbf{e^{obs}}. \qquad \textbf{Equation 8}$$

2.1 The least squares solution

A common way to solve the problem in Equation 8 is to use the sum of squared residuals:

$$Q \equiv \sum_{i=1}^{N} (d_i^{obs} - g_i(\mathbf{m}))^2 = \left|\mathbf{d^{obs}} - \mathbf{Gm}\right|^2 = \left|\mathbf{e^{misfit}}\right|^2 \qquad \textbf{Equation 9}$$

where $Q(\mathbf{d^{obs}},\mathbf{m})$ is a quality function describing the squared residual between the observed data and the model estimate. $Q(\mathbf{d^{obs}},\mathbf{m})$ should be minimised for the optimal model to be found. $\mathbf{e^{misfit}}$ is the error between the modelled and the observed data. If there are more data than unknowns ($N>M$) the problem is over determined, and therefore an exact solution can not be found. In this case the best estimate is found when Q is minimised. Then, for any possible **m**

$$Q^{LSQ}(\mathbf{d^{obs}},\mathbf{m^{LSQ}}) \leq Q(\mathbf{d^{obs}},\mathbf{m}). \qquad \textbf{Equation 10}$$

Since solving the inverse problem is now a problem of locating the minimum of Q it is solved by setting the derivatives of Q with respect to **m** in Equation 9 to zero and solving the resulting equation system:

$$\frac{\partial Q^{LSQ}}{\partial m_j} = \frac{\partial}{\partial m_j}\left[\sum_{i=1}^{N} e_i^2\right] = \sum_{i=1}^{N} 2e_i \frac{\partial e_i}{\partial m_j} = 0 \qquad \textbf{Equation 11}$$

where e_i is the residual of the i_{th} data. Since each data residual is a function of M model parameters (see Equation 1) the linear inverse problem from Equation 8 can now be re-written as

$$e_i(m_1,...,m_M) = d_i^{obs} - \sum_{k=1}^{M} G_{ik} m_k \qquad k = 1...M. \qquad \textbf{Equation 12}$$

and, since

$$\frac{\partial Q}{\partial m_j} = 0$$

as stated in Equation 11

$$\frac{\partial e_i}{\partial m_j}=\frac{\partial\left[d_i-\sum_{k=1}^{M}G_{ik}m_k\right]}{\partial m_j}=\frac{\partial d_i}{\partial m_j}-\frac{\partial G_{ij}m_j}{\partial m_j}=-G_{ij}\,. \qquad \textbf{Equation 13}$$

If Equation 13 is substituted to Equation 9 the result becomes

$$\begin{aligned}\frac{\partial Q}{\partial m_j}&=2\sum_{i=1}^{N}\left(d_i-\sum_{k=1}^{M}G_{ik}m_k\right)(-G_{ij})=\\&=-2\sum_{i=1}^{N}G_{ij}d_i+2\sum_{i=1}^{N}G_{ij}\left(\sum_{k=1}^{M}G_{ik}m_k\right)=0 \qquad j=1\ldots M\end{aligned}\ . \qquad \textbf{Equation 14}$$

Equation 14 is a linear system of equations with M unknowns that can be expressed in matrix formulation as

$$\mathbf{0}=-\mathbf{G}^{\mathbf{T}}\mathbf{d}^{\mathbf{obs}}+\mathbf{G}^{\mathbf{T}}(\mathbf{Gm}) \qquad \textbf{Equation 15}$$

or

$$(\mathbf{G}^{\mathbf{T}}\mathbf{G})\,\mathbf{m}=\mathbf{G}^{\mathbf{T}}\mathbf{d}^{\mathbf{obs}} \qquad \textbf{Equation 16}$$

and if the number of unknowns are the same as the number of observables the exact solution to the problem will be

$$\mathbf{m}^{\mathbf{LSQ}}\equiv(\mathbf{G}^{\mathbf{T}}\mathbf{G})^{-1}\mathbf{G}^{\mathbf{T}}\mathbf{d}^{\mathbf{obs}}. \qquad \textbf{Equation 17}$$

The least squares inverse mapping can now be written as

$$\mathbf{G}^{\mathbf{LSQ}}\equiv(\mathbf{G}^{\mathbf{T}}\mathbf{G})^{-1}\mathbf{G}^{\mathbf{T}} \qquad \textbf{Equation 18}$$

and the least squares model estimate is

$$\mathbf{m}^{\mathbf{LSQ}}\equiv\mathbf{G}^{\mathbf{LSQ}}\mathbf{d}^{\mathbf{obs}}. \qquad \textbf{Equation 19}$$

In the linear case, $\mathbf{m}^{\mathbf{LSQ}}$ can be obtained in one single step. However, if the case is non-linear the problem can not be solved in one single step and therefore an iterative scheme is necessary to obtain $\mathbf{m}^{\mathbf{LSQ}}$. This is discussed in Section 3.3 that describes the inverse modelling of surface wave seismic data.

2.2 The weighted and damped least squares solution

Sometimes the least squares estimate is not a very good solution to the inverse problem. For example differences in the residual of different data can require that some data is given a greater weight than others. This is done with the weighted least squares mapping

$$\mathbf{G}^{\mathbf{WLSQ}}=(\mathbf{G}^{\mathbf{T}}\mathbf{WG})^{-1}\mathbf{G}^{\mathbf{T}}\mathbf{W} \qquad \textbf{Equation 20}$$

which provides the weighted least squares estimate as

$$\mathbf{m}^{\mathbf{WLSQ}}=\mathbf{G}^{\mathbf{WLSQ}}\mathbf{d}^{\mathbf{obs}}. \qquad \textbf{Equation 21}$$

To stabilise matrix operations it might be necessary to damp the solution. The damped least squares mapping is

$$\mathbf{G}^{\mathbf{DLSQ}} = \left(\mathbf{G}^{\mathrm{T}}\mathbf{G} + \boldsymbol{\alpha}\mathbf{I}\right)^{-1}\mathbf{G}^{\mathrm{T}} \qquad \textbf{Equation 22}$$

and if Equation 21 and Equation 22 is combined we get the weighted damped least squares mapping that provides a robust solution for the non-linear problems:

$$\mathbf{G}^{\mathbf{WDLSQ}} = \left(\mathbf{G}^{\mathrm{T}}\mathbf{W}\mathbf{G} + \alpha\mathbf{I}\right)^{-1}\mathbf{G}^{\mathrm{T}}\mathbf{W} \qquad \textbf{Equation 23}$$

and the estimate becomes

$$\mathbf{m}^{\mathbf{WDLSQ}} = \mathbf{G}^{\mathbf{WDLSQ}}\mathbf{d}^{\mathbf{obs}}. \qquad \textbf{Equation 24}$$

In Equation 22 and Equation 23 **I** is the identity matrix and α is a Marquardt damping parameter (Marquardt, 1963).

2.3 Analysis of variance of the model parameters

The analysis of the certainty of the model parameters, or the analysis of their probability distribution, is also part of the solution to the inverse problem. Assuming that inverse problem is locally linear and that $\mathbf{e}^{\mathbf{obs}}$ is a stochastic vector with mean zero and covariance matrix $\mathbf{C}^{\mathbf{obs}}$, the a posterior covariance matrix, $\mathbf{C}^{\mathbf{est}}$, becomes

$$\mathbf{C}^{\mathrm{est}} = \left(\mathbf{G}^{\mathrm{T}}\mathbf{C}^{\mathrm{obs}}\mathbf{G}\right)^{-1} \quad \text{(Tarantola and Valette, 1982).} \qquad \textbf{Equation 25}$$

The variance of the estimated model parameters are the diagonal elements in $\mathbf{C}^{\mathbf{est}}$ and the standard deviations are the square root of the variances. Note the formal equivalence between **W** and $\mathbf{C}^{\mathbf{obs}^{-1}}$.

3 Laterally constrained inversion of surface wave seismic data

This chapter describes an algorithm for laterally constrained inversion (LCI) of surface wave seismic data. The LCI performs a parameterised, layered inversion of many datasets by coupling neighbouring shear wave velocity models together with lateral constraints on the model parameters (Auken and Christiansen, 2004), as illustrated in Figure 18 in the thesis. In addition to the formulation of the inverse problem and its solution, a forward response for Rayleigh wave dispersion curves (phase velocity versus frequency) from a shear wave velocity model is also described.

3.1 The data and model vectors

One surface wave sounding (as described in Section 3.2.2 in the thesis) form the phase velocity data vector

$$\mathbf{d} = (v_1,\ldots,v_N)^{\mathrm{T}} \qquad \textbf{Equation 26}$$

where every phase velocity data point corresponds to a certain frequency. To minimise the effects of non-linearity and to assure that data and model parameters are positive, logarithmic data is used:

$$\mathbf{d} = (\log(v_1),\ldots,\log(v_N))^{\mathrm{T}} \qquad \textbf{Equation 27}$$

The observational error can be assumed to be a stochastic Gaussian error and the observational data is then written as

$$\mathbf{d}^{\mathbf{obs}} = \mathbf{d}^{\mathbf{true}} + \mathbf{e}^{\mathbf{obs}} \qquad \textbf{Equation 28}$$

where the expectation value

$$\mathrm{E}\left[\mathbf{e}^{\mathbf{obs}}\right] = \mathbf{0}. \qquad \textbf{Equation 29}$$

If no information on how the standard deviation varies for different frequencies[1] is available a standard deviation of e.g. 5% can be assumed.

The covariance matrix will become

$$\mathbf{C}^{\mathbf{obs}} = \begin{bmatrix} {e_{1,1}^{obs}}^2 & \cdots & 0 \\ \vdots & \ddots & \vdots \\ 0 & \cdots & {e_{N,N}^{obs}}^2 \end{bmatrix} \qquad \textbf{Equation 30}$$

The $M{=}n_l{*}2\text{-}1$ model parameters are logarithms of shear wave velocities and layer thicknesses:

$$\mathbf{m} = (\log(v_{s1}),...,\log(v_{s,n_l}),\log(t_1),...,\log(t_{n_l-1}))^{\mathrm{T}}. \qquad \textbf{Equation 31}$$

3.2 The forward modelling

The function described here is the model response, **g** and

$$\mathbf{d} = \mathbf{g}(\mathbf{m}) \qquad (\textbf{Equation 3} \text{ repeated})$$

Theoretical dispersion curves for a layered elastic medium can be calculated with a matrix formulation based on wave propagation theory. In this study the stiffness matrix method proposed by Kausel and Roesset (1981) is used. Each layer (in a shear wave velocity model with i layers) is represented with a layer stiffness matrix ($\mathbf{SL}_i$) (see below), the half space is represented with a halfspace stiffness matrix (**SH**), where loads (l) and displacements (r) are expressed as a function of the material properties; compressional wave velocity (V_p), shear wave velocity (V_s), thickness (h), shear modulus (G) of each layer, and radian frequency (ω) and wave number (k). By satisfying the boundary conditions at each layer interface, all layer matrices are assembled to a system matrix (**S**) describing the complete layer model, Equation 32. Each point on a dispersion curve represents a solution to **S** where all boundary conditions are satisfied simultaneously. For modal solutions to exist, **S** must be singular, i.e. its determinant must be zero. The dispersion equation or characteristic equation then becomes Equation 33:

$$\mathbf{S}r = l \qquad \textbf{Equation 32}$$

$$f(f,k) = \det[\mathbf{S}] = 0 \qquad \textbf{Equation 33}$$

Numerically the problem is reduced to finding the determinant of a sometimes large and sparse matrix. The main disadvantage with the stiffness matrix approach is

---

[1] O'Neill (2003) show that the standard deviation is frequency dependent with smaller errors at high frequencies and larger errors at low frequencies, compared to what is assumed here. This behaviour can be determined by performing statistical analysis of multiple datasets.

that **S** becomes singular at the bulk wave numbers (V_p and V_s velocities) of the system. This can be a problem when tracing dispersion curves across these wave numbers.

Here the final matrix equations as given by Kausel and Roesset (1981) are presented, Equation 34 - Equation 52. The layer stiffness matrix is

$$[\mathbf{SL_i}] = \mathbf{C}\begin{bmatrix} \mathbf{S}_{11} & \mathbf{S}_{12} & \mathbf{S}_{13} & -\mathbf{S}_{23} \\ \mathbf{S}_{12} & \mathbf{S}_{22} & \mathbf{S}_{23} & \mathbf{S}_{24} \\ \mathbf{S}_{13} & \mathbf{S}_{23} & \mathbf{S}_{11} & -\mathbf{S}_{12} \\ -\mathbf{S}_{23} & \mathbf{S}_{24} & -\mathbf{S}_{12} & \mathbf{S}_{22} \end{bmatrix}$$

Equation 34

in which

$$\mathbf{S}_{11} = \frac{1}{t_s}\cos(t_p kh)\sin(t_s kh) + t_p \sin(t_p kh)\cos(t_s kh)$$

Equation 35

$$\mathbf{S}_{12} = \frac{3-t_s^2}{1+t_s^2}\left[1-\cos(t_p kh)\cos(t_s kh)\right] + \frac{1+2t_p^2 t_s^2 - t_s^2}{t_p t_s(1+t_s^2)}\sin(t_p kh)\sin(t_s kh)$$

Equation 36

$$\mathbf{S}_{13} = -t_p \sin(t_p kh) - \frac{1}{t_s}\sin(t_s kh)$$

Equation 37

$$\mathbf{S}_{22} = \frac{1}{t_p}\sin(t_p kh)\cos(t_s kh) + t_s \cos(t_p kh)\sin(t_s kh)$$

Equation 38

$$\mathbf{S}_{23} = -\cos(t_p kh) + \cos(t_s kh)$$

Equation 39

$$\mathbf{S}_{24} = -\frac{1}{t_p}\sin(t_p kh) - t_s \sin(t_s kh)$$

Equation 40

$$\mathbf{C} = \frac{(1+t_s^2)kG}{2\left[1-\cos(t_p kh)\cos(t_s kh)\right] + \left(t_p t_s + \frac{1}{t_p t_s}\right)\sin(t_p kh)\sin(t_s kh)}$$

Equation 41

t_p and t_s indicate tangents of wave propagation direction, as defined by

$$t_p = -i\sqrt{1-\frac{1}{l_p^2}}$$

Equation 42

$$t_s = -i\sqrt{1-\frac{1}{l_s^2}}$$

Equation 43

$$l_p = \frac{V_p}{c}$$

Equation 44

$$l_s = \frac{V_s}{c}$$

Equation 45

$$c = \frac{\omega}{k}$$ **Equation 46**

where *i* is the imaginary unit. The halfspace stiffness matrix is

$$[\mathbf{SH}] = \mathbf{C}\begin{bmatrix} \mathbf{SH}_{11} & \mathbf{SH}_{12} \\ \mathbf{SH}_{12} & \mathbf{SH}_{22} \end{bmatrix}$$ **Equation 47**

where

$$\mathbf{SH}_{11} = \frac{it_p(1+t_s^2)}{1+t_pt_s}$$ **Equation 48**

$$\mathbf{SH}_{12} = 2 - \frac{it_p(1+t_s^2)}{1+t_pt_s}$$ **Equation 49**

$$\mathbf{SH}_{22} = \frac{it_s(1+t_s^2)}{1+t_pt_s}$$ **Equation 50**

and

$$\mathbf{C} = kG$$ **Equation 51**

When the four-by-four **SL** matrices and the two-by-two **SH** matrix have been calculated for each layer they are assembled to obtain the global **S** matrix, Equation 52. For a layer model with four layers the system matrix then becomes:

$\mathbf{S} =$

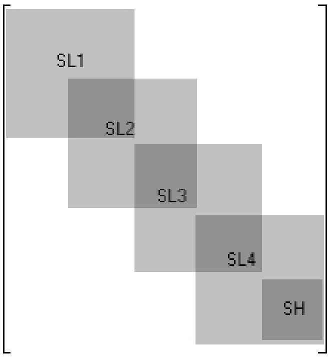

Equation 52

The estimated wave number for a certain frequency is found by searching through a range of wave numbers, and finding the one that gives a matrix determinant arbitrarily close to zero.

3.3 The inverse modelling

The underlying problem in a geophysical context is very often non-linear but can locally be treated as a linear problem. Different techniques can be used to reduce the effects of non-linearity; this is described in detail in e.g. Menke (1989). Here the established practice of linearised approximation with the first term of the Taylor expansion of the model formulation is followed. This gives

$$\mathbf{d}^{\mathbf{obs}} + \mathbf{e}^{\mathbf{obs}} = \mathbf{G}\left(\mathbf{m}^{\mathbf{true}} - \mathbf{m}^{\mathbf{ref}}\right) + \mathbf{g}\left(\mathbf{m}^{\mathbf{ref}}\right) \qquad \textbf{Equation 53}$$

that should be compared with the linear case in Equation 8. The notation follows that for Equation 8 and in addition **g** is the non-linear mapping of the model to the data space. If the true model, $\mathbf{m}^{\mathbf{true}}$, is sufficiently close to some arbitrary reference model, $\mathbf{m}^{\mathbf{ref}}$ the problem can be considered locally linear and:

$$\mathbf{G}\mathbf{m}^{\mathbf{true}} = \mathbf{d}^{\mathbf{obs}} + \mathbf{e}^{\mathbf{obs}}. \qquad \textbf{Equation 54}$$

3.3.1 The Jacobian matrix calculation

The Jacobian matrix, **G**, contains the partial derivatives of

$$G_{ij} = \frac{\partial d_i}{\partial m_j} = \frac{\partial \log(d_i)}{\partial \log(m_j)} = \frac{m_j}{d_i}\frac{\partial d_i}{\partial m_j} \qquad \textbf{Equation 55}$$

where the logarithm minimises the effects of non-linearity and ensures that the data and model parameters are positive. The partial derivatives are calculated using e.g. two point symmetrical difference

$$G_{ij} = \frac{g(m_j + \delta m) - g(m_j - \delta m)}{2\delta m}. \qquad \textbf{Equation 56}$$

3.3.2 The iterative solution

For the inverse modelling the weighted damped least squares criterion from Equation 24 is used. The quality function to minimise is

$$Q = \left|\mathbf{d}^{\mathbf{obs}} - \mathbf{G}\mathbf{m}\right|^2. \qquad \textbf{Equation 57}$$

To assure convergence it is required that some kind of damping is used in the iterative procedure, then:

$$\mathbf{m}_{\mathbf{i+1}} = \mathbf{m}_{\mathbf{i}} + \left(\mathbf{G}(m_i)^{\mathrm{T}}\mathbf{C}^{\mathbf{obs}^{-1}}\mathbf{G}(m_i) + \alpha\mathbf{I}\right)^{-1}\mathbf{G}(m_i)^{\mathrm{T}}\mathbf{C}^{\mathbf{obs}^{-1}}\left(\mathbf{d}_{\mathbf{obs}} - \mathbf{d}(\mathbf{m}_{\mathbf{i}})\right) \qquad \textbf{Equation 58}$$

so that

$$Q(\mathbf{d}^{\mathbf{obs}}, \mathbf{m}_{\mathbf{i+1}}) < Q(\mathbf{d}^{\mathbf{obs}}, \mathbf{m}_{\mathbf{i}}). \qquad \textbf{Equation 59}$$

This approach of damping is the Marquardt method mentioned before and α is set to the geometric mean of the diagonal elements in $\mathbf{G}^{\mathrm{T}}\mathbf{G}$ and then increased or reduced until $Q(\mathbf{d}^{\mathbf{obs}}, \mathbf{m}_{\mathbf{i+1}})$ improves or is minimised.

3.3.3 The laterally constrained inversion

For the laterally constrained inversion with n_i models (that each have n_l layers) and corresponding dispersion curves the data vector with N data values (for each dispersion curve N_i data values) becomes

$$\mathbf{d} = (v_{1,1}, \ldots, v_{N_1,1}, \ldots, v_{1,n_i}, \ldots, v_{N_{n_i},n_i})^{\mathrm{T}}. \qquad \textbf{Equation 60}$$

The model becomes

$$\begin{aligned}\mathbf{m} = (&\log(v_{s1,1}),\ldots,\log(v_{sn_l,1}),\log(t_{1,1}),\ldots,\log(t_{n_{l-1},1}),\ldots \\ &\ldots,\log(v_{s1,n_i}),\ldots,\log(v_{sn_l,n_i}),\log(t_{1,n_i}),\ldots,\log(t_{n_{l-1},n_i}))^{\mathrm{T}}\end{aligned} \qquad \textbf{Equation 61}$$

with $M = n_i(2n_l - 1)$ model parameters.

The lateral constraints are connected to the true model by

$$\mathbf{R}\delta\mathbf{m}^{\mathbf{true}} = \delta\mathbf{r} + \mathbf{e}^{\mathbf{r}} \qquad \textbf{Equation 62}$$

where $\mathbf{e}^{\mathbf{r}}$ is the error on the constraints with 0 as expected value, and $\delta\mathbf{r} = -\mathbf{Rm}^{\mathbf{ref}}$ provides the identity between the parameters tied by constraints in the roughening matrix **R**, containing the values 1 and –1 for the constrained parameters and 0 in all other places. The covariance matrix $\mathbf{C}^{\mathbf{R}}$ describes the strength, or variance of the constraints.

A priori information is included as:

$$\mathbf{I}\delta\mathbf{m}^{\mathbf{true}} = \delta\mathbf{m}^{\mathbf{prior}} + \mathbf{e}^{\mathbf{prior}} \qquad \textbf{Equation 63}$$

where $\mathbf{m}^{\mathbf{prior}}$ is the extra data with a priori information on model parameters, $\delta\mathbf{m}^{\mathbf{prior}} = \mathbf{m}^{\mathbf{prior}}\text{-}\mathbf{m}^{\mathbf{ref}}$, $\mathbf{e}^{\mathbf{prior}}$ is the error on the a priori data with 0 as expected value and **I** is the identity matrix with the dimension of the model vector. The variance in the a priori model is described in the covariance matrix, $\mathbf{C}^{\mathbf{prior}}$.

The inversion problem can now be written as

$$\begin{bmatrix}\mathbf{G}\\ \mathbf{I}\\ \mathbf{R}\end{bmatrix} \cdot \delta\mathbf{m}^{\mathbf{true}} = \begin{bmatrix}\delta\mathbf{d}^{\mathbf{obs}}\\ \delta\mathbf{m}^{\mathbf{prior}}\\ \delta\mathbf{r}\end{bmatrix} + \begin{bmatrix}\mathbf{e}^{\mathbf{obs}}\\ \mathbf{e}^{\mathbf{prior}}\\ \mathbf{e}^{\mathbf{r}}\end{bmatrix} \qquad \textbf{Equation 64}$$

or more compactly

$$\mathbf{G'}\cdot\delta\mathbf{m}^{\mathbf{true}} = \delta\mathbf{d'}+\mathbf{e'} \qquad \textbf{Equation 65}$$

The covariance matrix for the joint observation error, **e’**, becomes

$$\mathbf{C'} = \begin{bmatrix}\mathbf{C}^{\mathbf{obs}} & & \underline{\underline{\mathbf{0}}}\\ & \mathbf{C}^{\mathbf{prior}} & \\ \underline{\underline{\mathbf{0}}} & & \mathbf{C}^{\mathbf{R}}\end{bmatrix} \qquad \textbf{Equation 66}$$

The model estimate

$$\delta\mathbf{m}^{\mathbf{est}} = \left(\mathbf{G'}^{\mathrm{T}}\,\mathbf{C'}^{-1}\,\mathbf{G'}\right)^{-1}\mathbf{G'}^{\mathrm{T}}\,\mathbf{C'}^{-1}\,\delta\mathbf{d'} \qquad \textbf{Equation 67}$$

minimises

$$Q = \left(\frac{1}{N+M+A}\left[\left(\delta\mathbf{d'}^{\mathrm{T}}\,\mathbf{C'}^{-1}\,\delta\mathbf{d'}\right)\right]\right)^{\frac{1}{2}} \qquad \textbf{Equation 68}$$

where, A is the number of constraints, M is is the number of model parameters and N is the number of observed data.

3.4 Analysis of model estimation uncertainty

The a posteriori covariance of model parameters is calculated as in Equation 25 and standard deviations on model parameters are calculated as the square root of the diagonal elements in $\mathbf{C}^{\mathbf{est}}$**.** Because the model parameters are represented as logarithms, the analysis gives a standard deviation factor (STDF) on the parameter m_j that is defined by

$$\mathrm{STDF}(m_j) = \exp(\sqrt{C_{jj}^{est}})\,. \qquad \textbf{Equation 69}$$

Thus, the theoretical case of perfect resolution has a STDF=1. Well-resolved parameters are defined to have a STDF<1.2, which is approximately equivalent to an error of 20%, moderately resolved parameters fall within 1.2<STDF<1.5, poorly resolved parameters 1.5<STDF<2, and unresolved parameters have a STDF>2. Due to the linear approximation the uncertainty given by this analysis will be less accurate with increasing errors. Therefore, the analysis of the uncertainties is presented in intervals with increasing length.

References

Auken, E., and Christiansen A.V., 2004, Layered and laterally constrained 2D inversion of resistivity data, *Geophysics*, 69, 752-761.

Jacobsen, B.H., 2000, *geophysical inverse modeling*, lecture notes, Aarhus University, Course in discrete inverse modelling.

Kausel, E. and Roesset, J.M., 1981, Stiffness matrices for layered soils, *Bulletin of the seismological journal of America*, 71, 1743-1761.

Marquardt, D., 1963, An algorithm for least squares estimation of nonlinear parameters, SIAM, *Journal of Applied Mathematics*, 11, 431-441.

Menke, W., 1989, *Geophysical data analysis: discrete inverse theory* – Revised ed., San Diego Academic Press, International Geophysics Series.

O'Neill, A., 2003, *Full-waveform reflectivity for modelling, inversion and appraisal of seismic surface wave dispersion in shallow site investigation*, Doctoral thesis, The University of Western Australia.

Tarantola, A. and Valette, B., 1982, Generalized nonlinear inverse problems solved using a least squares criterion. *Reviews of Geophysics and Space Physics*, 20, 219-232.

Wisén, R. and Christiansen, A.V., 2005, Laterally and Mutually Constrained Inversion of Surface Wave Seismic Data and Resistivity Data, *Journal of Environmental and Engineering Geophysics*, 10, 251-262.